unibz junior researcher

Use of Biomass in South Tyrol

Energy Conversion and Distribution to the End User

Dario Prando

bu,press

bozen
bolzano
university
press

Freie Universität Bozen
Libera Università di Bolzano
Università Liedia de Bulsan

unibz junior researcher

Use of Biomass in South Tyrol

Energy Conversion and Distribution to the End User

Dario Prando

bu,press
bozen
bolzano
university
press

Cover design: doc.bz / bu,press
Printer: Druckstudio Leo, Frangart/o

www.unibz.it/universitypress

ISBN 978-88-6046-087-5
E-ISBN 978-886046-124-7

Contents

The unibz junior researcher series VII
Acknowledgements XI
Preface IX

1. Introduction and literature review 1
1.1 Biomass for CHP generation 2
1.2 Biomass for district heating 11

2. CHP plant based on biomass boiler and ORC generator 21
2.1 Materials and methods 24
2.2 Results and discussion 35
2.3 Main findings 42

3. CHP plant based on gasifier and ICE 45
3.1 Materials and methods 47
3.2 Results and discussion 51
3.3 Main findings 54

4. Critical issues on biomass-to-energy systems 55
4.1 Experimental setup 59
4.2 Results and discussion 63
4.3 Main findings 72

5. Integrated assessment of gasification systems for residential application 73
5.1 Methodology 75
5.2 Results and discussion 85
5.3 Main findings 92

6. Building refurbishment and DH systems 94
6.1 Materials and methods 97
6.2 Results and discussion 108
6.3 Main findings 121

7. Conclusions 123

Nomenclature 129
References 133

The author 153

The *unibz junior researcher* series

Especially at a time when universities are increasingly expected to produce tangible results, it is clear that one of their main tasks is to promote the work of their young scientists. The decision by the Free University of Bozen-Bolzano to publish the new series *unibz junior researcher,* enabling PhD students to present their research to a wider readership, is designed not so much to promote the work of individual scholars but rather to foster a common university culture. The idea is to publish studies which are exemplary, not just within the standards of the individual discipline, but also because of the wider significance of the issues they deal with and the way they are dealt with.

Due to the ever-increasing pressure in the academic world to publish papers in internationally-renowned journals, there is a danger that a lot of research reaches out to only a narrow field of specialists. But we maintain that it is precisely the role of the university to ensure that knowledge is transmitted to a wider audience, that discussion between different areas of research is stimulated and that a dialogue with a wider readership beyond the university is established. This promotes a public sphere that is better informed and more competent in debating. The studies which are published in the *unibz junior researcher* series will serve future PhD students as reference points for participation in such a culture of research. Engaging in research in isolation from the general public simply ignores the requirements of our times: Universities need to open up and academics need to learn to transmit their knowledge at various levels—all the more so considering the increasing complexity of research topics and the higher demands of research methods. This is the only way to justify public investment in universities, only in this way can universities fulfil their public mandate and contribute to a competent dialogue over impending societal issues.

The first issues of this series convincingly fulfil these criteria. They present PhD research projects judged as excellent by the examining commissions. The Free University of Bozen-Bolzano's excellent research environment has contributed greatly to these results: The authors were able to approach their research topics in a measured way, under the close supervision of members of the respective PhD advisory commission, who were able to offer a range of perspectives on the relevant research methodology. Furthermore, the university's generous bursary scheme gives PhD students the opportunity to spend periods of study and research abroad, and to thereby gain experience of how other universities conduct research on related topics. They could also present their research methodology and preliminary findings at international congresses – a valuable experience in improving communicative competences. Finally, the regional setting of our university gave them access to a rich variety of empirical data which shows that South Tyrol, while being an alpine region, is by no means represents "periphery". Instead, the research projects demonstrate that regional study objects can have international relevance because the condensed dimensions allow processes to be brought into focus more readily and changes to be monitored more precisely. The region of South Tyrol is indeed affected by global change, as witnessed for instance in the environmental field, where its sensitive alpine landscape is particularly susceptible to harmful developments. So it is possible to see South Tyrol as a sort of laboratory where we can register warning signs earlier and experiment with appropriate counter measures. A greater density of transformation processes can equally be seen in the social field. As a traditional border area, South Tyrol has always been at the crossroads of different cultures. Its historical experience with multilingualism, with different political and legal frameworks and with the cultural interaction of very different reference points for identity, makes for a background against which some of today's major social challenges such as migration or the globalised economy, can be analysed and interpreted.

These chances for new socially-relevant scientific insights find expression in the PhD studies selected for this series. The university authorities hope that these publications will allow the wider public to gain insights into the quality of the work of these young researchers, and to recognize that the fruits of the financial investment in this university have direct beneficial effects on the local society. I congratulate the authors chosen for this series and wish them every success in their scientific career hoping they will remain intellectually and emotionally linked to their university and to South Tyrol.

Walter Lorenz
Rector – Free University of Bozen-Bolzano

Acknowledgements

This research work was financially supported by the Autonomous Province of Bolzano in the main framework of the project "Sustainable use of biomass in South Tyrol: from production to technology". I thank Prof. Zerbe, who coordinated the project.

A special thanks goes to my supervisors Prof. Gasparella, Prof. Baratieri and Prof. Dasappa for teaching me the secrets of research and making me feel at home, both in Italy and in India. I am also grateful to Prof. Righetto, Prof. Zaffani and Prof. Longo, who lit my way from the middle school up to university.

I would like to thank all the friends who accompany me on my journey, in particular, the biomass guys, the buildings guys, the PhD guys and the CGPL guys.

Last but not least, my gratitude goes to my family, and to my wife Stefy in particular, for her constant support and for her enormous commitment for our new family.

Preface

This book is the result of a PhD research, based on both modelling and experimental studies in the area of renewable energy. The research was conducted in Italy at the Free University of Bolzano and complemented with research at the Indian Institute of Science in Bangalore (India). This collaboration was established through the SAHYOG project, which aims at strengthening the network between Europe and India. In addition, other cooperation initiatives with national and international scientific partners have been established, such as with the University of Florence, the University of Trento, the University of Innsbruck, and with companies such as Bioenergy 2020+, Bioenergie Renon, EcoResearch, Re-Cord, SIBE and Tis Innovation Park. This research was financially supported by the Autonomous Province of Bozen-Bolzano within the main framework of the project "Sustainable use of biomass in South Tyrol: from production to technology" coordinated by Stefan Zerbe.

Renewable energy and energy efficiency is at the top of the political agenda both in Europe and worldwide. The European Union has issued various directives for the promotion of the use of renewable energy and the energy efficiency of both buildings and energy conversion systems. All these measures are considered viable options to reduce both greenhouse gas emissions as well as the dependence on imported fossil fuels. Moreover, when referring to the efficiency of a system, it is imperative not to refer only to the nominal efficiency of each single component but to the global efficiency of the entire system. This aspect is a key point to develop efficient systems, and it requires tools and skills to identify the optimal solution for a specific application.

With this volume the author aims at providing an insight into the above-mentioned issues by presenting an integrated assessment of the performance of energy conversion systems based on lignocellulosic biomass. On the one hand, it focuses on the conversion of biomass into energy, on the other hand, on the distribution and matching of the generated heat to the demand, i.e. the final uses, considering the respective efficiencies. These two elements are complementary and both their efficiencies contribute to the overall performance of the whole system.

One of the challenges of this topic involves the improvement of biomass-to-energy systems identifying possible upgrading measures and—in particular for the gasification-based plants—the enhancement of the operational reliability. Nonetheless, the subsidy mechanism for the promotion of renewable energy should be revised since it strongly favours the profitability of electricity production compared to heat production. In this perspective, the first part of the work deals with the detailed monitoring of two commercially available plants—one based on combustion and one on gasification—in order to define the current energy performance achievable in practical applications. The experimentation has been supplemented with the modelling of the main components in order to identify potential improvements. Since the operational reliability of gasification systems is threatened by the presence of tar compounds in the producer gas, a base study on tar characterisation was carried out during the research at the Indian Institute of Science in Bangalore. In fact, tar is considered the main barrier for the development of gasification technology. However, the research has shown that technology packages do exist to meet the demand.

Another challenge that needs to be met is the prediction of the impact of building refurbishment on the energy performance of the systems. Nowadays, both subsidies and minimum requirements are set by the governments to promote improvements in building energy performance. This rapidly changes the building scenario and it also requires a constant update of the energy systems to be efficient in real operation. Furthermore, when considering the installation of small scale combined heat and power (CHP) systems based on biomass, there is a limit on the minimum scale available in the market. In this perspective, the CHP installation is rarely suitable for a single building and the use of district heating (DH) networks is required to justify this application. Nonetheless, the DH network should not compromise the heat distribution efficiency that would affect the global efficiency of the

system. In this framework, the second part of this work deals with the energy and economic assessment of the distribution and use of the heat generated by a plant. A numerical model, developed for the purpose, enables the simulation of both centralised users (building, flat) and distributed users (district heating). The impact on the whole system of both the refurbishment of the buildings and the potential improvement of the DH network has been investigated exploiting the prediction capabilities of the developed model.
The main results of this research highlight that, in most of the CHP plants, a considerable share of the heat is discharged into the environment because the subsidisation mechanism makes heat generation less profitable than electricity. Moreover, gasification systems have shown higher electrical efficiency than Organic Rankine Cycle (ORC) systems, however the latter could increase the performance if operated with a heat sink at low temperature. Therefore, the conversion of the current district heating networks to low temperature systems could considerably improve the heat distribution efficiency and, consequently, the efficiency of the whole system. The future refurbishment of buildings will be a great challenge for the DH networks, which will need to consider improvement measures, such as low temperature distribution and CHP system installation, to be competitive against alternative solutions.
This study is undoubtedly a tangible contribution to spread the know-how acquired from an extensive investigation into the sustainable use of ligno-cellulosic biomass and it paves the way for the implementation of efficient energy systems from a global perspective.

A. Gasparella – Free University of Bozen-Bolzano, Italy
M. Baratieri – Free University of Bozen-Bolzano, Italy
S. Dasappa – Indian Institute of Science, Bangalore, India

1. Introduction and literature review

Biomass, wood in particular, is the oldest source of energy used by mankind. It still represents roughly 9 % of the world's primary energy consumption and 65 % of the world's renewable primary energy consumption (Lauri et al. 2014). Nowadays, this renewable energy resource is considered as an option to reduce both greenhouse gas emissions and the dependence on imported fossil fuels (The European Parliament and the Council of the European Union 2009). The process involving growth and combustion of biomass is carbon neutral because CO_2, emitted during combustion, is sequestered by process of photosynthesis from the atmosphere during the growth of the plant. Furthermore, the emitted CO_2 is twenty times less active as greenhouse gas than methane which would be produced from the natural decomposition of biomass (Demirbas 2001). Nevertheless, biomass usually needs pre-processing to become a suitable fuel and has to be transported to the energy generation plant; all these steps negatively impact on the greenhouse gas emissions.

Cogeneration is defined as the combined production of heat and power and allows a primary energy saving compared to the separate production of the two energy streams. With regard to the limited availability of renewable resources, among them especially biomass resources, efficiency in terms of consumption and utilization becomes vital. Heat is the energy stream with lower quality and it is generated in most of the conversion processes. Thermodynamically, the lower the exit temperature of the flue gases from the process plant, the higher the efficiency of the polygeneration system. For this reason, a polygeneration system is suitable to be coupled to a DH system which enables exploiting heat at quite low temperature (i.e. < 100 °C). Furthermore, future implementation of the fourth generation DH (i.e. return/supply temperatures at 30/70 °C) will allow exploiting heat share that until now has usually been discharged into the environment .

The first part of this chapter deals with the main technologies for cogeneration based on biomass. CHP generation technologies are then compared; combustion-based systems (i.e. steam turbine, organic Rankine cycle and Stirling engine) and gasification-based systems (i.e. internal combustion engine and biomass integrated gasification combined cycle). Capacity (power level), efficiency, operation flexibility and field experience at the current state of the art have been reported for each technology.

The second part of the chapter deals with the implementation of biomass technologies in DH systems. A brief introduction about the architecture of DH systems has been complemented by an analysis of the potential benefits deriving from the use of biomass. The CHP systems, presented in the previous section, are analysed focusing on their application to DH networks. The discussion has been extended including the determination of the cost-optimal size, the role of thermal energy storage and the impact of biomass transportation on the energy chain. Moreover, the influence of extensive refurbishment on the buildings connected to DH grids is extensively analysed. The possible solutions that allow the DH systems to be competitive in the future are presented in accordance with the scientific literature. Finally, the smart grid concept has been introduced and its applicability to thermal networks is discussed highlighting the potential benefits for the thermal sector as well as for the entire energy system.

1.1 Biomass for CHP generation

In the past few years, there has been a great interest in renewable energy sources. On the one hand, energy demand has been constantly growing, strictly correlated to the increase of global population and to expansion of developing countries' economies (Nelson 2011). This aspect, combined with the depletion of fossil fuels, has in the last few years caused a considerable increase in the prices for fossil fuel energy on the global energy markets. On the other hand, industrialized societies are currently becoming more aware of the impacts of fossil fuel utilization on the environment and on human health, making the search for environmentally and socially acceptable alternatives increasingly important (Kaltschmitt et al. 2007). If compared to other renewable sources (e.g., wind or solar energy) biomass has the main advantage that, if well managed, it can ensure a constant supply of energy, its availability not being dependent on climatic conditions in the short and medium term. This is an essential aspect in the design of an integrated exploitation of different renewable sources.

Sustainable biomass feedstock should have no impact on the food chain. In particular, lignocellulosics biomass, as woody biomass, energy crops—that are cultivated for the purpose of energy generation—or even algae are some examples of them. In Fig. 1.1 a rough distinction between crops, residues, by-products and waste has been made to consider a wide spectrum of feedstock for polygeneration. After the harvesting or collection, biomass has to be subjected to different pre-treatments, which usually have the common purpose of energy densification. The biomass chain is then characterized by transportation and storage to the first stage of conversion, i.e. thermo-, physical- and bio-chemical. Intermediate fuels and chemicals (solid, liquid and gaseous) can be obtained starting from the original feedstock, which can be valorised through combustion in boilers and, prime movers or fuel cell stacks for heat and electricity generation both for stationary and automotive applications.

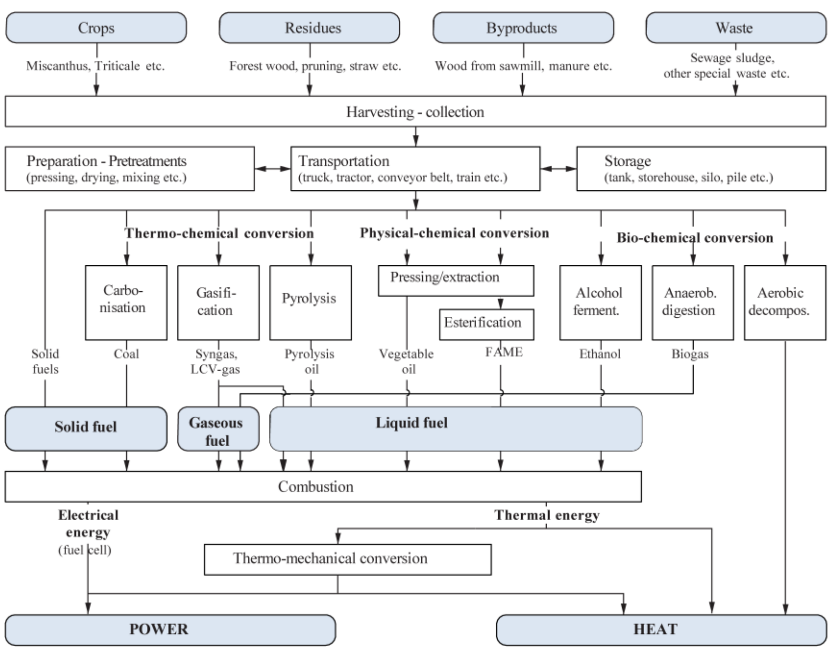

Fig. 1.1 – Schematic representation of different biomass-to-energy pathways (rounded boxes: energy carriers; boxes: conversion processes); Kaltschmitt et al. (2007).

The main technologies developed for converting biomass into thermal energy and electricity usually include a primary conversion stage that produces hot water, steam, gaseous or liquid products and a secondary conversion stage that transforms these intermediate products to heat and power. In the present section, the thermochemical processes are considered in detail and the different technologies are presented according to the following classification:

- combustion-based technologies producing steam or hot water, coupled to steam engines, steam turbines, Organic Rankine Cycle (ORC) and Stirling engines;
- gasification-based technologies producing gaseous fuels, coupled to internal combustion engines (ICEs), gas turbines (GTs), fuel cell stacks and micro-turbines.

1.1.1 Combustion-based technologies

The direct combustion of lignocellulosic biomass is a process mostly applied for the pure generation of heat by means of boilers. The boilers can be based on fixed bed combustion, fluidized bed combustion and pulverized bed combustion (Saidur et al. 2011). The fixed bed combustion boilers include grate furnaces, for large scale systems up to 20 MW_{th}, and underfeed stokers, for small-medium scale systems up to 6 MW_{th}. The former are suitable for biomass with high water content, high ash content, and irregular particle size since the grate allows a smooth transportation of the material and facilitates the drying phase. The latter, due to a simpler fuel load system, requires water content smaller than 35 %, homogeneous material and small ash content. The fixed bed combustion boiler can reach combustion efficiency up to 90 % at nominal thermal output (Van Loo and Koppejan 2008). The fluidized bed combustion boilers are typically used for large scale applications, more than 30 MW_{th}. These boilers have high fuel flexibility due to a mixed suspension of fuel and solid bed material that promotes a complete combustion with a lower excess of air. Thanks to the homogeneous combustion and the low excess of air, the fluidized bed boilers can reach a combustion efficiency of 95 % and low NOx emissions (Saidur et al. 2011). The pulverized combustion bed boilers are mostly used for large scale applications.

The fuel, small dried particles such as wood powder, are transported by air, which is also used as primary air for combustion. Combustion is then completed with the addition of secondary air. Low excess of air is required for a complete combustion because the suspended fuel and the combustive air are perfectly mixed. This results in high combustion efficiency and low NO_x emissions.
The direct combustion of lignocellulosic biomass can be coupled with different prime movers for cogeneration of heat and power. The most common prime movers consist of steam turbines, Organic Rankine Cycle generators and Stirling engines.
Steam turbines are typically used for applications with size in the range 0.5–500 MW_{el}. Turbines smaller than 0.5 MW_{el} are available but they have a niche market (Van Loo and Koppejan 2008). This technology is based on a thermodynamic direct cycle (i.e. Rankine cycle) that allows converting heat into mechanical work using water as working fluid. In the specific case, a steam boiler based on biomass generates high-pressure steam that is converted into mechanical work by means of a turbine. The mechanical work usually drives a generator to produce electrical power. The steam, after its expansion, is condensed at constant pressure and the saturated liquid is pumped from low to high pressure. The water at high pressure enters the steam boiler and repeats the cycle. The steam turbines, used for CHP generation, can be classified into two main typologies: non-condensing (or back pressure) turbines and extraction turbines. Non-condensing turbines exhaust the entire flow of steam to provide heat to the DH network. The network temperature level at the condenser determines the condensing temperature; lower temperatures increase the capacity of the turbine to generate work. Extraction turbines have different steam extractions from intermediate portions of the turbine to satisfy the requirements of the DH grid. The steam extractions are designed depending on the required pressure/temperature of the DH network. The extraction turbine enables a higher steam flow to the turbine, generating additional electricity, during the periods of reduced thermal power. The steam turbines benefit from the usability of a wide variety of biomass (i.e. forest wood, sawmill by-product and agricultural residues) because the combustion of biomass and the production of steam occur in different sys-

tems. This technology has also some drawbacks. The steam boiler requires a super-heater to avoid liquid drops in the turbine that would erode the turbine blades. This is an obstacle for the scaling down of the system to a simplified design. Furthermore, the use of steam required qualified personnel to operate the plant (Duvia and Guercio 2009). The scaling-down of this technology below 30 kW_{el} encounters some obstacles such as low electrical efficiency and high specific investment costs (Alanne et al. 2012).
The ORC generators are available for small-medium CHP applications, from 500 kW_{el} up to 10 MW_{el} (Duvia and Guercio 2009; Quoilin et al. 2013). The technology is based on the Rankine cycle, similar to a conventional steam turbine, but it operates with a high molecular mass organic fluid. The operation with this fluid is particularly suitable for low temperature heat sources. Other benefits are related to the use of the organic fluid. The coupled boiler does not require a super-heater due to the absence of liquid drops in the turbine. The organic fluid is not corrosive and thermal oil is used as a thermal medium, therefore offering high reliability and requiring little maintenance.. Furthermore, no licensed operators are necessary for the maintenance. The turbine has a large diameter, due to the large flow rate of the organic fluid, and low peripheral speed enabling the direct drive of the electrical generator without reduction gear. The ORC generators can reach an electrical efficiency up to 20 % at nominal load, but the efficiency is satisfactory also at partial load (Bini and Manciana 1996; Dong, Liu and Riffat 2009; Duvia and Guercio 2009). This technology is well established and commercially available from various manufacturers (Rentizelas et al. 2009). Nevertheless, ORC generators are considered less prominent for micro-scale application due to high specific investment cost and limited electrical efficiency (Dong et al. 2009; Quoilin et al. 2013).
The Stirling engine is a reciprocated engine externally heated. In the specific case, it is an external combustion engine because the heat is provided by means of biomass combustion. The cycle is closed in a loop with a gaseous working fluid (i.e. usually air, hydrogen or helium) that is compressed in the cold portion and expanded in the hot portion. These cyclic compressions and expansions convert heat into mechanical work. The reciprocating motion is then converted to circular motion by means of a crankshaft that turns a gen-

erator to produce electrical power. An internal regenerative heat exchanger is usually adopted to increase the thermal efficiency of the engine. There are various configurations in the architecture of the engine but all of them are based on the same principle. External combustion allows the use of a wide variety of biomass types (i.e. forest wood, sawmill by-product and agricultural residues). Unlike the internal combustion engine, the heat is provided with a continuous combustion enabling a complete burning of the fuel, reduced noise and little vibrations. Nevertheless, Stirling engines are slow to change the power output and a long warm-up (i.e. few minutes) is required to start the operation (Kongtragool and Wongwises 2003). This technology is mainly available in sizes smaller than 200 kW_{el}. The Stirling engine has a promising electrical efficiency up to 25 % (Biedermann et al. 2004a). The commercial introduction of the Stirling engine has started, but the investment cost is quite high because no mass production is available. Furthermore, the long-term experience with biomassfired boilers is limited. In accordance with the scientific literature, the development of new materials to improve the heat transfer to the working fluid are considered to be the key to the success of this technology (Kölling et al. 2014; Kongtragool and Wongwises 2003). In the specific case of biomass-fired boilers, a cleaning system for the reduction of ash deposition on the hot heat exchanger of the Stirling Engine can increase its availability (Biedermann et al. 2004b; Marinitsch et al. 2005).

1.1.2 Gasification-based technologies

The gasification of lignocellulosic biomass coupled with different prime movers is a promising technology for CHP generation. The gasification process consists of a partial oxidation in which the solid fuel is converted into a gaseous fuel, i.e. producer gas. The composition of the producer gas depends on various process conditions but mainly on the oxidant used, as shown in Table 1.1 (Bocci et al. 2014). The producer gas can be burnt to generate heat, but its use in prime movers for CHP production is a more valuable application. The most common prime movers are the internal combustion engine, the gas turbine and the fuel cell.

Gasification, compared with combustion, is more sensitive to changes in feedstock type, particle size, water content and ash content (McKendry 2002b). The gasifiers can be classified into three main categories: fixed bed, fluidized bed and entrained flow. The fixed bed gasifiers, , can be mainly divided into updraft (i.e. counter-current flows) and downdraft (i.e. co-current flows). In the updraft gasifier the biomass moves through drying, pyrolysis, reduction and oxidation zones whereas the gas flows in the opposite direction.

Table 1.1 – Producer gas composition with different oxidants (Bocci et al. 2014).

	Composition (vol. %)					LHV
Oxidant	H_2	CO	CO_2	CH_4	N_2	(MJ Nm^{-3})
Air	9–10	12–15	14–17	2–4	56–59	3–6
Oxygen	30–34	30–37	25–29	4–6	-	10–15
Steam/CO_2	24–50	30–45	10–19	5–12	-	12–20

This configuration allows a high conversion efficiency, but the producer gas usually has a high tar content mainly generated in the pyrolysis zone. Tar causes major fouling in the prime movers with consequent unscheduled plant stops (Paethanom et al. 2012). For this reason, the producer gas from an updraft gasifier is more suitable for direct firing (Bocci et al. 2014), but can also be used in prime movers if proper measures are taken to reduce the tar content (Han and Kim 2008; Pedroso et al. 2013). In downdraft gasifiers, biomass and oxidant flow in the same direction and, after drying and pyrolysis zones, they are forced to pass through a throat where oxidation at high temperature takes place. This enables the tar cracking with a resulting producer gas that is suitable for CHP production in prime movers. Downdraft gasifiers are usually smaller than 1 MW because the scaling-up does not allow uniform flow and temperature in the oxidation zone (Bocci et al. 2014). The second category of gasifiers involves the fluidized bed gasifiers. In this configuration, biomass and hot bed material (i.e. inert sand or catalyst) are intensely mixed and kept in a semi-suspended state enabling uniform temperatures in the entire bed. For this reason, the fluidized bed gasifiers accept a wide typology of biomass and are particularly suitable for large installations. This configuration is more complex than the fixed bed solution and the tar content in the producer gas is generally higher than downdraft technology, but lower than updraft technology (Milne and Evans 1998). The resulting producer gas, after proper cleaning, is mainly used in the internal combustion engine and also for CHP application (Ahrenfeldt et al. 2011). The last category involves the entrained flow gasifiers. This design does not have a solid bed, and the fuel is entrained with the gas stream. For the purpose, the fuel should be finely pulverized (i.e. 100–500 μm) and this is usually challenging due to the fibrous nature of biomass. Furthermore, after grinding the particles tend to stick together. The resident time of the fuel (i.e. a few tens of seconds) is considerably shorter than fluidized bed (i.e. a few minutes). The temperatures are very high (i.e. 1200–1500 °C) promoting the thermal cracking of tars but also causing ash melting (Knoef 2012; Veringa 2005). For this reason, the use of biomass containing ash requires slagging gasifiers that are more expensive due to the equipment to handle the molten ash in the form of slurry. The use of non-slagging gasifiers is considered a suitable approach when dealing with upgraded fuel such as pyrolysis oil, since it is almost free of ash and minerals.

Among the possible prime movers, reciprocating engines are the most used because they are based on an established technology with high reliability as a result of extensive research carried for fossil fuel usage. The ICE is commonly used for application in the size range 10–2000 kW_{el} (Bocci et al. 2014). However, modular installation foresees power plants up to 10 MWel. The producer gas has a lower heating value than natural gas and gasoline but, with some modifications, both Otto and Diesel engines can be used (Aung 2008). Furthermore, the particulate and tar content in the producer gas have to be reduced under required levels by means of proper cleaning sections. Indicative limits for both particulate and tar are 50 mg Nm^{-3} and 100 mg Nm^{-3} respectively (Hasler and Nussbaumer 1999; Spliethoff 2001). Some gasification systems coupled with ICE are successfully commercialized, but some technical and economic issues still have to be addressed.

Gas turbines are mainly applied with sizes larger than 1000 kW_{el} with a satisfactory electrical efficiency, usually higher than 25 % (Dong et al. 2009). Gas turbines have stricter limits than reciprocating engines in terms of particulate and tar content. Indicative limits are 20 mg Nm^{3} for particulate content and 8 mg Nm[3] for tar content (Hasler and Nussbaumer 1999; Milne and Evans 1998). The consolidation of this technology would enable the development of combined cycles based on gasification, i.e. Biomass Integrated Gasification Combined Cycle (BIGCC). According to (Veringa 2005), BIGCC is a promising technology for large scale power plants (i.e. 50–100 MW_{el}). This configuration enables a high power-to-heat ratio to be reached because additional electricity is generated by means of a steam turbine exploiting the high enthalpy content of the GT exhausts (Difs et al. 2010; Ståhl and Neergaard 1998).

There are other technologies in demonstration phase with promising efficiencies but several efforts will be necessary to reach their commercialization. Demonstration plants based on Solid Oxide Fuel Cell (SOCT) show they can reach electrical efficiency of 40 % (Bocci et al. 2014). Nevertheless, the limits for particulate and tar content in the producer gas are stricter than the gas turbine, and many other compounds (i.e. H_2S, SO_2, HCl) can compromise their operation.

The gasification process, compared with the combustion process, leads to higher electrical efficiency because it is not related to Carnot's law (Veringa 2005). The advantage is even more evident comparing systems smaller than 200 kW_{el}. Moreover, fuel cell is particularly promising given the higher efficiency due to direct conversion of chemical into electrical energy. Biomass gasification applied to CHP production is considered a promising technology for decentralized plants at sizes that have not been sufficiently efficient before, i.e. power plant smaller than 10 MW_{el} (Ahrenfeldt et al. 2011). However, the limited standardization of this technology increases the investment risk that is a factor that influences the decision of the investors (Rentizelas et al. 2009).

A comparison among the major technologies for CHP generation is shown in Table 1.2. The efficiencies are defined on the feedstock lower heating value and are comprehensive of the entire CHP system.

Table 1.2 – Comparison among the most common biomass CHP systems.

	Combustion-based CHP systems			Gasification-based CHP systems	
	ST	ORC	Stirling	ICE	BIGCC
Electrical Power	50 kW–250 MW	500 kW–10 MW	< 200 kW	10 kW–10 MW	50 MW–100 MW
CHP electrical efficiency	0.10–0.25	0.13–0.18	0.10–0.15	0.20–0.35	0.30–0.40
Power-to-heat ratio	0.10–0.35	0.20–0.25	0.15–0.20	0.40–0.50	0.70–0.90
Field experience	extensive	extensive	limited	sufficient	very limited

1.2 Biomass for district heating

The district heating (DH) is a system for distributing heat, produced in a central station, for various applications; the heat is usually used for space heating, water heating and low temperature industrial processes. Three main parts can be identified in a DH system; generation, distribution and consumption sections. The generation plant differs between pure heat generation (i.e. boiler) and combined heat and power (CHP) generation. The distribution grid is mainly based on pre-insulated pipes with length of few kilometres for micro DH and hundreds of kilometres for macro DH. The consumption section is a sub-station connecting the primary and the secondary networks with a direct or indirect connection, i.e. with or without a heat exchanger. According to Lund et al. (2014), the medium to transfer heat can be classified into four categories; steam (i.e. first generation DH), pressurized hot water over 100 °C (i.e. second generation DH), pressurized hot water below 100 °C (i.e. third generation DH) and low temperature water 30 °C–70 °C (i.e. fourth generation DH).

The DH systems offer many benefits for building owners and in general, for the hosting community. Reduced heating costs, safer operation and increased reliability are some of the benefits for the building owner. Improved energy efficiency, reduced emissions and opportunity to use local energy resources are advantages that involve the entire community. Nevertheless, limited know-how of this technology, the difficulty of finding appropriate sites and the high investment costs are the main obstacles for a large implementation of DH systems. Furthermore, government regulations to avoid potential monopoly of the DH owner is an aspect to take into account (Rezaie and Rosen 2012).

The DH system is very flexible in terms of energy sources; it can be based on non-renewable sources, renewable sources or a combination of the two sources. The non-renewable sources include fossil fuels, nuclear energy, cogeneration heat and waste heat from systems exploiting non-renewable sources. The renewable sources include biomass, geothermal, aerothermal and solar energy. Where geothermal energy is not available, biomass is the only non-intermittent on-site renewable resource for CHP generation (Wood and Rowley 2011). Biomass feedstock can be stored for later use increasing the flexibility of the DH system (Hall and Scrase 2012). Biomass used for DH applications is mainly lignocellulosic including forest and agricultural biomass. Forest biomass in particular is available throughout the year avoiding long-term storage (Castellano et al. 2009). In addition to the energetic benefits, the use of biomass creates jobs and promotes social and economic development of the local community (Openshaw 2010).

1.2.1 Heat generation and distribution in DH systems

In DH systems based on lignocellulosic biomass, the production section is usually based on thermochemical conversion processes such as combustion and gasification because their primary products, i.e. heat and producer gas, are suitable to be exploited in DH systems (Akhtari et al. 2014; McKendry 2002a). The technologies can be applied for pure heat generation, but DH systems are considered an excellent opportunity for CHP generation since the network acts as a large heat sink for the cooling water of the power generation processes (Magnusson 2012; Persson and Werner 2011). The CHP systems generate two energy outputs, i.e. heat and electricity, with characteristics that are considerably different (Börjesson and Ahlgren 2012). From both a thermodynamic and an economic point of view, electricity is a high-quality energy carrier since it can be converted into all other forms of energy. The quality of heat depends on the temperature level; a higher temperature

increases the generation of mechanical work. On this basis, the technologies should be compared considering both the overall efficiency, i.e. the sum of electrical and thermal efficiency, and the power-to-heat ratio (Puig-Arnavat et al. 2013).
The electrical efficiency of both non-condensing steam turbines and ORC generators depends on the pressure at the condenser. The lower the condensing pressure, the higher the work generated by the turbine and, therefore, the electrical efficiency. The condensing pressure is determined by the condensing temperature which depends on the temperature of the DH grid. According to Prando et al. (2015a), a reduction of the mean temperature network of 10 °C would increase the electrical efficiency of 1 % (absolute increment). For this technology, both the supply and return temperatures of the network should be kept as low as possible in order to increase electrical efficiency. Steam turbines are commonly used for large scale applications. The implementation of non-condensing steam turbines, rather than extraction steam turbines, allows a high flexibility of the system to follow the seasonal variation of the DH system; wide power-to-heat ratios can be achieved. Furthermore, the extraction steam turbines are particularly suitable to fulfil heat need at high temperature that is often required by industrial processes (ICF International 2008). The ORC generators are commonly used for applications with a size smaller than 2 MW_{el} (Van Loo and Koppejan 2008). According to Duvia and Guercio (2009), the electrical efficiency of ORC generators is not particularly penalized at partial load. For this reason, this technology allows acceptable performance also for DH networks with a far from constant heat load profile.. The Stirling engine is a technology developed for sizes smaller than 200 kW_{el}. The implementation of this technology is suitable for distributed generation in residential or commercial buildings and micro DH networks (Corria et al. 2006; Renzi and Brandoni 2014). According to Biedermann et al. (2004b), the electrical efficiency of the Stirling engines is slightly penalized at partial load operation. The gasification systems have a high electrical efficiency (i.e. 0.20–0.30) for a wide range of sizes (i.e. 10 kW_{el}-10 MW_{el}) (Dasappa et al. 2011). This technology is particularly promising for micro DH applications due to the high efficiency at the lowest sizes. Nevertheless, for the smaller sizes of the range (roughly less

than 200 kW_{el}) the gasification systems are usually not equipped to operate at partial loads; therefore, they should be installed in micro DH as base thermal load stations.

Some examples of the above-mentioned technologies are reported in this section.

The CHP plant in Güssing (Austria) is a well-known application of FICFB (fast internal circulating fluidized bed) steam gasifier coupled to two gas engines. The gasifier is fed by woodchip and it consists of two zones; a combustion zone that provides heat to the gasification zone by means of the circulating bed material. The producer gas is mainly composed of hydrogen (35–45 vol. % dry), carbon monoxide (19–23 vol. % dry), carbon dioxide (20–25 vol. % dry) and methane (9–11 vol. % dry), with a resulting heating value of 12 MJ Nm^{-3} on dry basis (Knoef 2012). The tar content in the raw gas is around 1500–4500 mg Nm^{-3} while after the cleaning section – i.e. fabric filter and oil scrubber – the clean gas has a very low tar content such as 10–40 mg Nm^{-3} (Ahrenfeldt et al. 2011). The clean gas is finally fed into two gas engines for a total production of 4.5 MW_{th} and 2.0 MW_{el}; the electricity is delivered to the local grid while the heat supplies the town of Güssing through the district heating network. The fuel input power is 8 MW therefore the overall electrical efficiency is about 25 % while the thermal efficiency is 56 %. From 2002 to 2008, the CHP plant operated with an average of 5700 h per year (Ahrenfeldt et al. 2011).

A well-known CHP plant − based on ORC − is located in Lienz (Austria). The plant is fed by woodchip that is combusted in a thermal oil boiler, equipped with a thermal oil economizer, with a nominal capacity of 6.5 MW_{th}. The thermal oil (300/250 °C) fed the ORC process that enables the production of 1 MW_{el} and 4.45 MW_{th}; the electricity is delivered to the local grid while the heat supplies the town of Lienz through the district heating network (80/60 °C). Furthermore, a small share of heat – from the heat recovery unit of flue gases – is directly delivered to the district heating network. The net electrical efficiency at nominal load is 18 % for the ORC process and 15 % for the entire CHP plant. The thermal efficiency at nominal load is 80 % for the ORC process and 65 % for the entire CHP plant. The plant is fully automated and ordinary maintenance requires an unlicensed operator for 3–5 h per week.

Plants based on this technology have a high reliability with more than 7000 h per year of operation (Obernberger et al. 2002).
The last example concerns a micro-scale CHP plant located in Bolzano (Italy). The downdraft gasifier is fed by woodchip with a moisture content lower than 10 %, calculated on wet basis. The producer gas is approximately composed of hydrogen (17 vol. % dry), carbon monoxide (22 vol. % dry), carbon dioxide (8 vol. % dry), nitrogen (51 vol. % dry) and methane (2 vol. % dry), with a resulting heating value of 4.7 MJ Nm-3 on dry basis. The raw gas is treated in the cleaning section – i.e. fabric filter – and the outlet gas has a tar content lower than 10 mg Nm^{-3}. The clean gas is finally fed into the gas engine that enables the production of 98 kW_{th} and 43 kW_{el}; the electricity is delivered to the local grid while the heat supplies the surrounding buildings. The gross electrical efficiency is 22 % and the thermal efficiency is 50 %. The plant is fully automated and requires a weekly stop for ordinary maintenance in order to avoid unexpected outages (Prando et al. 2014b).
The DH networks can extend over long distances and connect a large number of users, but the resulting heat load profile along the year is not constant. The sizing of the CHP could be based on the minimum heat demand, but the plant could be particularly small to justify a CHP plant installation. The determination of the cost-optimal size is a challenging calculation that needs to take into account many parameters such as electric efficiency, thermal efficiency, equivalent utilization time of the plant at rated output, investment costs, operational costs, subsidies for the use of renewable sources and other economic parameters (Sartor et al. 2014). This optimization is particularly important for biomass CHP plants, which, compared with fossil fuels plants, have higher investment costs and lower efficiencies. This is mainly due to the nature of the fuel that requires advanced systems to achieve satisfactory performance from both the energetic and environmental point of view. Considering a heat-driven plant, the equivalent utilization time of the plant at rated output depends on the match between heat load profile and the rated load of the plant. For example, Sartor et al. (2014) developed a model to investigate the cost of heat (COH) depending on the equivalent utilization time of the plant at rated output (τe). The study, as shown in Fig. 1.2, considers both natural gas boiler and biomass CHP defining the break-

even point. These results are valid for the reference Belgian situation but could be adapted to any situation changing the parameters of the model.

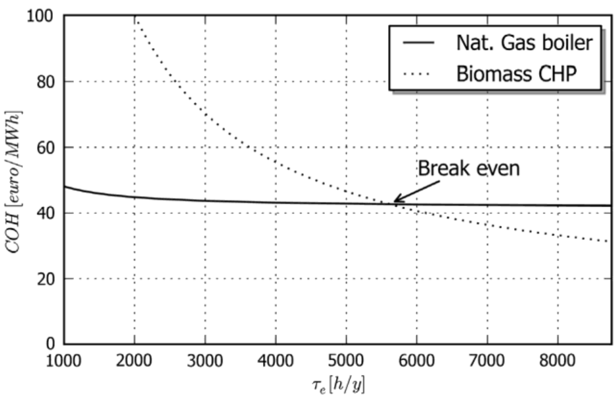

Fig. 1.2 – Cost of heat (EUR MWh^{-1}) depending on the equivalent utilization time (h year^{-1}) "Reproduced by permission of Kevin Sartor" (Sartor et al. 2014).

Heat storage plays an important role in the district heating, and it should be carefully sized depending on the generation system and load profile of the buildings. The hot water cylinder is the most common heat storage providing heat over periods of hours to days. In accordance with Wolfe et al. (2008), further development of this technology can be expected but radical change is unlikely. For both boiler and CHP systems, the heat storage enables the installation of systems with a smaller size because the peak loads can be supplied by the stored heat. Furthermore, it allows on-off operation of the production systems when the heat load is low, and both thermal and electrical efficiency would be particularly penalized (Ferrari et al. 2014). According to Nuytten et al. (2013), the implementation of a centralized heat storage, compared with a decentralized solution, enables higher flexibility of the CHP system; a decentralized solution causes exceptional peaks when the storage units have to be charged. This problem could be tackled by a future smart management in which the DH manager has full control of the decentralized storage units.

In the last years, several buildings have been refurbished, and extensive implementations of energy saving measurements are expected in the next

years (European Commission 2010). The decreasing heat need of the buildings causes a reduced utilization of the DH capacity with a consequent reduction of both the system efficiency and the revenues.
The existing DH systems need to be upgraded in order to be competitive, and builders of new DH constructions have to carefully consider the development of the building stock. An increase of DH utilization could be achieved with a network extension, but it strictly depends on the heat density of the considered area (Münster et al. 2012; Nielsen and Möller 2013). The reduction of heat demand is not considered a barrier for the DH systems in high density areas, but they will lose competitiveness in low heat density areas (Connolly et al. 2014; Persson and Werner 2011).
Another upgrade of the DH systems is the reduction of the grid temperatures (i.e. supply and return). Both heat exchangers and radiators are usually oversized because they are designed for the most critical weather condition. Actually, for most of the year, the heat load is smaller, and reduced network temperature could be implemented improving the distribution efficiency (Prando et al. 2015b). Furthermore, the use of control algorithms could be used to produce the lowest possible return temperature of the network (Lauenburg and Wollerstrand 2014). Innovative control system based on mass flow control by means of pumps with inverter could also be adopted to increase the heat transfer while reducing return temperature and pumping power (Kuosa et al. 2013). According to Gustafsson et al. (2010), the grid supply temperature should be used as an indicator of the outside temperature to control the temperature of the heating system of the buildings. The most suitable control curve between outdoor and network supply temperature should be customized for each DH system by means of simulation tools in order to increase network ΔT and consequently reduce the pumping power.
The state of the art shows the low temperature district heating (LTDH), i.e. 55/25 °C (supply/return), is a suitable solution for DH systems in low heat density area with low energy buildings (Li and Svendsen 2012). In accordance with Dalla Rosa and Christensen (2011), LTDH systems in areas with linear heat density of 0.20 MWh m^{-1} $year^{-1}$ are supposed to be feasible from an energetic and economic point of view. In existing DH systems, the DH

managers cannot force the users to adopt measures that aim to decrease the temperature level of their heating systems, but they could promote it by means of heat price depending on the temperature level.

Building refurbishment is not only an obstacle to DH efficiency, it can reduce the difference of thermal power between the heating season and the period with only DHW demand (Lund et al. 2014). According to Sartor et al. (2014), a more constant heat load enables a higher equivalent utilization time of the CHP system. In addition, involvement of the end-users for a proper use of the buildings could lead to a 60 % peak load reduction with significant benefits in terms of efficiency of the DH system (Dalla Rosa and Christensen 2011).

The transportation of biomass, both from the energetic and economic point of view, significantly influences the large-scale biomass plants because they cannot rely only on the resources locally available (Börjesson and Ahlgren 2012; Rentizelas et al. 2009). Fig. 1.3 qualitatively represents the volume of biomass (i.e. spruce pellet, spruce woodchip and rice straw) in order to have the same energy as for coal. In addition, the respective values for energy density are reported in Fig. 1.3 (Chiang et al. 2012; Knoef 2012). For this reason, biomass is considered suitable for small to medium scale applications decentralized on the territory. The development of decentralized biomass CHP plants can minimize transportation, electricity grid losses and heat distribution losses (Bang-Møller et al. 2011; Wolfe 2008). Furthermore, biomass resource is quite spread over most of the countries which can help to increase their energy independence (Sartor et al. 2014). The decentralization of the systems brings many benefits but also some drawbacks. Decreasing the size of a plant leads to smaller efficiency and higher specific investment costs. It is not possible to define the optimal solution valid for all the applications but each case has to be evaluated considering the technologies available at the size under consideration.

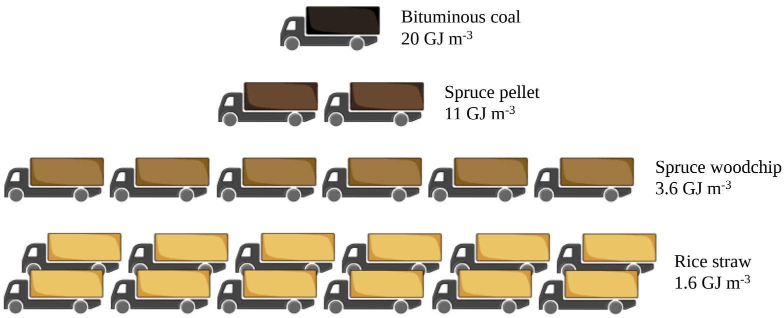

Fig. 1.3 – Comparison between coal and biomass (Clipart by Paola Penna).

1.2.2 Smart grid concept for thermal networks

According to Wolfe (2008), a high development of decentralized systems is expected for the next two decades, and this could be enhanced by system technologies such as active networks, smart metering and intelligent tariff-interactive load management. In the decentralized model, heat demand is less predictable than in a centralized model, therefore, more flexibility and active network management is required by DH systems. Furthermore, large development is expected for remote telecommunications since they are considered a suitable option for the control of both heat and electrical loads. According to Lund et al. (2014), the concept of smart thermal grids should be developed in the perspective of smart energy systems (i.e. electricity, thermal, cooling and other grids) in order to define synergies between the sectors and optimal solutions for each sector as well as for the entire energy system. Fig. 1.4 depicts a smart energy system. Moreover, the CHP systems produce heat and power at the same time, therefore; an integrated management of both electric and thermal grids is crucial (Rivarolo et al. 2013). Buildings in particular have the possibility to shift loads and reduce peaks for both the electricity and thermal demands, therefore, an interactive operation between buildings and grids would improve the performance of the whole system. Furthermore, time-varying prices and energy saving tips could strongly contribute to the successful implementation of the smart management of the system (Olmos et al. 2011). According to Xue et al. (2014), the building thermal masses could be used as thermal energy storage reaching the benefits previously mentioned. Nevertheless, the buildings should have proper building characteristics, i.e. thermal insulation layer on the external side of the building envelope, in order to achieve a high energy storage efficiency.

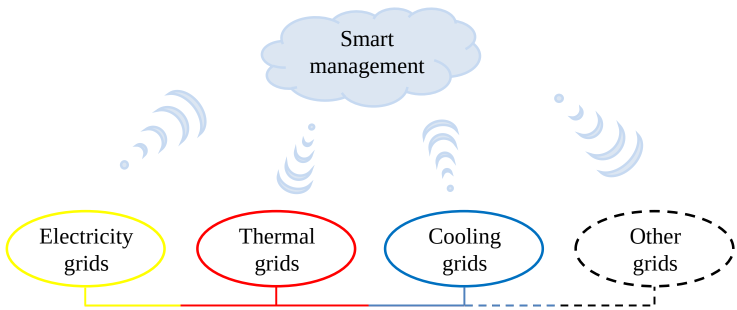

Fig. 1.4 – Smart energy system concept.

In future, DH systems should be completely based on renewable sources and CHP systems will have a key role for electricity balancing and grid stabilization (Lund et al. 2012). Since biomass is a non-intermittent on-site renewable energy, biomass CHP technologies could make a considerable contribution to the integration of intermittent renewable energy sources. In addition, the electrification of the transportation sector will further influence the dynamic behaviour of the electricity grid requiring smart management between vehicles and grid (Mwasilu et al. 2014). According to Ferrari et al. (2014), smart polygeneration grids designed for autonomous management enable the development of CHP systems, the reduction of energy distribution, the integration of renewable sources and the optimization of the system through the storage technology. However, the future of decentralized systems is strictly related to the development of new policies and price mechanisms promoting the transition of the energy companies from supply-focused to service-focused (Wolfe 2008).

2. CHP plant based on biomass boiler and ORC generator

In recent times, a lot of effort has been put worldwide into tackling climate change issues. One of the measures adopted by the European Union is known as the "20-20-20" target. One of the three targets consists of raising to 20 % the share of EU final energy consumption produced from renewable resources. Within this objective, the use of biomass could provide a substantial contribution to offset fossil fuel consumption, as stated in the European directive 2009/28/EC (The European Parliament and the Council of the European Union 2009). Another target of the European Union is the improvement of the EU's energy efficiency by 20 %; as stated in the European directive 2012/27/EU (The European Parliament and the Council of the European Union 2009), the promotion of cogeneration/polygeneration could contribute to achieve this objective.

Considering the combined heat and power (CHP) systems based on biomass, the internal combustion engines coupled with gasifiers and the ORC generators coupled with boilers are the most widespread technologies for sizes smaller than 1 MW_{el} (Bocci et al. 2014).

Gasification is considered a promising technology in terms of electric efficiency, but with a higher investment risk due to the lack of standardisation (Rentizelas et al. 2009; Kalina 2011). The overall electric efficiency of a gasification system ranges from 20 % at 100 kW_{el} to about 30 % at 1 MW_{el} size (Dasappa et al. 2011). This range of values is in accordance with recent works (Ahrenfeldt et al. 2013). In literature, there are different opinions about the maturity of such a technology. Some authors have stated that only few systems have been economically demonstrated at small scale (Dong et al. 2009) while others suggest that the gasification systems in operation are prototypes for demonstration purpose (Quoilin et al. 2013). Nowadays, several small scale gasifiers coupled with internal combustion engines (< 1 MW_{el}) are successfully commercialized and operated in several applications (Vakalis et al. 2013; Vakalis et al. 2014). However, some technical and economic issues have still to be addressed.

ORC is a well proven and used technology with investment, operational and maintenance costs that are lower if compared to gasification (Rentizelas et al.

2009; Maraver et al. 2013). The gasification systems have an investment cost 75 % higher and a maintenance cost 200 % higher than ORC-based systems (Quoilin et al. 2013). However, some authors reported that boiler-ORC coupling has a similar specific investment cost as gasifier-ICE one (Wood and Rowley 2011), or even higher (Huang et al. 2013). Beyond the conflicting opinions, the authors agree that the investment cost has a considerable impact on the business plan for both the technologies. The electric efficiency of the ORC process is in the range 6–17 % (Rentizelas et al 2009); the upper limit refers to a size of around 1 MW_{el}. The ORC process of the plant in Lienz (i.e. 1 MW_{el}) reaches a net electric efficiency at nominal load of 18 % and a net electric efficiency of the whole CHP system of 15 % (Obernberger et al. 2002). In such plants, heat is transferred to the ORC working fluid by means of a thermal oil coming from the biomass boiler. Therefore, also the biomass boiler efficiency plays a significant role in the overall plant efficiency.

Even though the efficiency of the ORC is lower than other CHP technologies, it requires very low maintenance work and thus very low O&M and personnel costs. In addition, organic fluids, thanks to their high molecular weight, have low enthalpy drop in the expander and, as a consequence, higher mass flow rates, if compared with water. Higher flow rates implies the use of larger turbines and therefore the effect of gap losses, fluid-dynamic losses and all the other machine losses are proportionally reduced. The overall efficiency of an ORC turbine is greater than 90 % and the performance is not particularly penalised at part load (Turboden 2014; Exergy 2014). However, its capacity to generate mechanical work is affected by the choice of the organic working fluid, the ORC configuration and the setting of the operating parameters; all these choices have to be determined accordingly with the specific application (Branchini et al. 2013; Algieri and Morrone 2013; Peris et al. 2014). Nevertheless, the investment cost is rather high and this is the main obstacle to an extensive use of this technology. Moreover, the power-to-heat ratio is usually lower than 0.25, therefore, a large share of heat should be valorised to make this technology competitive (Quoilin et al. 2013)

As far as efficiency is concerned, the main nominal specifications of each system are declared by the manufacturer. However, the performance in real operation could differ considerably from the nominal one due to the custom installation and the matching between heat supply and heat demand. Moreover, the national energy policy, with the subsidization of electricity production from power plant based on non-photovoltaic renewable sources (Ministry of the economic development 2012), distorts the value of electricity and heat, strongly promoting electricity generation and penalising heat valorisation (Prando et al. 2014a). As a consequence, CHP systems with low, or even negative, primary energy saving could have positive business plans. In this perspective, there is a substantial potential for the improvement of the energy performance of all the technologies. The ORC has a low power-to-heat ratio but a satisfactory performance at partial load that favours heat load tracking (Rentizelas et al. 2009; Dong et al.2009). However, the subsidisation of electricity production, as previously mentioned, encourages the maximisation of the electric output of the ORC generator even if the heat share is not completely exploited (Noussan et al. 2013).

Besides the CHP plant technology, district heating (DH) systems play a key role in promoting large scale renewable energy integration and can improve the matching of heat supply to heat demand. Furthermore, the determination of the proper size of the plant, depending on the annual heat demand profile, is essential to achieve a high annual average efficiency (Sartor et al. 2014; Barbieri et al. 2012; Brandoni and Renzi 2014).

The current energy infrastructure in South Tyrol (Italy) includes more than 70 plants based on woody biomass, most of them supplying heat to residential districts (Agency for environment of the Autonomous Province of Bolzano 2014). The thermal power of these plants ranges from 100 kW to 10 MW and most of them are based on direct combustion. So far, 12 plants operate an ORC generator, and some others are based on fixed bed gasifiers coupled with an internal combustion engine for the combined generation of heat and power. As a case study, a CHP system in Renon in South Tyrol is considered whose mass and energy balance of the CHP system − based on an ORC generator coupled with a biomass boiler – is presented. The assessment has been carried out experimentally, monitoring the fluxes of energy and mass, and supplemented with the modelling of the ORC generator. The main energy parameters of the system were monitored for a whole year of operation and the input biomass of the boiler was measured twice at two different power loads. The results highlight the present performance and the main losses of the plant. The potential improvements of the energy performance are also discussed. A thermodynamic model, calibrated to simulate the ORC operation, was developed in Matlab-Simulink environment using REFPROP 9 software; it allows us to predict the potential improvements of the ORC generator performance considering different management strategies of the system. In particular, the potential improvement of electric efficiency, due to the reduction of the average DH network temperature, is presented. Furthermore, electricity consumption of the plant auxiliaries is shown in detail. Finally, the impact of the subsidisation on the performance of the plant is discussed.

2.1 Materials and methods

2.1.1 CHP system layout

The CHP plant, considered in the present monitoring activity, is located in Renon (Bolzano, Italy). It is connected to a DH network delivering heat to 250 users of different sizes (single buildings, apartment houses and hotels). The network length is about 23 km of steel pipe for a total water volume of approximately 500 m^3. The nominal DH supply temperature is 90 °C and the DH return temperature depends on the users' demand and on the DH pump management.

The CHP system consists of a biomass boiler, an ORC generator and a biomass dryer (see Fig. 2.1). The boiler is a moving grate furnace − with a nominal power of 5.9 MW_{th} − fed with wood chips (G30-G50), mainly spruce forest residues from the surroundings (70 %) and a small share of wood waste from sawmills (30 %). The feedstock is pre-treated in the drying section till the water content is in the range 15–25 % on a wet basis. Woodchips are loaded into the boiler by means of racks moved by hydraulic cylinders that operate at regular time intervals. The output ash from the combustion is collected and properly disposed. The generated heat is entirely delivered to the ORC section by means of thermal oil, with a supply temperature of 310 °C and a return temperature of 240 °C, at nominal condition.

Fig. 2.1 – Biomass boiler, ORC generator and biomass dryer (from left to right).

The ORC generator is based on the traditional Rankine cycle and it is operated with octamethyltrisiloxane (MDM), which is the organic fluid employed in most of the large scale commercial ORC plants. The thermo-physical properties of the octamethyltrisiloxane make it particularly suitable for low temperature heat sources such as biomass combustion. Furthermore, the system is equipped with a regenerator to improve the efficiency of the thermodynamic cycle and with a split system that permits a more efficient utilisation of the thermal power by the boiler (i.e. increase of the boiler efficiency) and maximises the electric power production (Bini and Manciana 1996; Duvia and Guercio 2009). At nominal condition, the ORC generator produces 1.0 $MW_{el,net}$ and 4.8 MW_{th}. In the investigated plant, the electricity is completely delivered to the national grid and the thermal power, discharged by the thermodynamic cycle, is used for both the DH network and the biomass dryer. The dryer is connected in series, downstream from the heat exchanger of the DH network, therefore it is fed at a lower temperature (see Fig. 2.2).

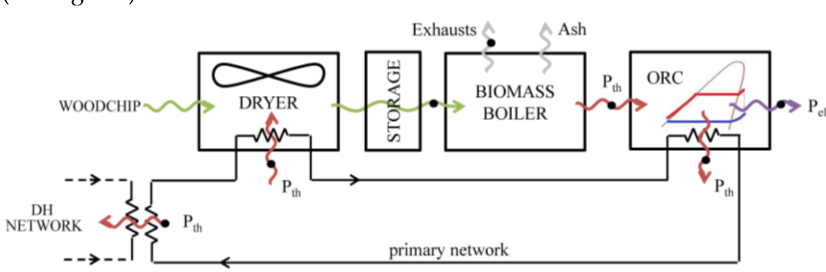

Fig. 2.2 – Layout of the CHP plant (the monitoring points are highlighted with black dots).

2.1.2 Monitoring setup

The CHP plant was analysed in detail and both energy and mass balances were carried out with the aim of determining the performance of the system in real operation. The plant was monitored for two different power loads: 79 % and 94 % of the nominal power, respectively. The monitoring was carried out for 4–6 hours under steady-state conditions. In this time span, the following parameters were measured and recorded: mass rate and moisture of woodchips, generated electricity and mass flow and temperatures (supply and return) of thermal oil (boiler-ORC circuit) and condenser cooling water (ORC-DH/dryer circuit). The woodchip input was weighed with a balance having a load range of 0–50 t and a measurement uncertainty of ± 20 kg (k=2). The thermal power production was measured by means of a multi-functional integrator (Supercal 531 – Sontex) that combines two resistance thermometers and a static fluidic oscillator flow meter. The instrumentation has an accuracy of the energy measurement chain that is in accordance with the strictest limit stated in UNI EN 1434-1:2007.

Table 2.1 – Specifications of the different measuring devices.

Parameter	Instrument	Range	Uncertainty (k=2)
Biomass mass	balance	0–50 t	± 20 kg
Moisture	Humimeter BMA	5–70 %	± 1.0 %
C, H, N	Perkin Elmer 2400 series II	-	± 0.3 %
Ash fraction	Zetalab ZA	-	± 0.21 %
Heating value	IKA C5000 c.p. 2/10	-	± 0.2 MJ kg^{-1}
Thermal power	SONTEX Supercal 531	-	± $(3+4\cdot\Delta T_{min}/\Delta T+0.02\cdot Q_{nom}/Q)$ %
Temperature	PT100	2–200 °C	± (0.15+0.002·T) °C
Thermoil temperature	Thermocouple k	0–375°C	± 2.5 °C
Electric power	HT PQA820	10–200 A	± (0.7 % reading + 0.03) kW
CO	MRU vario plus industrial	0–2000 ppm	± 10 ppm
CO_2		0–3 % vol.	± 0.5 % reading
O_2		0–21 % vol.	± 0.2 % vol. abs

The electricity production of the ORC generator was recorded from the meter integrated in the plant and the electricity consumption of the main auxiliaries was measured by means of a power analyser (HT PQA820). The output ashs was not measured because several conveyor belts are used, and it was not possible to determine, with a satisfactory accuracy, the ash discharged during the monitoring. The amount of produced ash was estimated indirectly by means of the amount of woodchips at the inlet of the boiler and by means of the ash content determined through a proximate analysis. In order to assess the energy and mass balances, a set of analyses was carried out on the feedstock (in accordance with the reference normative), moisture content (EN 14774: 2009), heating value (EN 14918: 2010) and ash content (EN 14775: 2010); see Fig. 2.3. Three samples of the feedstock were collected for each monitoring, according to EN 14778: 2011 standard. Table 2.1 reports the specifications of the abovementioned instruments.

Fig. 2.3 – Measurement of water content in a oven, heating value in a calorimeter and ash content in a muffle (from left to right).

The electric and thermal efficiencies of the CHP system were calculated as a ratio between the input and the output energy in the time span of the monitoring. Electrical efficiency is calculated considering the net electricity production.

$$\eta_{el,net} = \frac{E_{el} - E_{aux}}{m_b \cdot LHV_b} \quad (1)$$

$$\eta_{th} = \frac{E_{th}}{m_b \cdot LHV_b} \quad (2)$$

where E_{el} refers to the gross value, while m_b and LHV_b refer to the test fuel on "as received" basis. The power-to-heat ratio was calculated as a ratio between the gross electric power and the thermal power generated by the plant. The combined standard uncertainties of the abovementioned indexes was determined in accordance with the guide for the expression of uncertainty in measurement (ENV 13005:1999).

Boiler efficiency was calculated using an indirect method that implies the measurement of the losses occurring in the boiler. In order to determine the losses, the temperature and the main compounds in the flue gases was measured. A gas analyser (MRU vario plus industrial) was used to measure O_2 (with electrochemical cell), CO and CO_2 (with non-dispersive infrared sensor) content in the combustion flue gas. The detailed equations for the determination of the boiler efficiency are reported below:

$$\eta_{th,boil} = 1 - (f_A + f_B + f_U + f_D) \tag{3}$$

$$f_A = \frac{\left(t_{fg} - t_{room}\right) \cdot \left[\frac{c_{pmd} \cdot \left(C_b - C_{res}\right)}{0.536 \cdot \left(CO + CO_2\right)} + c_{pmw} \cdot 1.224 \cdot \left(9H + w\right) \right]}{LHV_b} \tag{4}$$

$$f_B = \frac{12644 \cdot CO \cdot \left(C_b - C_{res}\right) / \left(0.536 \cdot \left(CO + CO_2\right)\right)}{LHV_b} \tag{5}$$

$$f_U = \frac{335 \cdot C_r}{LHV_b} \tag{6}$$

$$f_D = \frac{\alpha \cdot S_{boil} \cdot \left(t_{surf,boil} - t_{room}\right)}{LHV_b} \tag{7}$$

where LHV_b refers to the test fuel on an as received basis.

The ORC generator has several measuring probes embedded in the plant that are used to monitor the performance of the system. Besides the electricity production, the temperature and the pressure of the ORC working fluid in different section (condenser, regenerator, evaporator and turbine) were recorded. These data allow a detailed evaluation of the thermodynamic behaviour of the plant as well as the nominal and the part load operation of the turbine, as it will be described in section 2.3.

Moreover, input thermal power – supply ($T_{s,oil}$) and return ($T_{r,oil}$) temperatures and oil mass flow ($\dot{m}_{oil}$) –, output thermal power – supply ($T_{s,w}$) and return ($T_{r,w}$) temperatures and water mass flow ($\dot{m}_{w}$) – and the electric power (P_{el}) were measured and recorded for the whole year 2012 with a time step of 1 minute (see Fig. 2.4). This dataset enables us to obtain a complete overview of heat utilization and the correlation between electric/thermal power and the average network temperature. The collected data was pre-processed to filter data corresponding to either unexpected or planned outages of the plant due to detected anomalies or to the maintenance program (scheduled twice a year) that cause temporary stoppage of the plant and, consequently, lack of data.

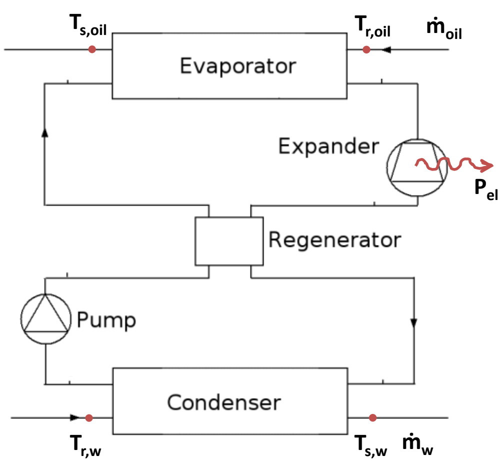

Fig. 2.4 – Layout of the ORC generator (the monitoring points are highlighted with red dots)

2.1.3 ORC generator model

The ORC generator under analysis was modelled through a thermodynamic approach that involves the main operating parameters. The biomass boiler supplies the required heat to the thermal oil which is pumped to the economizer and to the evaporator of the ORC module; in these heat exchangers the working fluid is pre-heated and vaporized respectively. Downstream of the evaporator, the vapour expands in a turbine, which is directly connected to a synchronous electric generator rotating at a constant speed of 3000 rpm. After the expansion, vapour flows to a regenerator and then in the condenser; the thermal power rejected by the condenser is used to heat the water flow in the primary circuit of the DH network. The thermodynamic cycle is finally closed when the liquid organic fluid is pumped to the evaporation pressure and flows to the heat regenerator. The thermodynamic properties of the working fluid (MDM) were provided by the REFPROP 9 software (NIST 2012). The described model of the generator allows an interesting evaluation and a sensitivity analysis on the performance of the system.

As a reference, the thermodynamic cycle of the modelled ORC plant is reported in Fig. 2.5 for the nominal operating conditions (i.e. for an electric power output of 1 $MW_{el,net}$). The cycle involves the following processes: the MDM is pumped from low to high pressure and it then enters the HRVG (i.e. pre-heater, evaporator and super-heater) where it is heated at constant pressure to become a dry saturated vapour (1–3); the dry saturated vapour expands through the turbine which drives the electric generator (3–4); the outlet vapour flows through the regenerator where enthalpy recovered from vapour cooling (4–cond) is used for liquid pre-heating (1–r); finally, the vapour enters the condenser where it is condensed at a constant pressure to become ~~a~~ saturated liquid (4–1). A more detailed description of each single state will be presented below. As a reference state, both enthalpy and entropy are set to zero for the saturated liquid at the normal boiling point.

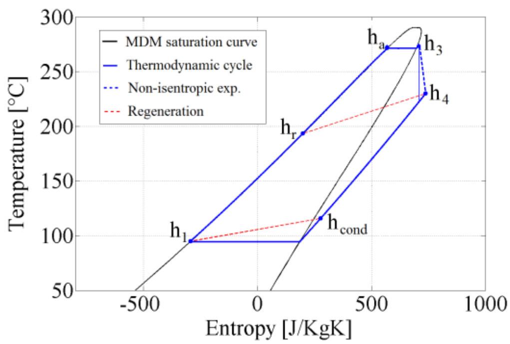

Fig. 2.5 – T-S diagram of the organic Rankine cycle with regeneration

The ORC working parameters are collected for different operating points at nominal load and part load with the aim of defining a proper model of the system. In order to fully define the Rankine thermodynamic cycle the following parameters must be known: condensing pressure (p_c), vapour evaporating pressure (p_v), superheating maximum temperature (t_3), pinch point temperature (t_{pp}) at the heat recovery vapour generator (HRVG). The thermal oil inlet and outlet temperatures at the HRVG are recorded, thus it is possible to evaluate the thermal power that is fed to the vapour cycle as:

$$P_{th,to} = \dot{m}_{to} \cdot c_{p,to} \cdot \left(t_{to,in} - t_{to,out} \right) \qquad (8)$$

The evaporation temperature and pressure of the thermodynamic cycle were monitored by the plant control system. Combining this data with the measured temperature of the thermal oil it was possible to define both the pinch point and the corresponding thermal oil and MDM temperatures; the pinch point is particularly important for the evaluation of the heat exchange between the thermal oil and the working cycle; its value in nominal condition is 20 °C. The pinch point occurs at the inlet of the evaporator; therefore the MDM mass flow rate can be evaluated as:

$$\dot{m}_V = \frac{P_{th,pp,to}}{h_3 - h_a} \qquad (9)$$

The experimental measurements show that a superheating of about 3 °C is adopted in the boiler to ensure the complete evaporation of the working fluid; thus the enthalpy of point h_3 does not lie exactly on the saturation vapour curve, but in the superheat region.

Given these evaluations, Fig. 2.6 reports the heat exchange graph of the thermal oil and the MDM during the pre-heating and evaporating process, in nominal conditions. MDM reaches a temperature of around 275 °C with a pressure of 1060 kPa and the conveyed thermal power is about 5.9 MW_{th}. Thermal oil enters the heat exchanger at about 310 °C with a mass flow rate of 34.5 kg/s.

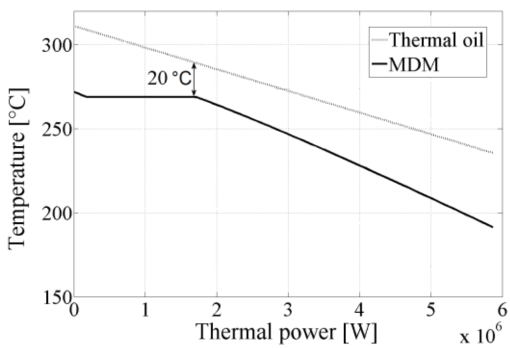

Fig. 2.6 – Thermal oil and MDM temperatures at the ORC plant boiler

The silicon oil vapour is then expanded in the turbine which is an impulse machine directly connected to a synchronous electric generator rotating at a constant speed of 3000 rpm. Thanks to the availability of the experimental temperature and pressure of the MDM at the inlet and the outlet of the expander, it was possible to assess a nominal isentropic efficiency of the turbine of 80 %.

The electric power produced by the turbine is:

$$P_t = \dot{m}_v \cdot (h_3 - h_4) \cdot (\eta_{el,t} \cdot \eta_{m,t}) = \dot{m}_v (h_3 - h_{4,is}) \cdot (\eta_{is,t} \cdot \eta_{el,gen} \cdot \eta_{m,t}) \qquad (10)$$

In order to extend the experimental results and to define an off-design model of the system, the turbine isentropic efficiency was assessed according to the equation proposed by Keeley (1988) which was also used by (Calise et al. 2014; Gabbrielli 2012]:

$$\eta_{is,off} = \eta_{is,d} \sin\left[0.5\pi\left(\frac{\dot{m}_{v,off}\,\rho_d}{\dot{m}_{v,d}\,\rho_{off}}\right)^{0.1}\right] \tag{11}$$

The vapour at the turbine outlet is used to preheat the liquid siloxane to the enthalpy value h_r (see Fig. 2.5), by means of a regenerator. Vapour cools down through the regenerator so the enthalpy of the siloxane at the inlet of the condenser is h_{cond}. The regenerated thermal energy fed to the liquid MDM can be evaluated as:

$$P_{th,reg} = \dot{m}_V \cdot (h_r - h_1) = \dot{m}_V \cdot (h_4 - h_{cond}) \tag{12}$$

Since the temperature and the pressure at the inlet and the discharge of the regenerator are known from the measurements, it was possible to evaluate the regenerator efficiency (ε):

$$\varepsilon = \frac{h_r - h_1}{h_4 - h_1} \tag{13}$$

which, in nominal condition, is 0.73.

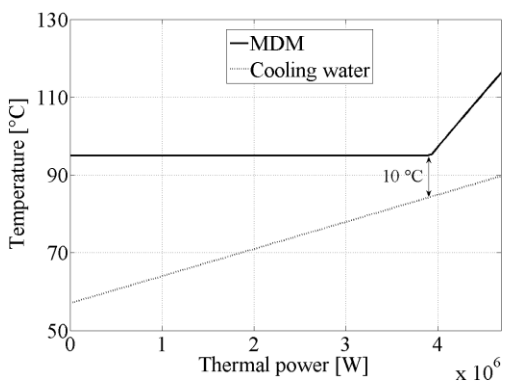

Fig. 2.7 – Thermal oil and MDM temperatures at the ORC plant condenser

Downstream from the regenerator, vapour enters the condenser and is used to exchange heat with the primary circuit of the DH section. With a similar procedure to that presented for the evaporating section, the heat exchange graph (Fig. 2.7) is also evaluated for the condensing section. Condensing pressure and temperature closely depend on the temperature of the cooling fluid according to the formula:

$$t_c = t_{cf,pp} + \tau \tag{14}$$

The water temperature of the primary DH circuit and the water mass flow rate are known from the measurements, so the siloxane condensing pressure can be evaluated by defining the temperature difference in the condenser at the pinch point. In accordance with the experimental data, the pinch point in the condenser is 10 °C in nominal operating conditions. The thermal power recovered at the condenser can be defined as:

$$P_{th,c} = \dot{m}_V \cdot (h_{cond} - h_1) \tag{15}$$

The trend of the temperature of the MDM and the cooling water and the thermal heat exchanged at the condenser are presented in Fig. 2.7 for the nominal working conditions.
The thermodynamic cycle is closed by the pumping process that allows the MDM pressure to be increased from the condensation to the evaporation value. The power consumption of the pump can be calculated as:

$$P_p = \dot{m}_v \left(h_2 - h_1\right) / \left(\eta_{el,p} \eta_{m,p}\right) = \dot{m}_v \left(h_3 - h_{4,is}\right) / \left(\eta_{is,p} \eta_{el,p} \eta_{m,p}\right) \tag{16}$$

The pump is controlled in part load conditions by an inverter that regulates the rotational speed according to the required evaporation pressure and siloxane mass flow rate.
In conclusion, the net electric power output of the ORC process is:

$$P_{el,ORC,net} = \left(P_{el,t} - P_{el,p}\right) \tag{17}$$

Table 2.2 reports the assumptions that were made in terms of components' and machines' efficiency.
The model was validated with the acquired experimental data and it allows us to perform some evaluations on the performance of the system under varying operating conditions. As an example it is possible to calculate the electric performance of the ORC plant as a function of the evaporating pressure of the MDM. At the same time, a sensitivity analysis of the condensing

pressure can be performed in order to define the performance loss of the system with increasing condensing temperature.

Table 2.2 – Machines' and components' efficiency assumptions for the ORC plant model

Assumed efficiencies	Symbol	Value
Pump isentropic efficiency	$\eta_{is,p}$	0.70
Electric generator efficiency	$\eta_{el,gen}$	0.97
Pump electric motor efficiency	$\eta_{el,p}$	0.90
Pump mechanical efficiency	$\eta_{m,p}$	0.98
Turbine mechanical efficiency	$\eta_{m,t}$	0.98

2.2 Results and discussion

2.2.1 ORC generator

The model of the ORC generator was calibrated on the nominal load, however it shows prediction capabilities also at partial load. The comparison between the experimental data and the modelling data of the ORC generator is reported in Table 2.3. The table compares the main key parameters of the ORC generator at two different power loads of the plant. The average deviation between measured and modelling values is about 4 %.

Table 2.3 – Comparison between experimental and modelling data of the ORC generator.

	Part load 1		Part load 2	
	Meas.	Model	Meas.	Model
$P_{el,net}$ (kW)	828	820	556	560
P_{th} (kW)	4148	4131	3386	3320
p_{evap} (kPa)	966	930	716	630
p_{cond} (kPa)	19.8	19.2	21.8	20.9
t_3 (°C)	271.7	265.9	251.4	243.5

The electric efficiency of the ORC generator strongly depends on the evaporation pressure (spanning from 100 kPa to 1400 kPa) as reported in Fig. 2.8; these results are obtained by means of the ORC generator model. The efficiency curves do not show a linear increasing trend with the evaporation

pressure, but they progressively flatten. This trend resembles the theoretical thermodynamic Rankine cycle with constant condensation conditions and progressively increasing evaporation pressure. Moreover, the inefficiencies of the real thermodynamic cycle amplify the curve flattening. The dotted vertical line, depicted in Fig. 2.8, represents the nominal evaporation pressure of the plant, which is 1060 kPa (evaporating temperature of 272 °C). The electric efficiency is calculated for different values of the condensing temperature and the solid black line refers to the nominal condensing condition of 95 °C (condensing pressure of 16.5 kPa). The other curves refer to higher condensing temperatures, which usually occur during the operation of the plant in summer months, and to lower condensing temperatures, that could be achieved by decreasing the DH network temperatures.
At the nominal evaporation and condensing pressure, the net electric power produced by the ORC generator is about 1 $MW_{el,net}$. Higher evaporating pressures ensure a slight increase in the electric efficiency but significantly higher thermal oil temperatures and working fluid pressures are required. The net electric efficiency of the ORC generator reaches its maximum value (i.e. 17 %) in nominal operating conditions and it is significantly influenced by the condensing temperature and poorly affected by the evaporation pressure over the nominal condition.

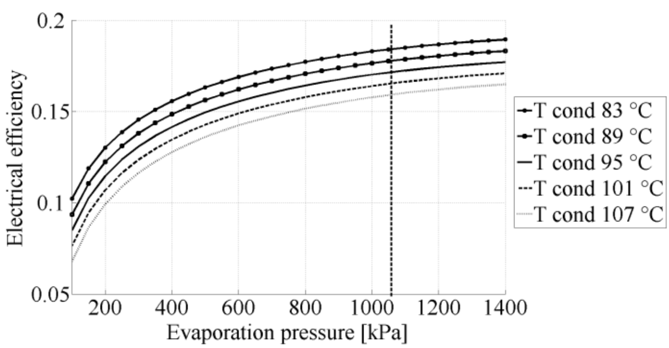

Fig. 2.8 – Net electric efficiency of the ORC generator as a function of the evaporating pressure and the condensing temperature

The experimental data collected for the whole year 2012 highlighted a correlation among ORC electric efficiency, electric load and mean temperature of the

primary network. Fig. 2.9 shows the experimental data of the whole year 2012 (data points whose colour represents the fraction of the total electric load), the trend line of the experimental data (dotted curve) and the operating curves at constant electric load simulated with the ORC model (solid curves). First of all, the graph highlights the efficiency penalisation when the ORC generator is operated at partial load. The plant is operated in order to track the heat load; however, partial load operation corresponds to higher temperature of the primary network because the plant management strategy aims to increase the discharged heat, in order to maximise electricity production. This management strategy is a consequence of the Italian subsidisation policy for plants based on renewable energy, such as biomass (Ministry of Economic Development 2012). The subsidy consists of a high feed-in tariff on the electricity generated by the plant – the main share of the incentive − and a bonus for the electricity generated in high efficiency cogeneration (Ministry of Economic Development 2011) – a negligible share of the incentive. Further information about the influence of the subsidisation on the business plan of a biomass CHP plant is reported in literature (Prando et al. 2014a).
The solid curves, reported in Fig. 2.9, represent the simulated operating curves at different electric loads (i.e. 0.4, 0.6, 0.8, 1) that have been determined through the developed model. The graph highlights that, for a pre-fixed electric load, higher values of the ORC electric efficiency can be reached by decreasing the mean temperature of the primary network. As the mean temperature of the primary network reduces, also the condensing temperature – and therefore the condensing pressure − of the thermodynamic cycle decreases and thus the specific work of the cycle grows. As an example, a reduction of 10 °C of the mean primary network temperature would lead to an increase in the electric efficiency of the ORC generator of about one percentage point. Nevertheless, the reduction of the network temperature is a measure that has to be assessed with an integrated approach considering the entire DH system (from the generating plant to the final users); the minimum network temperature depends on the characteristics of the buildings connected to the DH system (Prando et al. 2014a).

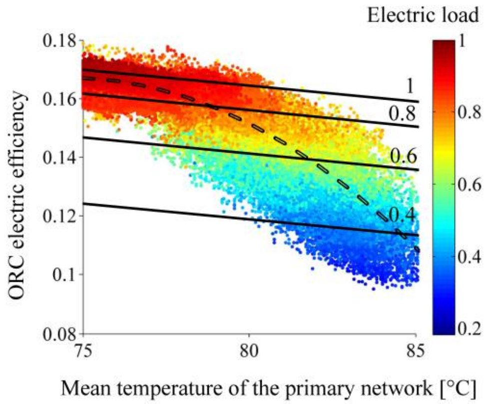

Fig. 2.9 – Net electric efficiency of the ORC generator as a function of the mean temperature of the primary network and the electric load; experimental data (dots), trend line of the experimental data (dotted curve) and operating curves at constant electric load simulated through the model (solid curves).

2.2.2 Monitoring activity

The monitoring of the entire system, including the measurement of the input biomass into the boiler, was carried out at two different power loads: 79 % and 94 %. The results of energy and mass flow measurements, complemented with their expanded uncertainty, are reported in Table 2.4. The uncertainty on the evaluation of the generated ash is rather high because the ash production was indirectly calculated, as mentioned in section 2.2. The biomass, delivered to the plant by the local farmers, has a water content between 20 % and 60 % and after the drying process it reaches a value of around 15 %. In accordance with the legislation in force in South Tyrol, ash is a by-product of the plant that has to be disposed and, according to the manager of the plants, its disposal cost is around 150 EUR t^{-1}.

The energy performance, calculated as stated in section 2.2, is reported in Table 2.5. However, quality of woodchips − moisture content, feedstock typology, particle size, ash content, heating value, etc. − can influence the yield of the system. Electric efficiency has been calculated as net value, considering the consumption of the auxiliaries. The comparison of the efficiency at different power loads highlights that the plant performance is not particularly penalised at partial load. This is mainly due to the ORC generator that preserves its efficiency at partial load.

Table 2.4 – Experimental measurement of the energy and mass input/output of the plant (uncertainty refers to k=2).

	Power load (%)	
	79	94
Gross electric power (kW_{el})	837 ± 6	996 ± 7
Auxiliaries consumption (kW_{el})	261 ± 2	286 ± 2
Thermal power (kW_{th})	4160 ± 3	4709 ± 3
Input power (kW_{th})	6290 ± 110	7140 ± 127
Biomass consumption (“as received”) ($kg\ h^{-1}$)	1454 ± 20	1703 ± 20
Biomass water content on wet basis (%)	14.4 ± 1.0	15.6 ± 1.0
Biomass LHV on “as received” basis ($MJ\ kg^{-1}$)	15.6 ± 0.3	15.1 ± 0.3
Ash production (on dry basis) ($kg\ h^{-1}$)	11.2 ± 5.2	11.5 ± 6.0

Table 2.5 – Experimental measurement of the plant main indexes of energy performance (uncertainty refers to k=2).

	Power load (%)	
	79	94
Net electric efficiency (-)	0.091 ± 0.003	0.099 ± 0.003
Thermal efficiency (-)	0.662 ± 0.012	0.660 ± 0.012
Power-to-heat ratio (-)	0.201 ± 0.001	0.212 ± 0.001

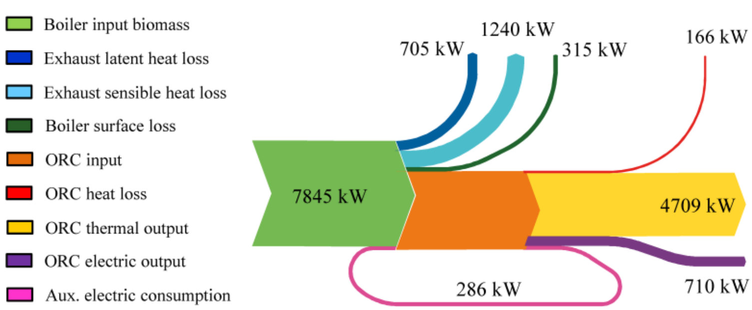

Fig. 2.10 – Sankey diagram of the system at 94 % power load.

The energy balance of the plant, operated at 94 % power load, is shown in detail in Fig. 2.10. The biomass input power was calculated using the HHV of biomass (i.e. 16.6 MJ kg^{-1} "as received" basis). The exhaust latent thermal power (705 kW) accounts for 9 % of the boiler input power on HHV basis. This share refers to the thermal power required to vaporise both the water content of biomass (25 %) and the water produced during the oxidisation of the hydrogen in the biomass (75 %). The exhaust sensitive thermal power (1240 kW) is due to the discharge of the hot flue gases at the chimney, at a temperature of around 240 °C, which accounts for 16 % of the boiler input power on HHV basis. The boiler surface losses (315 kW) account for 4.0 % of the boiler input power on HHV basis. The gross efficiency of the boiler is around 78 % on LHV basis and 71 % on HHV basis. A further exploitation of both sensitive and latent exhaust heat could considerably improve the efficiency of the boiler. The potential would be larger if integrated with the reduction of the network temperature. The chemical heat loss in the flue gases and the heat loss due to combustible constituents in the residues were detected to be a negligible share (<0.05 %) and are not reported in Fig. 2.10. The CO content in the flue gases was around 20 ppm at 10 % oxygen concentration. The ORC thermal loss (166 kW) accounts for 2.1 % of the boiler input power on HHV basis. The electricity consumption of the auxiliaries (286 kW) is 29 % of the gross electric power. Finally, the useful net power shares are the ORC electricity output (710 kW) and the ORC thermal output (4709 kW) that account respectively for 9.1 % and 60 % on HHV basis, and 9.9 % and 66 % on LHV basis.

The electricity consumption of the main auxiliaries was monitored and it is reported in Fig. 2.11. At nominal power load, the electric self-consumption is around 300 kW_{el}; therefore it is 28 % of the ORC output electric power. Almost 65 % of the electricity consumption is due to the following four auxiliaries; the organic fluid pump of the ORC generator (20.0 %), the extractor of the boiler flue gases (19.9 %), the thermal oil pump to exchange heat from the boiler to the ORC section (12.6 %) and the fan of the condensation section (10.9 %). The condensation section is also used to partially condense the water in the flue gases and dilute them with fresh air in order to avoid the formation of plume at the chimney outlet; it is not used to recover the latent heat of the exhausts.

The auxiliaries' consumption has been monitored also at 60 % of the power load (summer season) and it accounted for 207 kW_{el} – i.e. 34 % of the ORC output electric power. The main auxiliaries are the same identified at nominal load with the exception that the condensation section fan is off, because there is no plume formation at the chimney in the summer season, and the ventilator of the biomass dryer section accounts for the 8.7 % of the total electric consumption (18.0 kW).
The thermal output of the ORC generator is used for both DH network and biomass drying. Fig. 2.12 shows the ORC thermal output (blue line) and the thermal power provided to the DH network (green line). The DH demand is displayed in the graph as cumulative curve while the ORC thermal output is plotted corresponding with the time series of the DH demand. A comparison between the two curves highlights that, on yearly basis, half of the produced heat (47 %) is used by the DH network. The remaining heat share (53 %) is delivered to the biomass drying section, that is operated when extra heat – not required by the DH network – is available. The dried biomass is properly stored in a covered storage to be used over the whole year. The dryer is fed in series, downstream from the heat exchanger of the DH network; therefore, it is fed at a lower temperature (70–80 °C). The drying section is manually operated in batch mode with consequent management inefficiencies. An automatic and continuous drying process would permit a considerable reduction of the drying heat share. The DH demand is higher than the ORC thermal output for a very short time span in the winter season and during the boiler/ORC maintenance period; in this case a backup diesel boiler is operated to meet the demand of the DH network.

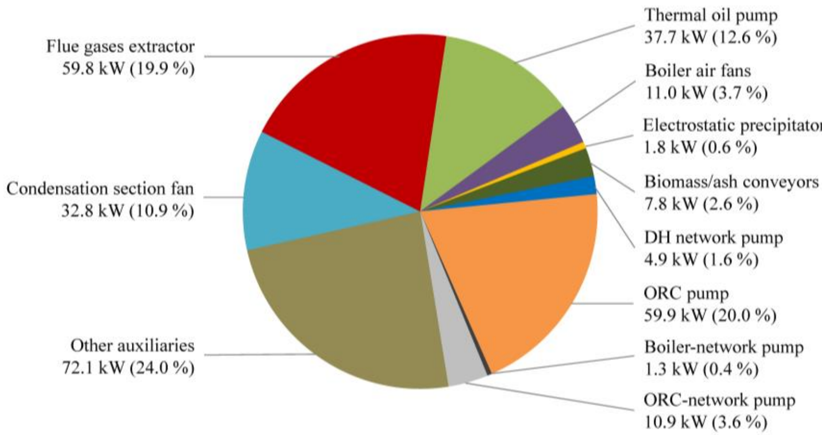

Fig. 2.11 – Auxiliaries electric self-consumption of the plant at nominal power load.

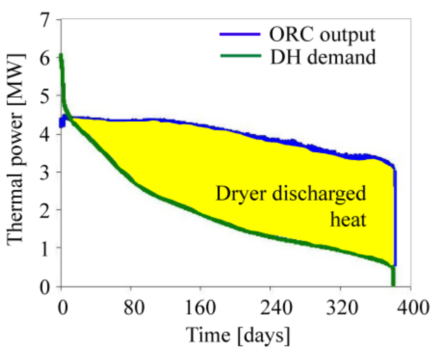

Fig. 2.12 – Thermal power generated by the ORC generator and supplied to the DH network for the year 2012.

2.3 Main findings

This study focuses on the monitoring of the energy performance of a biomass boiler coupled with an ORC generator in a DH context. The assessment was supplemented by means of a calibrated model of the ORC generator in order to carry out some predictions for different management strategies of the system. The monitored plant is a flexible system because its performance is not particularly penalised at partial load. As an example, the penalisation of the electric efficiency is around 8 % considering the plant operating at 80 % of the nominal power load. However, the subsidisation for renewable sources promotes the nominal load operation – discharging part of the cogenerated heat – in order to maximize electricity production. Since the maximum ORC plant load depends on the amount of thermal power that can be discharged, high network temperature is set to increase the rejected heat and thus the electricity production, even if the electric efficiency is penalized.

Numerical results are in good agreement with the monitored data, therefore the developed model shows some significant prediction capabilities. An evaluation of the sensitivity of the electric performance of the ORC plant at varying working conditions shows that the condensing temperature is the most significant parameter, while the evaporating pressure has a lower influence. For a pre-fixed electric load, higher values of the ORC electric efficiency could be reached by decreasing the mean temperature of the primary network. For example, a reduction of 10 °C of the mean primary network temperature would lead to an increase in the electric efficiency of the ORC generator of about one percentage point.

The analysis of the boiler losses highlighted that the exhaust latent thermal loss and the exhaust sensitive thermal loss account for 9 % and 16 % of the boiler input power, respectively. A further exploitation of both sensible and latent exhaust heat shares could considerably improve the efficiency of the boiler. However, this measure should be integrated with a reduction of the DH network temperature that would enable a higher heat recovery at lower temperature. The detailed analysis of the plant electricity consumption highlights that, at nominal power load, 65 % of the electric consumption is due to the following auxiliaries: flue gases extractor, thermal oil pump, ORC pump and condensation section fan. The installation of efficient devices would considerably contribute to reduce the electricity self-consumption. Furthermore, the fan of the condensation section operates only to avoid plume formation at the chimney, therefore the exploitation of the exhaust latent heat share would relieve its significant electric consumption.

More than 50 % of the ORC output heat is used to dry the woodchips; therefore, a further detailed analysis on the energy effectively used for the drying process would be essential to optimise the plant operation. In addition, driers' operation is not automated but it is manually handled in batch mode with consequent management inefficiencies. An automatic and continuous drying process would permit a considerable reduction of the drying heat share and a consequent improvement of the global efficiency of the system. Nonetheless, the subsidisation of electricity production greatly increases the value of electricity and does not optimise the valorisation of the generated heat. In this perspective, there is less interest to improve the efficiency of the drying section that is also operated as an air cooler which leads to an increase in the discharged heat and, therefore, electricity production.

3. CHP plant based on gasifier and ICE

Biomass-to-energy technologies are renewable and carbon neutral (Faaij et al. 1997), nonetheless a constant supply of the feedstock should be ensured in order to achieve continuous operation. It should be also noted that most of the thermal conversion technologies are feedstock-specific, in the sense that the design parameters, i.e. air input, temperature, retention time, are optimized for fuels of a specific range of parameters as size, moisture, fine matter content and heating value (Vakalis et al. 2013). Therefore, the corresponding technologies are developed in accordance with the available fuels, along with other factors such as economic incentives and local conditions (Vakalis et al. 2013). The supply of biomass for energetic utilization in future could also be "restricted" not only by competition for resources, but also by the application of the cascade principle which has been formulated by the EU forest strategy (SWD 2013). The cascade principle indicates that biomass should be utilized in the following order of priority: wood based products, re-use, recycling, bioenergy and disposal. The reasoning behind the cascade principle is that the life cycle of biomass should be maximized in order to ensure the viability of the bio-economy but also to bring some balance to the market due to subsidies in the bioenergy sector. Nonetheless, a counter argument is that the bioenergy sector utilizes mainly biomass of lower quality like various residues (forestry, industrial, harvesting) and low-quality wood. In addition, free markets tends to maximise the value of the production, thus the entrepreneur is in fact primarily interested in generating high added value products from the feedstock. A further highly discussed element of the cascade approach by Directive is also related to who will decide and how on which is the best use of the feedstock.

Considering the CHP systems based on biomass, boiler-ORC and gasifier-ICE are the most used technologies for sizes smaller than 1 MW_{el}. According to Rentizelas et al. (2009), ORC is a well proven and used technology with a lower investment cost and also lower operational and maintenance costs if compared to gasification. Quoilin et al. (2013) stated that gasification systems have an investment cost 75 % higher and a maintenance cost 200 % higher than ORC-based systems. On the other hand, boiler-ORC is considered to have a similar specific investment cost to gasifier-ICE, according to Wood and Rowlay (2011), and even higher according to Huang et al. (2013). Beyond the conflicting opinions, the authors agree that the investment cost has a considerable impact on the business plan for both the technologies. The net electrical efficiency of the ORC process is in the range of 6–17 % (Rentizelas et al. 2009); 17 % refers to ORC with a size of around 1 MW_{el}. According to Obernberger et al. (2002), the biomass ORC plant in Lienz (i.e. 1 MW_{el}) reaches a net electrical efficiency at nominal load of 18 %. The electrical efficiency of the whole system (i.e. boiler and ORC) is slightly lower than the above-mentioned values due to the efficiency of the boiler that is around 90 % (Obernberger et al. 2002). On the other hand, gasification systems are considered a promising technology in terms of electrical efficiency, but with a higher investment risk due to the lack of standardisation (Rentizelas et al. 2009). According to Dasappa et al., the overall electrical efficiency of a gasification system is in the range of 20 % at 100 kW_{el} to about 30 % at a MW level. This range of values is in accordance with the review carried out by Ahrenfeldt et al. (Ahrenfeldt et al. 2013). In 2009, Dong et al. (2009) stated that only few systems have been economically demonstrated at small scale. In 2013, Quoilin et al. (2013) stated that the gasification systems in operation are prototypes for demonstration purposes. Nowadays, several small scale gasifiers coupled with internal combustion engines (i.e. smaller than 1 MW_{el}) are successfully commercialized and used in several applications (Vakalis et al. 2013; Vakalis et al. 2014). However, some technical and economic issues have still to be addressed.

In order to compare the performance of gasification systems, technical standards have recently been developed (CTI 2013). European but also Italian standards and guidelines are currently adapting to the development of new innovative technologies, and have embraced the fact that biomass gasification has reached an important turning point, since it is also able to be applied to small plants which do not belong to the refinery industry but can be considered as co-generation plants.

3.1 Materials and methods

3.1.1 Plant layout

The CHP plant, chosen for the monitoring activity, is located in San Leonardo in Passiria (Bolzano, Italy). It is connected to a single-family house. The supply temperature is approximately 90 °C and return temperature depends on the user demand.

The CHP system is modular with two production lines in parallel composed of a biomass gasifier and an internal combustion engine (ICE). The gasifier is a downdraft gasifier (Joos-Gasifier design) with a nominal input power of around 200 kW_{th} (see Fig. 3.1). The woodchips − with water content lower than 15 % on wet basis − are conveyed through an air-tight loading auger to the reactor. The feedstock is a blend of the main species − spruce, larch, fir and pine − representative of the area in which the plant is located. The output char (i.e. solid carbonaceous residue) from the gasifier is collected and properly disposed. The ICE − 8 cylinders (V-shape) and 5.7 litres equipped with turbo-compressor – allows generating 45 kW_{el} and 120 kW_{th} (at rated conditions) (Spanner 2014). The thermal power is recovered with three heat exchangers in series; ICE coolant, exhausts cooling and producer gas cooling (see Fig. 3.2).

Fig. 3.1 – Gasification section of the investigated system.

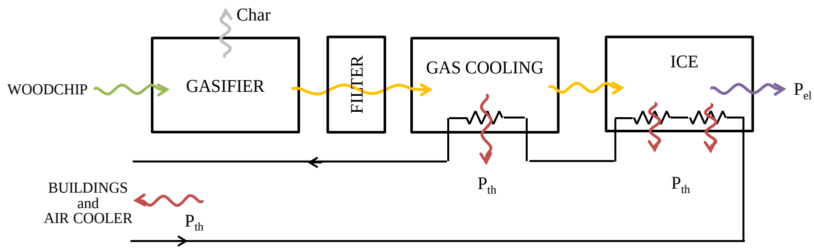

Fig. 3.2 – Layout of the power plant (gasifier-ICE).

3.1.2 Monitoring setup

The measuring and monitoring of the plant described in this chapter was carried out in accordance with the "Raccomandazione CTI 13". It is a draft guideline highlighting the aspects that have to be carefully evaluated during the contracting and commissioning of a gasification systems (i.e. classification, requirements, rules for bidding, ordering, construction and testing). The "raccomandazione CTI 13" was published by the Italian Thermo-technical Committee (CTI) for plants which produce and utilize producer gas obtained by gasification of ligno-cellulosic biomass (CTI 2013).
Input woodchips, thermal power (i.e. temperatures and mass flow) and electric power were recorded for around 5 hours. Woodchips are loaded by means of an auger that operates at regular time intervals. The monitoring time span has been established in order to neglect the loading buffer and have steady-state operation of the system. The input woodchips were weighed with a balance; 0–100 kg and accuracy 0.1 kg for the gasifier-ICE plant. The total amount of char has been collected in a sack and weighed in a balance (0–150 kg range, accuracy 0.05 kg). The thermal production has been estimated using temperature difference (in/out) on the hydraulic circuit and water volume flow rate (see Fig. 3.3). The temperatures were measured by means of thermocouples (type T) and the volume flow was measured by means of a transit-time ultrasonic flow meter (Riels AP5190-AP1090HT). Both the signals of thermocouples and flow meter have been acquired by means of a data logger unit (Agilent 34970A). The electricity production has been read on the meter set on the plant.

Fig. 3.3 – Monitoring of both electric power through a power analyser and thermal power through a flow meter and thermocouples (from left to right).

In order to assess energy and mass balances, a set of analyses was carried out on the feedstock; moisture content (EN 14774: 2009), heating value (EN 14918: 2010) and ash content (EN 14775: 2010). Three samples of feedstock were collected – at different times – in accordance with the EN 14778: 2011 standard. The electric and thermal efficiencies were calculated as a ratio between input and output energy in the time span of monitoring. The electricity consumption of the ancillary equipment was recorded by means of a power analyser (HT PQA820), as shown in Fig. 3.3. The electric and thermal efficiencies are calculated as:

$$\eta_e = \frac{E_e - E_{aux}}{m_b \cdot LHV_b} \tag{1}$$

$$\eta_t = \frac{E_t}{m_b \cdot LHV_b} \tag{2}$$

where E_e is the electric energy, E_{aux} is the electric self-consumption of the auxiliary equipment, E_t is the thermal energy, m_b is the amount of biomass, LHV_b is the lower heating value of the input biomass calculated on “as receive” basis.

The exergy concept could be used to assess the quality of energy. In the present case, exergy is a good indicator for the maximum amount of work that can be exploited from a stream (Perrot 1998). There are two main different types of exergy, physical and chemical (potential and kinetic exergy are almost negligible in this case). The former depends on the difference of the temperature and the pressure between the system and the environment. The latter is related to the type of the substances and their composition. As the different processes propagate, irreversibilities take place and decrease the maximum work that the system is able to exploit. A valid term of comparison could also be exergy degradation. The general equation for exergy calculation is the following:

$$B = h - h_0 - T_0 \cdot (s - s_0) \tag{3}$$

where B is exergy, h is enthalpy, s is entropy and T is temperature. The values h_0, s_0, T_0 are the relevant values at standard conditions. Physical exergy is highly dependent not only on the relative temperature and pressure of a stream, but also on the physical state of matter, i.e. for a perfect gas with a constant C_p the physical exergy is:

$$B_{ph} = C_p \cdot [(T - T_0) - T_0 \cdot (\ln \frac{T}{T_0})] + R \cdot T_0 \cdot \ln(\frac{p}{p_0})] \tag{4}$$

As mentioned above, chemical exergy is dependent on the composition. Relations developed by Morris and Szargut (1986), provide straightforward correlations of the substances and their heating value by a factor, known as β factor:

$$B_{ch} = \beta \cdot LHV \tag{5}$$

For biomass the β factor is:

$$\beta = \frac{1.0414 + 0.0177 \cdot [\frac{H}{C}] - 0.3328 \cdot [\frac{O}{C}] \cdot (1 + 0.0537 \cdot [\frac{H}{C}])}{1 - 0.4041 \cdot [\frac{O}{C}]} \tag{6}$$

For the calculations, char is considered to be graphite. Moreover, the chemical molar exergy of the gaseous compounds is also retrieved from tables (Morris and Szargut 1986). The chemical exergy of these substances is reported in Table 3.1.

Table 3.1 – Chemical exergy of substances (Morris and Szargut 1986).

Substance	Chemical exergy
Carbon Monoxide	275 kJ/mol
Hydrogen	236 kJ/mol
Methane	831 kJ/mol
Carbon (graphite)	410 kJ/mol
Carbon Dioxide	20 kJ/mol

The sum of chemical and physical exergy gives the overall exergy (if kinetic and potential exergy are negligible).

$$B = B_{ph} + B_{ch} \tag{7}$$

3.2 Results and discussion

3.2.1 Mass and energy analysis

The gasifier is constantly operated at nominal power load. However, quality of woodchips − moisture content, feedstock typology, particle size, ash content, heating value, etc. − can influence the capacity of the system. During the monitoring the CHP plant was operated at 95 % of the nominal power load.

Energy and mass flow data are reported for the monitored plant in Table 3.2. A share that accounts for the 8 % of the total heat is recovered in the gasification section − producer gas cooling − and the remaining share is recovered in the ICE − cylinder and exhausts cooling. However, only part of the generated heat is used, a considerable amount of heat (not measured) is discharged into the environment because the buildings connected to the plant have low heat demand for a large period of the year (e.g., summer time spring and autumn). Since the gasifier requires a low moisture content in the feedstock – which means higher purchase cost − a dryer section coupled with the gasifier could considerably improve the valorisation of the generated heat. The valorisation of heat is considered to be less important than electricity valorisation and this is due to the Italian subsidisation policy for plants based on renewable energy (Ministry of the economic development 2012). The subsidy consists of a high feed-in tariff on the electricity delivered to the national grid by the plant – main share of the incentive − and a bonus for the only electricity generated in high efficiency cogeneration (Ministry of the economic development 2011) – negligible share of the incentive. A study about the influence of subsidisation on gasification plants is reported in Prando et al. (2014).

Nowadays in South Tyrol, the discharged char has to be disposed of and, according to the manager of the plants, the cost is around 150 € t^{-1}. This substance is mainly composed of carbon (70 %) and the remaining share is mainly ash. It means that 2.4 % of the input energy of woodchips is disposed along with char.

Table 3.2 – Energy and mass input/output of the plant.

Power load (%)	95
Electrical power (kW_{el})	42.8
Auxiliary self-consumption (kW_{el})	6.8
Thermal power (kW_{th})	98.1
Input power (kW_{th})	196.3
Biomass consumption (kg h^{-1})	49.6
Biomass water content on wet basis (%)	6.6
Biomass LHV on "as receive" basis (MJ kg^{-1})	17.8
Char production (kg h^{-1})	0.74

The calculated energy performances are reported in Table 3.3. The self-consumption of the auxiliaries was measured and the electrical efficiency was calculated as net value. At the current stage of development, small scale gasification systems are designed to operate at nominal load in order to guarantee a proper quality of producer gas. Fig. 3.4 reports the energy flows of the CHP plant. The main loss is the thermal loss of the gasifier reactor that is roughly 22 % of the input energy.

Table 3.3 – Main indexes of energy performance.

Power load (%)	95
Net electrical efficiency (-)	0.183
Thermal efficiency (-)	0.499
Power-to-heat ratio (-)	0.436

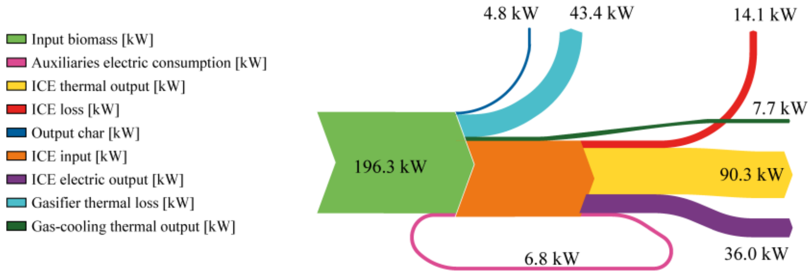

Fig. 3.4 – Sankey diagram for the energy flows of the plant.

3.2.2 Exergy analysis

In Fig. 3.5, the flow of exergy is shown. We observe significant exergy losses after each process due to irreversibilities. The low exergic content of generated heat streams is due to their relatively low temperature. Thus we could say that although the energy content in the heat streams is significant, its quality is relatively low. The major factor for the exergy losses is the heat transfer that takes place between the oxidation zone of the gasifier and the surroundings. Its contribution is particularly enhanced by the high temperature of the discharged heat. Moreover, the exergy loss in the CHP engine is also considerable.

The overall exergetic efficiency of the gasifier is calculated dividing the sum of chemical and physical exergy of the producer gas that exits the gasifier with the total exergy input. In this case it is around 63 %. Similarly, the exergetic efficiency of the whole plant is around 31 %.

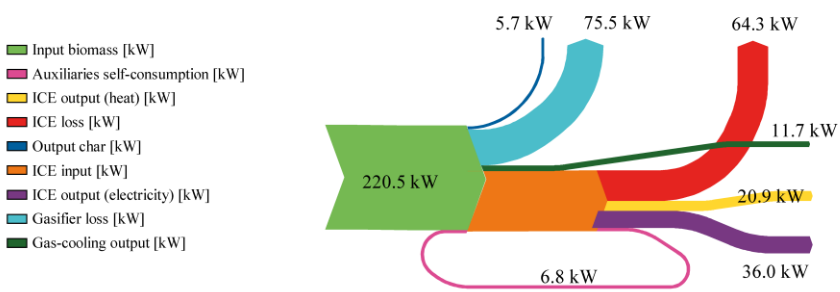

Fig. 3.5 – Flow of exergy and exergy losses (MJ h^{-1}).

3.3 Main findings

The net electric efficiency of the plant was measured as 18.3 % while thermal efficiency was measured as around 49.9 %. Nevertheless, small gasification systems are designed to operate at nominal load. It means they should be installed as base thermal load stations. The coupling of a biomass dryer section is considered a suitable option to improve the recovery of useful heat because of the low moisture content required by the gasifier. The discharged char has a disposal cost that could be tackled by the application of sustainable solutions which aim to valorise this by-product. It has a residual energy content (2.4 %) that make it attractive for further use in the energy chain.

The exergetic efficiency of the gasifier is 63 % while the one of the whole plant is 31 %. Although exergy is a useful concept when we want to pursue electricity production, this is not necessarily the case of cogeneration plants. Although the district heating stream has a relative low "energy quality" (exergy), the purpose is not only the production of mechanical work but also the transfer of heat, thus the exergy index cannot reflect the full extent of utilization possibilities for the output streams. As a support of the previous argument, biomass gasification has by-products, such as char, which are usually not utilized for either electricity or heat production, or could even have other applications (i.e. soil enhancer or pesticide absorbent on agricultural fields, filters, catalysts). Therefore, the performance of these kinds of co- or poly-generation plants should be estimated by means of a more integrated approach.

4. Critical issues on biomass-to-energy systems

Biomass can be converted into energy by means of different thermo-chemical processes such as combustion, pyrolysis and gasification. In particular, gasification is considered as an interesting process to expand the utilisation of biomass. Low-temperature air/steam blown biomass gasification enables the conversion of the solid fuel into a combustible gas commonly known as producer gas, while high temperature oxygen blown gasifiers generates so called syngas. The composition of the producer gas mainly depends on the feedstock characteristics and the conditions of the gasification process (i.e. temperature, gasifying agent, pressure, etc.) and the chemical/physical characteristics of the feedstock. As an example, the composition and the heating value of the producer gas depending on different oxidants is reported in Table 4.1 (Bocci et al. 2014; Sandeep and Dasappa 2014).

Table 4.1 – Producer gas composition with different oxidants (Bocci et al. 2014; Sandeep and Dasappa 2014).

	Composition (vol.%)					LHV
Oxidant	H2	CO	CO2	CH4	N2	(MJ Nm^{-3})
Air	9–10	12–15	14–17	2–4	56–59	3–6
Oxygen	30–34	30–37	25–29	4–6	-	10–15
Steam/CO2	24–50	30–45	10–19	5–12	-	12–20
Oxy-steam	45–51	13–25	15–20	1–4	-	7–10

The producer gas can be used in different prime movers (i.e. internal combustion engine, gas turbine, fuel cell) for the combined production of heat and power. The producer gas has a high potential to replace fossil fuel for decentralised energy generation, but it contains some undesired compounds (e.g., tar, particulate, fly ash, etc.) that have to be reduced in order to guarantee a proper operation of the prime mover.

The presence of tar in the producer gas is one of the main technology barriers for the development of the gasification systems (Asadullah 2014; Ruiz et al. 2013). Tar is a bituminous oil present in the producer gas in vapour phase that is difficult to remove with a simple condensation and it causes the clogging of filter and valves and the corrosion of the metallic components (Anis and Zainal 2011). The tar limit depends on the utilisation of producer gas in downstream applications. The internal combustion engine is considered to be more tolerant to tar than the gas turbine. The tar limit is around 100 mg Nm^{-3} for internal combustion engines using naturally aspirated while it is 5 mg Nm^{-3} for turbocharged engines and gas turbines (Milne and Evans 1998; Hasler and Nussbaumer 1999; Spliethoff 2001). The solid oxide fuel cells are not particularly sensitive to tar content in the producer gas (Hofmann et al. 2009) but desirable to have lower tar. Nevertheless, the effect of the fuel gas impurities on fuel cells is not well documented in scientific literature.

Besides the determination of the tar content limit, it is essential to identify the compounds that are critical for the operation of the system. As an example, the internal combustion engine is particularly sensitive to heavy tar, which creates deposition in the engine manifold and on the cylinder wall. PAH compounds do not cause deposition problem but can impact on the pollutant emissions of the engine exhausts and on the waste water of the gas conditioning (Hasler and Nussbaumer 2000). Milne and Evans (1998) defined the rule of thumb for the production of tar depending on the gasifier design: updraft at 100 g Nm^{-3}, fluidised bed at 10 g Nm^{-3} and downdraft less than 1 g Nm^{-3}. Furthermore, they suggested a classification of tar into four product classes: primary products which are characterised by cellulose-derived, hemicellulose-derived and lignin-derived methoxyphenols; secondary products which are characterised by phenolics and olefins; alkyl tertiary products which are mainly methyl derivatives of aromatic compounds; and condensed tertiary products which are PAH series without substituents. The four categories of tar correspond to different maturation temperatures; primary products are cracked before the tertiary products appear. The updraft gasifiers produce mainly primary tar with some degree of secondary character, the fluidised bed gasifiers produce secondary and tertiary tar, and the downdraft gasifiers produce mainly tertiary tar (Milne and Evans 1998). Nonetheless, the tar concentration depends on several parameters such as temperature, pressure, moisture/size/ash content of feedstock, gasifying medium, catalyst and additives, equivalence ratio (ER), resident time, etc.

Temperature is considered a fundamental parameter for the formation and maturation of tar. Higher operating temperatures reduce the overall tar production but with a progressive aromatisation of the evolved compounds (Hernández et al. 2013; Li and Suzuki 2009). A well-known scheme developed by Elliott (1988) summarises the maturation of tar with the temperature; mixed oxygenates at 400 °C, phenolic ethers at 500 °C, alkyl phenolics at 600 °C, heterocyclic ethers at 700 °C, PAH at 800 °C and larger PAH at 900 °C.
Besides the classification scheme proposed by Milne et al., another classification of tar in five classes based on solubility and condensability of different tar compounds is reported in Table 4.2 (Devi et al. 2005). The temperature increase promotes the decomposition of class 1 (GC-undetectable) and class 2 (heterocyclic aromatics) tar, while it fosters class 3 (light aromatic) and class 5 (heavy PAH compounds) tar (Han and Kim 2008). According to Bergman et al. (2002), the tar dew-point is a key parameter to assess the condensation issues and it depends on the tar concentration. Bergman defined the correlation for each tar class and highlighted that class 5 dominate the dew-point of tar, since at low concentration (e.g. <1 mg m^{-3}) a dew-point below 100 °C can be obtained (Li and Suzuki 2009). Nevertheless, depending on the concentration in the producer gas, also class 2 (heterocyclic aromatics) and class 4 (light PAH compounds) tar should be partially removed to avoid condensation which can foul engine and turbine (Anis and Zainal 2011).

Table 4.2 – List of tar compounds that are considered for different tar classes (Devi et al. 2005).

Tar class	Class name	Property	Representative compounds
1	GC-unde-tectable	Very heavy tars, cannot be detected by GC	Determined by subtracting the GC-detectable tar fraction from the total gravimetric tar
2	Heterocyclic aromatics	Tars containing hetero atoms; highly water soluble compounds	Pyridine, phenol, cresols, quinoline, isoquinoline, dibenzophenol
3	Light aromatic (1 ring)	Usually light hydrocarbons with single ring; do not pose a problem regarding condensability and solubility	Toluene, ethylbenzene, xylenes, styrene
4	Light PAH compounds (2–3 rings)	2 and 3 rings compounds; condense at low temperature even at very low concentration	Indene, naphthalene, me-thylnaphthalene, biphenyl, acenaphthalene, fluorene, phenanthrene, anthracene
5	Heavy PAH compounds (4–7 rings)	Larger than 3-rings, these components condense at high-temperatures at low concentration	Fluoranthene, pyrene, chrysene, perylene, coro-nene

Although higher temperatures decrease the tar content, some other factors limit the operating temperatures because high values lead to lower gas heating value, lower char conversion and higher risk of sintering (Devi et al. 2003). Also increasing ER leads to lower tar production due to a higher amount of oxygen for the oxidation of the volatile matter; nevertheless, the remaining tar undergoes a progressive aromatisation. However, the optimal ER values are a trade-off between gas quality, process efficiency and tar production (Hernández et al. 2013).

A study carried out by Yu et al. (2014) shows the tar formation for the major biomass components (i.e. cellulose, hemicellulose and lignin). PAHs represent the largest component of gasification tar. The relative percentage of PAHs increased with temperature. The relative percentages of PAHs for cellulose, lignin and hemicellulose increase from approximately 65–70 % at 800 °C to approximately 90–95 % at 1000 °C. Lignin, due to its molecular structure, has a higher tar yield and produces more stable components (PAHs derived primarily from phenols and its derivatives). For cellulose and hemi-cellulose, PAHs are derived primarily from benzene, toluene, ethylbenzene and xylene isomers (BTEX) and miscellaneous hydrocarbons.

Few studies regarding the tar analysis of a gasifier operated with coconut shell are present in scientific literature. Sheeba et al. (2009) tested coir pith in a circulating fluidised bed gasifier at different temperature (650–1020 °C) and ER (0.18–0.31) and he recorded a tar content of around 7–11 g m^{-3}. Senapati tested coconut coir in prototype of entrained flow gasifier at different temperature (976–1100 °C) and ER (0.21–0.30) and he found out tar content around 4.8–26.3 g m^{-3} (Senapati and Behera 2012). Moreover, the scientific literature lacks studies presenting a detailed analysis of the compounds detected in the tar of the producer gas when the gasifier is operated with coconut shell.

In this section, a comprehensive screening of the tar present in the raw producer gas was carried out for a small open top gasifier (about 1 kg h^{-1} as input biomass) operated with Casuarina woodchip and coconut shell as fuels. The analysis of tar was conducted with two different approaches available in the scientific literature such as gas chromatography-mass spectrometry (GC-MS) analysis and the gravimetric approach. Furthermore, tar collection was operated with two different solvents − isopropyl alcohol (IPA) and hexane − in order to compare their capability to dissolve tar compounds.

4.1 Experimental setup

4.1.1 Open top gasifier

The gasifier considered here is a micro scale unit reproducing the open top twin fire gasifier developed at the IISc (Indian Institute of Science) (Dasappa et al. 2011). The gasifier is a downdraft type and has a long cylindrical reactor with open top and air nozzles in the oxidation zone. The remaining char and ash are extracted by means of a bottom screw. This design is particularly suitable for generating low-tar producer gas. The dual air entry (i.e. through the top and through the nozzles) enables the flame front to move towards the top of the reactor, increasing the thermal bed and improving the gas resident time. The resident time of the gas, in the high temperature environment along with the hot reactive char, ensures cracking of higher molecular weight (MW) compounds. Furthermore, the tar cracking improves the overall gasification efficiency (CGPL 2014; Mahapatra and Dasappa 2014; Dasappa et al. 2004).

Fig. 4.1a shows the typical layout of an open top downdraft gasifier while Fig. 4.1b shows the picture of the gasifier that was used for the experimental tests. The gasifier was operated with two different feedstocks: Casuarina woodchip and coconut shell (see Fig. 4.2). Both materials are dried in an oven to reach a water content of around 5 %, calculated on wet basis. In order to collect the tar, the producer gas was spilled before the gas conditioning section, as depicted in Fig. 4.1b; the gas was then delivered to the tar sampling system and treated as described in section 2.2. During the tar sampling, both the temperature of the oxidation zone and the composition of the producer gas were continuously monitored and recorded.

(a)

(b)

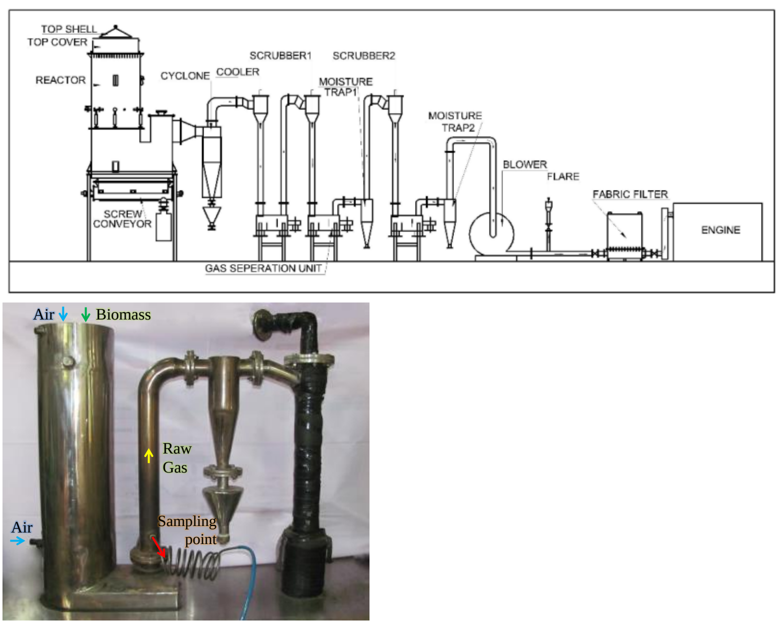

Fig. 4.1 – Typical open top downdraft gasifier: scheme (a) and picture of the system (b).

(a) (b)

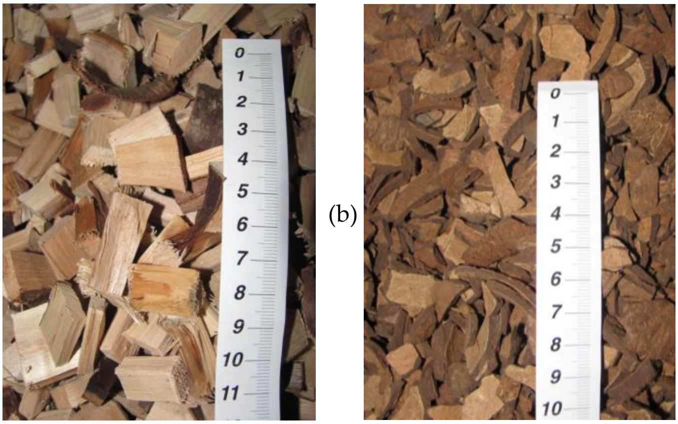

Fig. 4.2 – Casuarina woodchip (a) and coconut shell (b)

4.1.2 Tar sampling system

The equipment, used for the collection of tar, is composed of one empty bottle (i.e. moisture trap) and four bottles filled with a solvent (i.e. impinger bottles). A scheme of the setup is reported in Fig. 4.3. Each sampling was carried out using two different solvents: IPA (polar solvent) and hexane (non-polar solvent). Hexane has a lower boiling point, compared with IPA, therefore a larger evaporation of the solvent is expected. Nevertheless, hexane is a non-polar solvent and could differently impinge on tar. All the bottles were kept in an ice bath at 0 °C and atmospheric pressure (~ 89.5 kPa). The flow rate, bubbling through the impinger bottles, was set at 0.36 m^3 h-1 with a sampling time from a minimum of 1.5 h to a maximum of 4 h. The raw gas at the sampling point had a temperature around 330 °C.

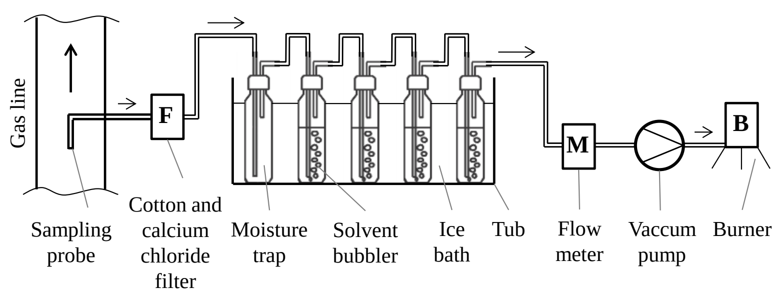

Fig. 4.3 – Scheme of the tar sampling setup.

After the sampling procedure, the samples were collected in a bottle. Both connection tubes and impinger bottles were rinsed with the used solvent and the rinsate added to the main solution. Finally, the entire solution was filtered by means of a paper filter and stored in an air tight bottle at a temperature of 5 °C. A sub-sample (10 ml) of each filtered solution was stored for the determination of the individual tar compounds by means of GC-MS analysis. The remaining part was used for the determination of gravimetric tar by means of solvent evaporation at ambient temperature (~ 30 °C) and ambient pressure (~ 89.5 kPa). The residues, after the gravimetric procedure, were re-dissolved in 10 ml of IPA and analysed by means of GC-MS analysis. The experiments were repeated three times for each feedstock (i.e. Casuarina woodchip and coconut shell) and each solvent (i.e. IPA and hexane). The results of the experiments are reported in the next chapters with the label composed by the number of the trial (i.e. 1, 2 and 3) and the indication of the used solvent (i.e. "ipa" for IPA and "hex" for hexane).

4.1.3 GC-MS analysis

The samples, collected by means of the tar sampling equipment, were analysed through a GC (GC Clarus 680 – Perkinelmer) coupled with MS (MS Clarus SQ8T – Perkinelmer). The GC Clarus 680 was equipped with a capillary column (Elite-5 – Perkinelmer); length: 30 m, internal diameter: 0.25 mm, film thickness: 0.25 μm, temperature limits: -60 to 325–350 °C, phase reference: 5 % diphenyl and 95 % dimethyl polysiloxane (low bleed). The temperature programme was set as follow: 30 °C held for 5 min, a ramp of 10 °C min-1 up to 150 °C followed by another ramp of 25 °C min^{-1} up to 320 °C. The carrier gas was high purity helium (99.999 %) with a flow rate of 1.0 ml min^{-1}. The injector temperature was set at 300 °C and the injection volume at 0.5 μl with a split ratio of 30:1. The transfer line and the ion source temperature were set at 200 °C and 180 °C, respectively. The MS was operated in electron ionisation mode (70 eV), full scan mode (range: 30–300 Da) and with a solvent delay of 2.7 min. The detected peaks were identified by means of NIST spectral library 2.0g (2011). Furthermore, the quantification of the main compounds (i.e. benzene, toluene, styrene, phenol and naphthalene) were carried out through MS detector in SIR (single ion recording) mode and by means of external standards.

4.2 Results and discussion

4.2.1 Process characterization

Both temperature in the oxidation zone and composition of the raw gas were monitored and recorded. No substantial differences were observed for both oxidation temperature and gas composition while operating the gasifier with Casuarina woodchip rather than coconut shell. The temperature in the oxidation zone was 900 ± 50 °C with both feedstocks and the composition of the producer gas as reported in Fig. 4.4. The standard deviation of the measurements was calculated and reported with whiskers in the graph on the top of each bar. The lower heating values (LHV) are 3.12± 0.22 MJ kg^{-1} and 3.03±0.11 MJ kg^{-1} for Casuarina woodchip and coconut shell, respectively.

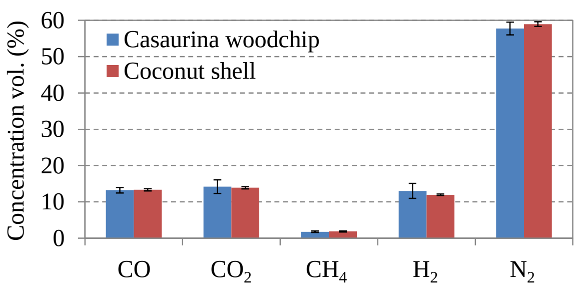

Fig. 4.4 – Composition of the producer gas (volumetric concentration on dry basis) for Casuarina woodchip (LHV=3.12±0.22 MJ kg^{-1}) and coconut shell (LHV=3.03±0.11 MJ kg^{-1}).

4.2.2 Calibration curves

The quantification of the main compounds was carried out by means of external standards. The calibration curves are reported in Fig. 4.5 (IPA as solvent) and Fig. 4.6 (hexane as solvent). The calibration curve is a linear regression calculated for three points at different concentrations and, therefore, different area of the chromatogram peak. The area was elaborated on the basis of the signal recorded by the MS detector operating in SIR mode (see Fig. 4.7). The chromatogram starts at 2.7 minutes because of the solvent delay (time required by the solvent to leave the column). The analysis was repeated three times for each point and the average value and the standard deviation (whiskers in the graphs) are reported in Fig. 4.5 and Fig. 4.6. The quantification of the compounds in the collected samples was elaborated by means of the calibration curves reported in these graphs.

The compounds that were not calibrated with the external standards, were quantified by means of estimated calibration curves that were determined on the basis of the correlation between the above-mentioned calibration curves and the molecular weight of the compounds. Each compound has its own correlation between area and concentration, as displayed in Fig. 4.5 and Fig. 4.6. In particular, as expected, Fig. 4.8 shows the correlation between calibration curves and molecular weight. For a predetermined concentration; the higher the MW, the higher the signal from MS detector and therefore the area of the chromatogram peak. The MW for the calibrated compounds are reported with parentheses: benzene (78.11 g mol^{-1}), toluene (92.14 g mol^{-1}), phenol (94.11 g mol^{-1}), styrene (104.15 g mol^{-1}), naphthalene (128.17 g mol^{-1}). In the graphs, benzene and naphthalene are displayed in the opposite extremes of the curves stack since they are considerably different in terms of MW. For each un-calibrated compound, an estimated calibration curve was elaborated on the basis of the calibration curves displayed in Fig. 4.8 and the corresponding MW. Therefore, for each un-calibrated compound, it is possible to estimate its concentration in the sample by means of the estimated calibration curve.

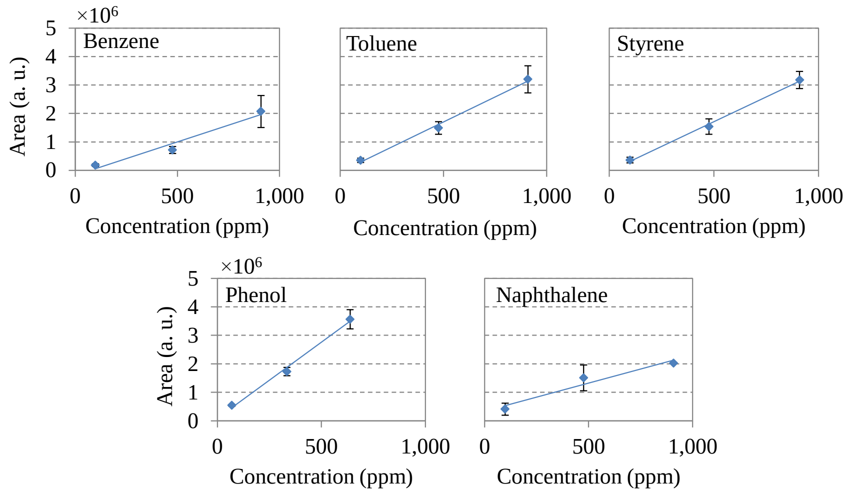

Fig. 4.5 – Calibration curves for the main compounds (IPA as solvent).

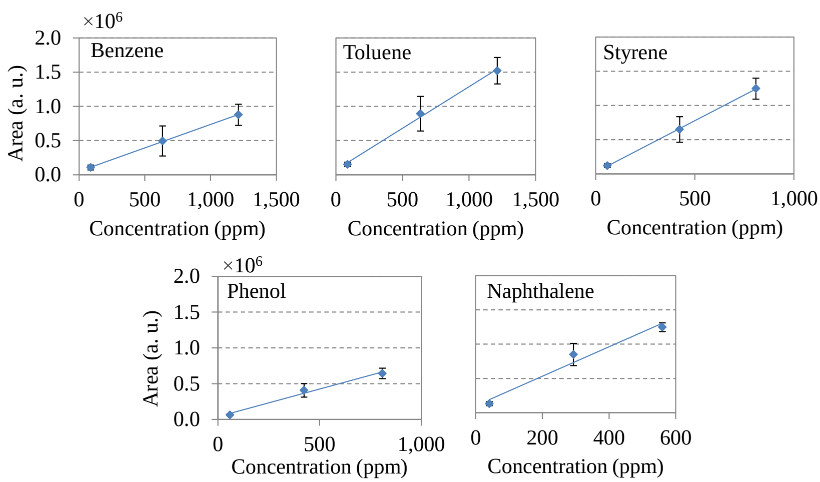

Fig. 4.6 – Calibration curves for the main compounds (hexane as solvent).

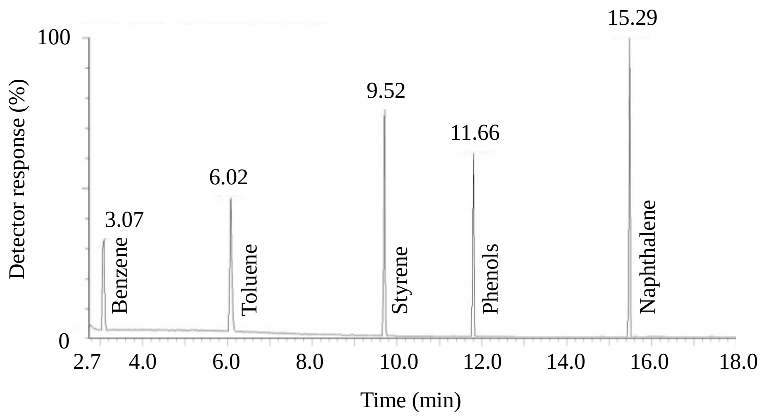

Fig. 4.7 – Total ion current chromatogram from GC-MS analysis of a standard blend (solvent delay: 2.7 min).

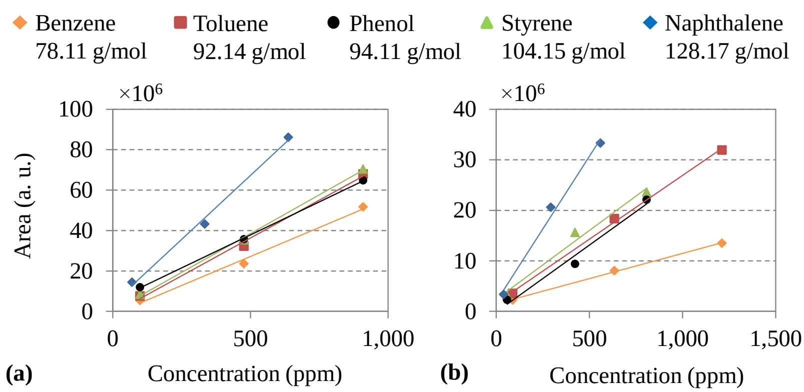

Fig. 4.8 – Calibration curves; IPA as solvent (a), hexane as solvent (b).

4.2.3 GC-MS analysis and gravimetric tar

The quantification of the tar compounds in the raw gas was carried out through the GC-MS analysis of the collected samples. The concentration of each compound was calculated by means of the detected area and the calibration curve. The area was elaborated on the basis of the signal recorded by the MS detector operating in full scan mode (see Fig. 4.9). All the analyses were repeated twice and the average value are reported in the following tables.

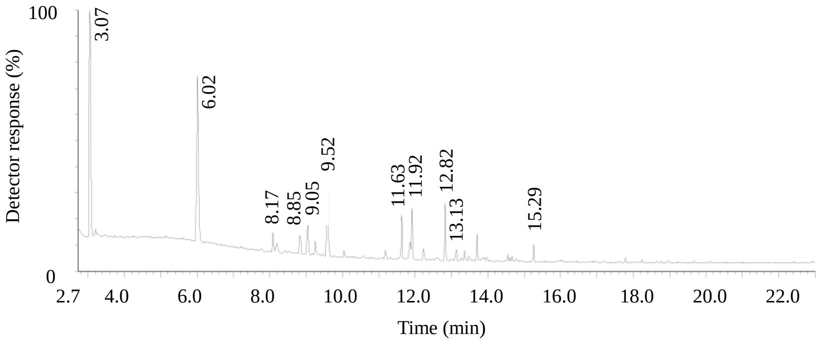

Fig. 4.9 – Total ion current chromatogram from GC-MS analysis in full scan mode of the sample 1_ipa obtained from gasification of coconut shell (solvent delay: 2.7 min).

Table 4.3 refers to the producer gas from Casuarina woodchip and Table 4.4 refers to coconut shell. The results are reported using both IPA and hexane as solvent. No considerable differences were observed using IPA rather than hexane. Nevertheless, IPA is easier to handle since its boiling point is higher compared to the one of hexane. Tables 4.3 and 4.4 report the average values calculated considering all the samples for each feedstock. Only gravimetric tar was calculated for the sample "1_hex", for both Casuarina woodchip and coconut shell, due to technical problems during the experiments. Furthermore, the total amount of tar (measured and estimated) and the percentage of estimated tar on the total one are reported in the tables. The order of magnitude of the total tar content is in accordance with the scientific literature that states it is around 1 g Nm^{-3} for a downdraft gasifier (Milne and Evans 1998). The detected tar compounds are mainly class 3 tar (i.e. light aromatics). Benzene and toluene account for an average share of 70 % of the total detected tar for both the feedstocks. Gravimetric tar is considerably lower (almost one order of magnitude) than the total tar detected in the collected samples. This is due to evaporation of the lighter compounds (e.g., benzene, toluene, etc.) during the gravimetric procedure. Only heavy hydrocarbons are expected to be present in the gravimetric tar residues, further discussion is reported in section 3.4.

The determination of tar content has to be restricted depending on the downstream application, not including the compounds that are not harmful for the considered application. As an example, considering an internal combustion engine, the organic compounds with a boiling point lower than about 100°C (e.g. benzene and toluene) should not be considered (Milne and Evans 1998).

Table 4.3 – Quantification of tar compounds (mg Nm^{-3}) in the raw gas when the gasifier is operated with Casuarina woodchip.

Sample #	IPA (solvent)				Hexane (solvent)			
	1 ipa	**2 ipa**	**3 ipa**	**Avg. ipa**	**1 hex**	**2 hex**	**3 hex**	**Avg. hex**
Benzene	160	102	108	**123**	-	93	116	**104**
Toluene	86	68	64	**73**	-	117	98	**108**
Styrene	38	0	7	**15**	-	35	22	**28**
Phenol	0	25	0	**8**	-	10	16	**13**
Naphthalene	4	33	0	**12**	-	2	1	**2**
Furans *	0	0	0	**0**	-	5	4	**4**
Cycloheptatriene *	0	0	0	**0**	-	2	0	**1**
Furfurals *	0	3	0	**1**	-	8	4	**6**
Dimethyl heptene *	0	0	0	**0**	-	0	0	**0**
Ethylbenzene *	7	10	0	**6**	-	16	10	**13**
Xylenes *	10	13	0	**8**	-	20	13	**16**
Anisole *	0	4	0	**1**	-	5	2	**4**
Benzofurans *	12	17	0	**9**	-	13	7	**10**
Indenes *	8	19	0	**9**	-	9	6	**8**
Acetic acid *	0	0	19	**6**	-	0	8	**4**
Cresols *	0	0	0	**0**	-	1	0	**0**
Cyclohexane *	3	0	5	**3**	-	0	0	**0**
Total GC-MS	327	294	201	**274**	-	337	309	**323**
Total Estimated * (%)	12	22	12	**15**	-	24	18	**21**
Gravimetric tar	73	41	30	**48**	72	45	60	**59**

* concentration estimated by means of estimated calibration curves

The results can be compared in terms of tar content depending on the used feedstock. Coconut shell has higher values for most of the compounds. The total amount of tar for coconut shell is 489 mg Nm^{-3} (IPA as solvent) and 405 mg Nm^{-3} (hexane as solvent) while for Casuarina woodchip is 274 mg Nm^{-3} (IPA as solvent) and 323 mg Nm^{-3} (hexane as solvent). Benzene and toluene are the compounds that mainly enhance the difference of the total tar values determined by means of GC-MS analysis. The gravimetric tar is similar for both the feedstocks because the lighter compounds (e.g., benzene, toluene, etc.) are evaporated during gravimetric procedure. The amount is 48 mg Nm^{-3} (IPA as solvent) and 59 mg Nm^{-3} (hexane as solvent) for Casuarina woodchip, and 52 mg Nm^{-3} (IPA as solvent) and 79 mg Nm^{-3} (hexane as solvent) for coconut shell.

Table 4.4 – Quantification of tar compounds (mg Nm^{-3}) in the raw gas when the gasifier is operated with coconut shell

	IPA (solvent)				**Hexane (solvent)**			
Sample #	**1 ipa**	**2 ipa**	**3 ipa**	**Avg. ipa**	**1 hex**	**2 hex**	**3 hex**	**Avg. hex**
Benzene	292	86	268	**215**	-	141	193	**167**
Toluene	156	55	225	**146**	-	109	87	**98**
Styrene	59	0	7	**22**	-	33	26	**29**
Phenol	10	44	16	**23**	-	32	46	**39**
Naphthalene	2	32	0	**11**	-	1	2	**2**
Furans *	0	0	0	**0**	-	4	0	**2**
Cycloheptatriene *	0	0	0	**0**	-	0	0	**0**
Furfurals *	12	9	0	**7**	-	10	3	**7**
Dimethyl heptene *	0	0	0	**0**	-	0	0	**0**
Ethylbenzene *	13	4	1	**6**	-	9	4	**7**
Xylenes *	20	10	0	**10**	-	16	9	**13**
Anisole *	0	3	0	**1**	-	2	7	**5**
Benzofurans *	29	20	0	**16**	-	18	17	**18**
Indenes *	22	21	0	**14**	-	11	14	**12**
Acetic acid *	16	24	0	**13**	-	4	8	**6**
Cresols *	0	0	0	**0**	-	1	0	**0**
Cyclohexane *	5	0	4	**3**	-	0	0	**0**
Total GC-MS	637	308	521	**489**	-	392	418	**405**
Total Estimated * (%)	18	30	1	**16**	-	19	15	**17**
Gravimetric tar	50	44	63	**52**	138	54	46	**79**

* concentration estimated by means of estimated calibration curves

In scientific literature there are several studies about the characterisation of tar, nevertheless, differences in the gasification technology, reaction temperatures and used feedstocks make it difficult to compare the results. The results of this study agree with the generalised tar composition for a downdraft gasifier: tar is mainly composed of tertiary aromatics (e.g., benzene, naphthalene, phenanthrene and pyrene) and tertiary alkyl aromatics (e.g., toluene, indene, phenol) (Milne and Evans 1998). These results are also in accordance with Hernandez et al. (2013) that found BTEX as the main constituents of tar (60–70 % wt.). Similar results were obtained from the characterisation of tar content in the syngas produced in a downdraft type fixed bed gasification system from dried sewage sludge (Phuphuakrat et al. 2010). However, Jordan et al. (2012) found results that significantly differ from the generalised tar composition outlined by Ref. (Milne and Evans 1998). They characterised the tar produced during gasification of fuel cane bagasse in a 50 kW_{el} air-blown downdraft autothermal gasifier, and showed that the main compounds of tar are 4-methylphenol, 1,2-benzediol, styrene, m-xylene and pyrene.

The fluidised bed design, if compared to the downdraft one, generates a producer gas with a higher tar content, mainly due to the lower gasification temperature, while the tar composition depends also on the gas residence time (Kinoshita et al. 1994; Van Paasen et al. 2004). In particular, the class 4 and heavy class 5 tar concentrations increase, while the class 2 and 3 tar concentrations decrease, with increasing the gas residence time (Van Paasen et al. 2004). According to Nemanova et al. (2011), the main tar components of an atmospheric fluidised bed gasifier are naphthalene (58.7 %), phenanthrene (6.6 %), indene (6.1 %). A study carried out by Michel et al. (2011) with a fluidised bed steam gasifier showed mainly the presence of PAHs (naphthalene, anthracene and biphenylene) in the producer gas; naphthalene as dominant compound with a share between 30 % and 70 %, depending on the catalyst used. Similar results were obtained by Aigner et al. (2009) and Koppatz et al. (2011), PAHs were found as the main components of tar, where naphthalene accounts between 30 % and 45 % depending on the catalyst used.

In the present study, the concentration of naphthalene, in the producer gas of an open top gasifier, was detected to be significantly low. Contrary to benzene, naphthalene is particularly sensitive to temperature and it undergoes two different reactions, one is the naphthalene polymerisation leading to soot formation and the other one is the naphthalene cracking leading to lighter species, such as benzene (Jess 19996; Gerund et al. 2008). In the open top reactor, the higher resident time (as mentioned in section 2.1) besides the high temperature of the oxidation section promotes the naphthalene conversion.

Finally, the tar level in the raw producer gas of the open top gasification technology is satisfactory: results obtained with the gravimetric approach are around 50–80 mg Nm^{-3}, as mentioned above. If compared to other well-known gasifiers, the open top gasifier has less tar than the air-blown updraft gasifier in Harboøre (80 g Nm^{-3}) and the steam fluidised-bed gasifier in Güssing (1.5–4.5 g Nm^{-3}) (Ahrenfeldt et al. 2013). Moreover, the tar level is not much higher than the one of the "Viking" gasifier (15 mg Nm^{-3}), that has an extremely low tar concentration due to the two-stage gasification process (Henriksen et al. 2006).

4.2.4 GC-MS analysis on gravimetric tar residues

The residues, obtained after gravimetric tar, were re-dissolved in 10 ml of IPA and analysed by means of GC-MS. Most of the detected compounds has MW higher than 150 g mol^{-1}; as expected, the lighter compounds were evaporated during the gravimetric procedure. The detected compounds are mainly class 4 (light PAH compounds) and class 5 (heavy PAH compounds) tar. For both Casuarina woodchip and coconut shell the main compounds detected on the gravimetric tar residues are acenaphthylene, methylparaben, dibenzofuran, fluorene, phenantrene, anthracene, pyrene, fluorantene and benzo[a,b,c]fluorene. According to several authors (Morf 2001; Namioka 2009; Jess 1996), compounds such as fluorantene and pyrene are soot precursors. Moreover, class 1 tar – GC-undetectable compounds (Table 4.2) − are the primary components of soots.

None of the compounds, identified in the gravimetric tar residues, was highlighted in the analysis of the collected sample because they were present with a concentration lower than the one of the detected compounds. It was not possible to estimate the concentration of the compounds in the gravimetric residues due to the considerable difference of MW with respect to the standard compounds reported in Fig. 4.8.

4.3 Main findings

In this chapter, a comprehensive screening of the tar present in the raw producer gas was carried out for a small open top gasifier operated with Casuarina woodchip and coconut shell as fuels. The main objectives of this research are the comparison of different approaches for the sampling and analysis of tar, and the assessment of the capability of the considered gasification technology to produce low-tar producer gas.

The tar sampling procedure was carried out with both IPA and hexane in order to define the capability of each solvent to dissolve tar. The results highlighted that there is not considerable difference using IPA rather than hexane as solvent. Nevertheless, IPA is easier to handle due to its higher boiling point.

The analysis of tar was performed with two different approaches available in the scientific literature such as the GC-MS analysis and the gravimetric approach. The GC-MS analysis on the collected samples highlighted that tar is mainly composed of light aromatic compounds, where benzene and toluene account for about 70 % of the total detected tar. The gravimetric tar was roughly one order of magnitude smaller than tar amount detected in the collected samples by means of GC-MS analysis. Moreover, GC-MS analysis on the gravimetric tar highlighted that most of the compounds have a MW higher than 150 g mol^{-1} and correspond to light and heavy PAH compounds. The two approaches for the determination of tar in the producer gas – GC-MS on collected sample and gravimetric tar – have different capabilities and have to be used depending on the downstream application of the gasification system.

The tar content values were detected to be higher when coconut shell is used in the gasification process. Nevertheless, the compounds that enhance the difference are mainly benzene and toluene. Considering the rest of the compounds, the gasification of Casuarina woodchip rather than coconut shell has a similar tar content in the producer gas.

Finally, the open top reactor turned out to be a gasifier design with excellent performance in terms of tar content in the producer gas. Regardless of the used feedstock (i.e. Casuarina woodchip or coconut shell), the gravimetric tar in the raw producer gas is about 50–80 mg Nm^{-3}.

5. Integrated assessment of gasification systems for residential application

In Europe, energy use in buildings accounts for around 40 % of total energy consumption. Therefore, reduction of energy consumption and use of energy from renewable sources in the building sector are important measures to meet the climate and energy targets set by the European Union (The European Parliament and the Council of the European Union 2009; The European Parliament and the Council of the European Union 2010). Furthermore, among the different renewable energy sources, biomass could provide a significant contribution to developing distributed generation systems and offset fossil fuel consumption (Lund et al. 2005; Algieri and Morrone 2013). There is also an increasing interest in the cogenerative production of heat and power because it can increase the overall efficiency of energy systems and reduce the global CO_2 emissions (Rosato et al. 2013a; Angrisani et al. 2011). PES of CHP systems is extensively analysed in literature; Pohl and Diarra (2013) analysed the influence of plant-side and demand-side characteristics, Rosato and Sibilio (2013b) investigated the effects of transient operation of CHP systems and Angrisani et al. (2013) assessed the advantages of thermal load sharing by means of a thermal micro-grid. Fumo et al. (2009) emphasised the importance to evaluate the primary energy saving of a CHP system design before the economic viability. Boschiero (2014), Pagliarini et al. (2012) and Piacentino et al. (2014) highlighted the benefits related to the implementation of trigeneration systems and discussed the importance of proper policies supporting this technology. The European Parliament, with the directive 2012/27/EU, promotes cogeneration based on useful demand for heating or cooling (The European Parliament and the Council of the European Union 2004; The European Parliament and the Council of the European Union 2012).

The most common technology to convert biomass into heat and power is based on a biomass boiler coupled with Organic Rankine Cycle (ORC). For sizes larger than 500 kW_{el}, the ORC technology is reliable and highly standardized with reasonable investment and operational costs. According to Quoilin et al. (2013) and Rentizelas et al. (2009), at these sizes, ORC systems can reach net electrical efficiencies up to 17 %. According to Dong et al. (2013) and Maraver et al. (2009), the ORC technology is less attractive for small scale applications because economies of scale penalise both the efficiency and the specific cost.

According to Joelsson and Gustavsson (2009), CHP systems based on biomass gasification represent a promising technological solution and a possible alternative to conventional biomass cogeneration systems. The integration of biomass gasification with high efficiency power generation systems can define competitive scenarios, but it is an investment option with strong dependency on the support policies (Wetterlund and Söderström 2010; Difs et al.2010).

The high efficiency that can be reached by gasification systems enables the development of energy models based on distributed generation at sizes that have not been sufficiently efficient until now. Moreover, the decentralization of energy production would lead to various benefits, e.g., reduction of the transmission and distribution losses, exploitation of the local resources and reduction of the energy used for the transportation of the feedstock (Rentizelas et al. 2009; Hawkes and Leach 2007).

The research concerning the coupling of biomass gasification with traditional power generators (gas engines and gas turbines) is well documented by Dong et al. (2009) for the small-scale and micro-scale systems and by Fagbenle et al (2007) for the large-scale systems. Benefits and obstacles of innovative generation systems, such as fuel cells, are described by Baratieri et al. (2009) and Tommasi et al. (2006). The implementation of gasification-based CHP for rural areas, where the electrical network does not exist, is discussed by Coronado et al. (2011) and Lee et al. (2013). Besides the development of mathematical models for a given biomass processing system, the simulation of a complete energy conversion plant is usually carried out through models that offer advantages in the evaluation of process performance in different operating conditions (2012). However, the evaluation of the overall system performance still requires further development to evaluate each technology as integrated into the complete chain (biomass pre-processing, biomass energy conversion, energy distribution, final use).

Moreover, small-scale and micro-scale CHP systems based on biomass are not a completely consolidated technology and some technical and economic issues have still to be addressed (Dong et al. 2009). Nevertheless, micro CHP systems based on gasification have been recently introduced into the market, and they can be used for small industrial application or building with several users (e.g., hotels) (Burkhardt GmbH 2013; Spanner Re² 2013). At the current stage, the management of gasification start-stop operations is quite complex, requiring a continuous operation of the system and subsequent dissipation of excess heat when there is no specific demand.

In this chapter, an assessment of the energy performance of a biomass micro-CHP system for residential application was carried out by means of an integrated approach. The power plant is based on biomass gasification, and the end-user consists of some blocks of flats. The overall energy performance was evaluated for various contexts; different size and operational time of the generation system, and different building configurations. The energy assessment was conducted for the complete chain from the production stage to the final user and to this purpose a multistage model was developed and applied. The evaluation was performed in terms of PES with respect to a reference conventional technology of separate production of heat and power based on biomass. In addition, the economic analysis of a test gasification system of 30 kW_{el} was performed either with or without subsidizations for the generated electricity.

5.1 Methodology

5.1.1 Building stock characterisation

In the application of the integrated approach proposed in this chapter, four buildings close to each other and heat distribution network – supplied by a common central system – were modelled. The geometrical and thermo-physical characteristics are the same for the four buildings, but different configurations were studied by varying some features (i.e. insulation level, kind of glazing and windows orientation), in order to evaluate different heat load profiles. The selected cases are designed to allow correlating their main features to the performance (both energetic and economic) of the cogeneration system and are not chosen to represent the Italian building stock.

Each building consists of ten floors, each one with 100 m^2 of floor area without internal partitions and 3 m of internal height. The ratio between the dispersing surface area and the net volume of each building (S/V) is 0.47 m^{-1}. The vertical surfaces of the envelope face the cardinal points. For each building, the floors of the flat at the ground level is considered in thermal contact with an unheated highly ventilated basement, and hence modelled as exposed to the external environment, without solar and infrared radiations exchanged with the sky dome.
The opaque elements have a simplified two-layer structure, with a 20 cm thick layer of massive clay block (thermal conductivity 0.25 W m^{-1} K^{-1}, density 893 kg m^{-3}, specific heat capacity 840 J kg^{-1} K^{-1}) on the internal side, and an insulating polystyrene layer (thermal conductivity 0.04 W m^{-1} K^{-1}, density 40 kg m^{-3}, specific heat capacity 1,470 J kg^{-1} K^{-1}) on the external side, with variable thicknesses. The effect of the thermal bridges was neglected. All the surfaces, both the internal and the external sides, have a solar radiation absorption coefficient of 0.3, with the exception of the internal floors and the external roof that have a coefficient of 0.6. The ratio between the area of the glazing and the internal floor is 11.67 %. The windows are double-glazed with a thermal transmittance of the glazing area equal to 1.1 W m^{-2} K^{-1}. The frame area is 20 % of the whole window area (14.56 m^2) and its thermal transmittance is 1.2 W m^{-2} K^{-1}. The ventilation rate is constant and equal to 0.3 ACH, in accordance with the Italian technical specification UNI/TS 11300-1:2008 (UNI 2008a). The internal gains have been assumed constant and equal to 4 W m^{-2}, half radiant and half convective (UNI 2008a). The heating air temperature set-point has been set to 20 °C in accordance with the UNI/TS 11300-1:2008 prescriptions for residential buildings (UNI 2008a). The residential buildings are located in Milan with 2,404 Heating Degree Days (HDD) with respect to a base temperature of 20 °C. This location, in accordance with the Italian climatic classification, refers to the climatic zone E (2100 HDD–3000 HDD) that is the most characteristic and populated in northern Italy.
Different building configurations were evaluated for the buildings previously described considering alternative options for some of the characteristics. Three possible thicknesses were considered for the insulating polysty-

rene layer of the opaque elements; 0, 5 and 15 cm, which provide average thermal transmittances respectively equal to 1.03, 0.45 and 0.21 W m^{-2} K^{-1} (i.e. uninsulated, poorly insulated and well-insulated buildings). As concerns the transparent components, which are all positioned on a single façade, two options were analysed; east or west oriented. These two possibilities allow having the maximum solar gain in the morning (east oriented) rather than in the afternoon (west oriented). Finally, two glazings with different solar heat gain coefficients, SHGC, (0.608 and 0.352) were considered in order to assess two different levels of solar heat gains. Combining the alternatives related to the insulation of the opaque components, the positions of the transparent ones and the glazing SHGC, 12 different building configurations were obtained.

The simulation of the building dynamic behaviour was conducted by means of EnergyPlus 7.1, a validated software for the simulation of real buildings (U.S. Department of Energy 2013). As comparison of the considered alternatives, Fig. 5.1 shows the space daily heating load profiles for the 12 building configurations in January (winter season) and April (middle season).

As regards the thermal losses of the delivery section, the simplified approach of seasonal values – proposed by the technical specification UNI TS 11300-2:2008 (UNI 2008b) – was adopted. Concerning the space heating system, the emission and distribution efficiencies depend on the envelope insulation level in agreement with the technical specification UNI TS 11300-2:2008 (UNI 2008b). The heating system is based on radiators; the emission efficiency is 0.90 for the cases without thermal insulation, 0.93 for those ones with 5 cm of insulation and 0.95 for those ones with 15 cm of insulation. The distribution efficiencies are equal to 0.97, 0.98 or 0.99, respectively for 0 cm, 5 cm and 15 cm of insulation. The control efficiency can be considered 0.94 for all cases and corresponds to on/off temperature control for each thermal zone of the building.

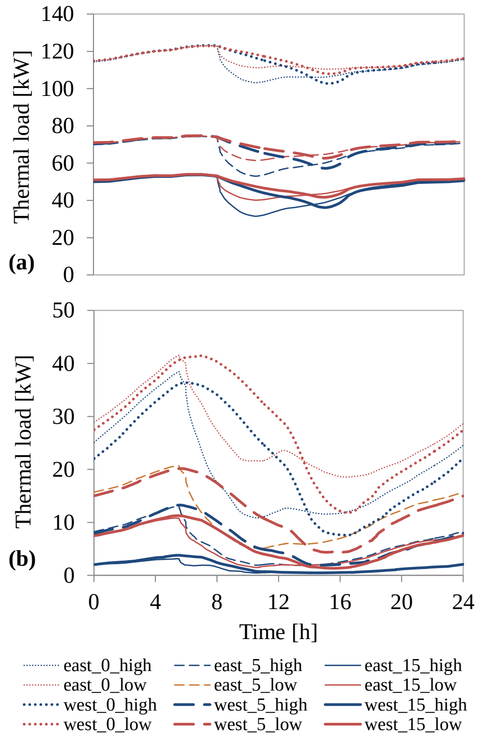

Fig. 5.1 – Average space daily heating load profile for four buildings (each with ten apartments) for an average day of January (a) and April (b). Building configurations: window orientation (east, west), insulation thickness (0, 5 and 15), SHCG (high, low).

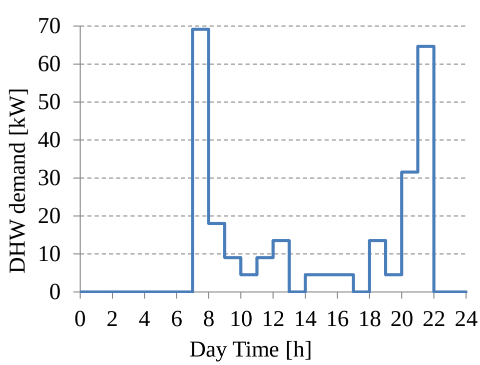

Fig. 5.2 – Average daily tapping pattern for 40 families with shower use.

The domestic hot water demand (DHW) was determined considering an average daily tapping pattern for a family with shower use in accordance with the EN 15316-3-1:2008 (CEN 2008). The contemporary DHW demand of 4 buildings (10 flats per building) was determined in accordance with the UNI 9182:2010 (UNI 2010). Fig. 5.2 shows the daily DHW demand considered in the integrated building-system analysis. The domestic hot water system is characterized by an emission efficiency of 0.95 because no devices for the control of supply are considered in the system (UNI 2008b). The distribution thermal loss was considered negligible since the distribution pipes are well insulated.

5.1.2 Power plant layout

The power plant was simulated with a multistage model by means of Matlab-Simulink environment. The gasification stage model was developed and validated by Baratieri et al. (2008), and it is based on the thermochemical equilibrium using the Cantera solver and the Gri-Mech thermodynamic properties (Smith et al. 2013). The developed multistage model has a general predictive capability that allows defining both electrical and thermal energy production depending on the considered operating conditions.

The power plant layout considered in this study (Fig. 5.3) is based on the generation and use of the producer gas to generate electrical and thermal power. The producer gas generation section was modelled as a downdraft fixed bed gasifier operating in ideal conditions, which can simulate different equivalence ratios (ER) – i.e. the actual air-fuel ratio divided by the stoichiometric air-fuel ratio – and therefore both pyrolysis (ER = 0) and air gasification processes (ER > 0). The simulated overall gasification process can be endothermic or exothermic depending on the equivalence ratio. For an endothermic process, the heat is provided through a burner fed by a producer gas spilling. For an exothermic process, the heat is simply discharged. The pressure inside the gasifier is considered to be atmospheric. Before feeding the CHP, the producer gas is piped through heat recovery and clean-up sections. Heat exchangers are assumed to be adiabatic with the producer gas being cooled from the gasification temperature to 150 °C. This temperature was chosen to minimize tar condensation that would clog up the heat exchanger. The clean-up section can be considered a condenser where tar and water vapour are condensed and cooled to 25 °C. The share of heat exchanged in the clean-up section is discharged to the environment due to heat losses to the surroundings. Pressure losses due to the ancillary equipment and to the filters were not considered. Electricity consumption of the auxiliaries was considered as much as 17 % of the gross electricity production (Ministry of Economic Development 2012).

In this study, poplar wood was considered as feedstock for the gasification process due to its availability in northern Italy. Its elemental composition, moisture content and heating value (Table 5.1) were employed as inputs for the thermochemical equilibrium model. The feedstock characteristics are reported on as received (ar) basis, i.e. considering the water content in the feedstock mass (Van et al. 1995).

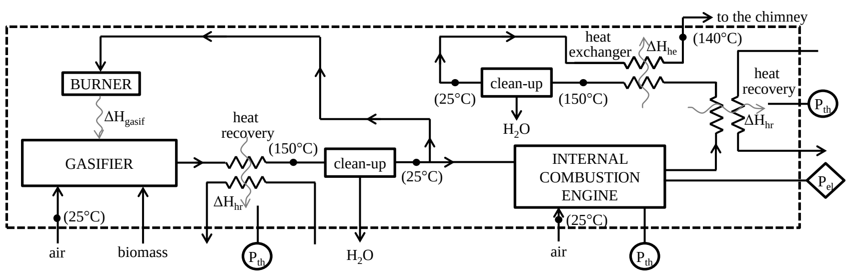

Fig. 5.3 – Schematic diagram of the power plant layout.

Table 5.1 – Characteristics of poplar wood.

moisture	ash	C	H	O	N	LHV	Ref.
[%wtar]						[MJ/kgar]	
15.0	1.1	41.2	5.0	37.2	0.4	14.936	(Van et al. 1995)

The producer gas coming from biomass gasification is exploited in an internal combustion engine (ICE) based on Otto cycle. As for the gasifier, also the processes in the CHP were modelled at thermodynamic equilibrium in a Matlab-Simulink environment. The Otto cycle was modelled as a fuel–air cycle. Combustive air and producer gas are compressed in isentropic conditions according to a specified volume ratio (v_1/v_2). Then complete combustion occurs at constant volume, followed by an isentropic expansion of exhaust gases and a discharge of exhaust gases at constant volume. The efficiency of the real cycle was calculated considering a ratio between the useful work and the work of the air-fuel cycle of 70 % (Heywood 1988); the complementary share of input energy was considered to be recovered both through the cylinder coolant and the exhaust gas cooling (Fig. 5.3). The exhaust gases from CHP are processed by means of a heat exchanger and a clean-up system with the same features previously described for the gasification section. Purified exhaust gas is then ready to be heated up to 140 °C through a heat exchanger and piped to the chimney. Nowadays, the clean-up section is not implemented for small scale plants, such as the one evaluated here. However, it was considered as a precautionary measure in a future perspective of extensive development of decentralised generation in residential areas. The Otto cycle is generally optimized in order to operate with gasoline which has different properties with respect to the producer gas. If compared to gasoline, producer gas has a higher auto-ignition temperature, hence it allows the adoption of higher volumetric ratio for the engine. In this analysis, volume ratio was fixed to 15 (Sridhar et al. 2001). The conversion efficiency from mechanical to electrical power is assumed as 94 % (Alberti et al. 2014). Thermal power is recovered by means of adiabatic heat exchangers, from both the gasification and CHP sections. The power-to-heat ratio was calculated as electrical power divided by the thermal power of the whole power plant. Furthermore, electrical and thermal power were computed to evaluate the electrical (1) and thermal (2) efficiency.

$$\eta_{el} = \frac{P_{el}}{LHV_{biom} \cdot Q_{m,biom}} \tag{1}$$

$$\eta_{th} = \frac{P_{th}}{LHV_{biom} \cdot Q_{m,biom}} \tag{2}$$

where LHV_{biom} is the lower heating value of the biomass and $Q_{m,biom}$ is the mass flow rate of biomass, P_{el} is the CHP electrical power and P_{th} is the thermal power recovered from both the gasifier and CHP.

Gasification temperature and equivalence ratios were optimised to reach the highest possible electrical efficiency since electricity is a form of energy of high quality. The gasification temperature were evaluated between 500 °C and 1000 °C, with a step of 25 °C, and the equivalence ratio was evaluated between 0.0 and 0.6, with a step of 0.025. The efficiencies obtained in this optimization procedure were used for the integrated analysis of buildings and the biomass gasification system.

5.1.3 Integrated analysis of building and CHP system

In Italy, gasification systems usually run without taking care of the dissipated heat due to the feed-in tariff on the electrical production (EUR/kWh_{el}) that is more attractive than heat valorisation. The incentive is paid by the electrical services management company (i.e. GSE – Gestore Servizi Elettrici), which is the State-owned company that operates the mechanisms of promotion and support of the renewable energy sources in Italy (Ministry of the economic development 2012).

At the current technical stage, the gasifier systems usually require complex procedures to reach a steady state operation; a partial or on/off operational mode is not yet considered feasible. According to these considerations, the power plant is supposed to run continuously for a period centred on the coldest day of the year. The electricity production is entirely delivered to the electrical grid that acts as an ideal storage. In contrast, only a fraction of the thermal production is useful: when buildings have reduced or no heat demand, thermal power has to be dissipated. Nevertheless, a thermal energy storage (TES) could enhance the useful heat, even if the system is not supposed to operate on/off. A preliminary analysis has shown that implementation of TES – with volume up to 10 000 litres – would enable exploiting an additional share that is smaller than 2 % of the heat produced by CHP system. In this study, a conservative assessment was carried out neglecting the contribution of TES.

The primary energy saving was calculated to evaluate the advantage in adopting a cogeneration system instead of the separate production of heat and power. In accordance with the Directive 2004/8/EC (The European Parliament and the Council of the European Union 2004), PES was calculated as:

$$PES = 1 - \frac{1}{\frac{CHP\ H\eta}{Ref\ H\eta} + \frac{CHP\ E\eta}{Ref\ E\eta}} \tag{3}$$

where CHP Hη is the thermal efficiency defined as annual useful heat output divided by the CHP fuel input, CHP Eη is the electrical efficiency defined as annual electricity divided by the CHP fuel input, Ref Hη is the efficiency reference value for separate heat production, Ref Eη is the efficiency reference value for separate electricity production. The reference efficiencies depend on the construction year of the power plant and the fuel supply. The values are reported in the Italian decree of the 4th august 2011 (Ministry of the economic development 2011). Considering the plant construction in 2013 and wood as fuel supply, Ref Eη is equal to 0.33 and Ref Hη is equal to 0.86. In accordance with the Italian decree, Ref Eη has to be corrected considering the average ambient temperature (i.e. 11.3 °C for the considered application) and the connection line voltage (i.e. 400 V for the considered application): the resulting value of Ref Eη is 0.315.

PES values were evaluated for all building configurations, for power plant sizes between 10 kW_{el} and 100 kW_{el}, with a step of 5 kW_{el}, and for operational period durations of between 1,560 h (65 days) and 8,760 h (365 days), in steps of 400 h.

5.1.4 Economic analysis

As described in the results section, PES analysis highlighted some building configurations more relevant than others. These configurations were considered for further study, such as economic analysis.

Firstly, a differential cash flow between the CHP plant and a traditional non-condensing gas boiler (reference case) was evaluated in subsidization regime. The traditional gas boiler was also considered in the CHP scenario as back-up of the CHP system. The subsidisation is mainly the feed-in tariff paid by GSE on the net electricity delivered to the grid; for the considered power plant, the tariff is guaranteed for 20 years. Moreover, a bonus per cogenerative electricity is paid by GSE if the CHP system has high efficiency; for a power plant smaller than 1 MW_{el}, the PES has to be higher than zero. The cogenerative electricity depends on the useful heat from cogeneration, and it is calculated according to the Directive 2004/8/EC (The European

Parliament and the Council of the European Union 2004). The electricity purchased by the users was not considered in the analysis since, in both scenarios, it is completely drawn from the national grid. This is a common practice since the incentive tariff is higher than the electricity price, and the incentive is not paid for the self-consumption electricity share.

In addition, a second differential cash flow was determined without subsidization. In this case, GSE offers a "simplified purchase & resale arrangements" to trade the electricity produced with renewable sources (GSE 2013).

The economic analysis is performed by calculating two indexes: the discounted payback time (PBT) – to evaluate the time required to recover the investment cost – and the annual worth (AW) – to estimate the annual revenue of owning and operating an asset over its entire lifespan. The gasifier lifespan (80 000 h) was adopted as a reference for the length of the investment analysis. As regards the engine, a lifespan of 40 000 h was used. The considered real interest rate is 3 % (European Commission 2012).

Table 5.2 – Parameters for the economic analysis.

Parameter	Value	Ref.
IC, gasifier + engine [EUR/kW$_{el}$]	4500	[a]
IC, engine [EUR/kW$_{el}$]	500	[a]
maintenance cost [EUR/kWh$_{el}$]	0.050	[a]
biomass cost [EUR/t]	165	[b]
feed-in tariff [EUR/kWh$_{el}$]	0.229	(Ministry of the economic development 2012)
cogeneration bonus [EUR/kWh$_{el}$]	0.040	(Ministry of the economic development 2012)
heat valorization [EUR/kWh$_{th}$]	0.057	(AEEG 2013)
electricity revenue (GSE)* [EUR/kWh$_{el}$]	0.120	(GSE 2013)
real interest rate [%]	3.00	-

[a] M. Prussi, personal communications, October 2013, C.R.E.A.R. University of Florence

[b] V. Francescato, personal communications, September 2013, A.I.E.L.

* Alternative to comprehensive incentive and cogeneration bonus

Table 5.2 reports the investment costs (IC), the operational costs, the feed-in tariff, the electricity price guaranteed by GSE for the "simplified purchase & resale arrangements" and the revenues (VAT and other taxes excluded) required to perform an economic analysis. The economic valorisation of the heat due to the CHP was calculated considering the natural gas savings of the back-up non-condensing boiler. Considering a seasonal efficiency of the back-up boiler of 93 %, natural gas LHV of 34.9 MJ/Sm^3 and natural gas cost for residential use equals to 0.51 EUR/Sm^3, the thermal power is valorised at 0.057 EUR/kWh_{th} (AEEG 2013).

Finally, a sensitivity analysis of the main parameters (i.e. IC, biomass cost, feed-in tariff, cogeneration bonus, heat valorisation) on both net present values (NPV) and AW was presented for the representative power plant configuration.

5.2 Results and discussion

5.2.1 Gasification section

The results of the optimization procedure – carried out on the gasification system to maximise the electrical efficiency – are reported in Fig. 5.4. The iso-efficiency curves have been plotted interpolating the points in which the electrical efficiency has been calculated, as explained in methods section. The maximum electrical power was obtained for a gasification temperature of 800 °C and ER of 0.1. In this configuration, the CHP electrical efficiency results 0.23 and the CHP global efficiency results 0.85. The global efficiency has been computed as the sum of the electrical and the thermal efficiency. The output power-to-heat ratio corresponds to 0.375. The energy optimization of the producer gas generation section corresponds to the complete conversion of carbon. A share of 26 % of the producer gas is used to feed the heater that provides heat to the gasifier (endothermic process). The total thermal power is recovered by the heat recovery section of the gasifier (15 %) and by the ICE section (85 %).

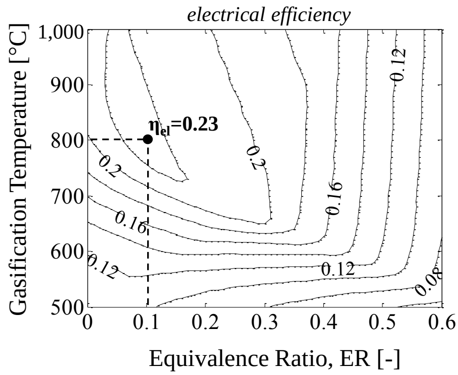

Fig. 5.4 – Electrical efficiency of the whole power plant layout depending on the equivalence ratio and the gasification temperature.

5.2.2 Power plant and buildings

The results of PES analysis for all the considered building configurations (12 alternatives) are shown in Fig. 5.5. The graph reports the curves corresponding to a PES equal to zero, i.e. the CHP system and the separate production of heat and power have the same consumption of fuel. The iso-PES curves have been plotted interpolating the points in which the PES index has been calculated, as explained in methods section. The curves show clusters for the building configurations with the same thermal insulation of the opaque envelope. The orientation and SHGC of the windows partially affect the PES, slightly shifting the curves inside these clusters. For this reason, the results of the energetic and economic analysis have been shown in detail for three building configurations with 0, 5, 15 cm of thermal insulation of the opaque components and high SHGC west-oriented windows, for which the resulting curves appear in the middle of the clusters.

Fig. 5.6 shows the detailed results of PES analysis for the three building configurations with different thermal insulation of the opaque components. Positive areas of PES have been detected for the three building configurations. PES index is related to the exploitation of the produced heat, therefore, the less heat is discharged the larger is PES. Short operational time and small plant size usually allow higher primary energy saving values, but there are some limitations that have to be considered. First of all, plants smaller than 30 kW_{el} are not commercially available. Furthermore, lower operational times (e.g., shorter than 4000 h) could lead to high payback periods.

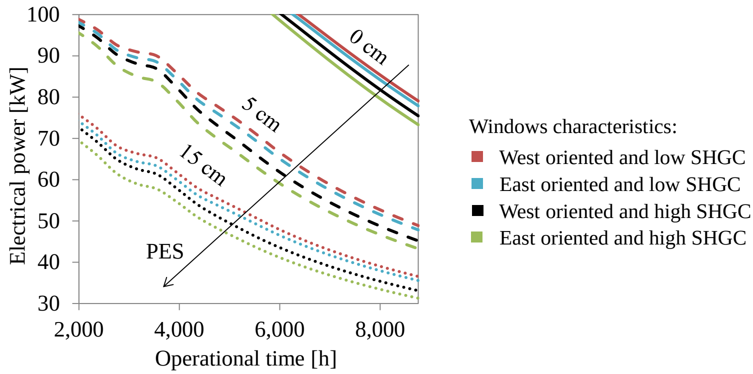

Fig. 5.5 – Curves of PES equal to zero depending on the power plant size and the operational time for all the considered building configurations.

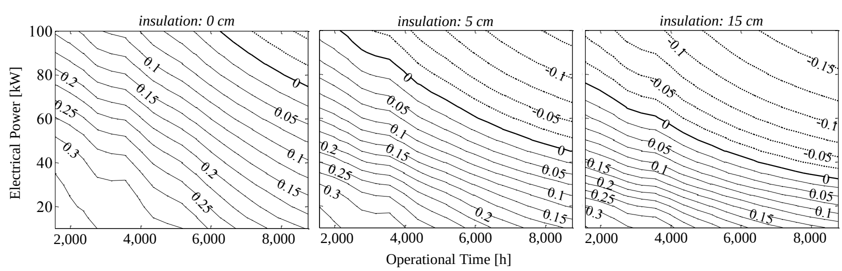

Fig. 5.6 – Iso-PES curves depending on the power plant size and the operational time for three building configurations (0, 5, 15 cm of the thermal insulation of the opaque envelope).

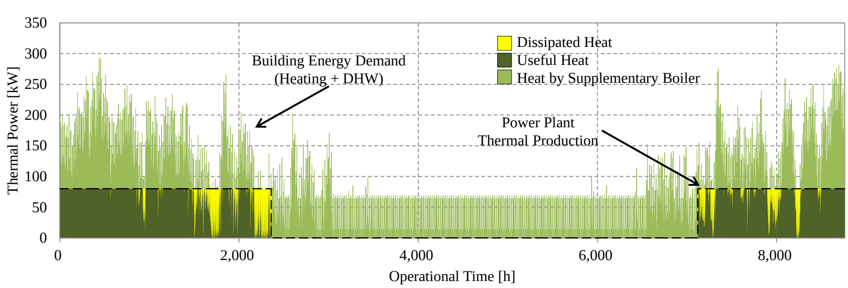

Fig. 5.7 – Heat demand of the building without thermal insulation in the opaque envelope and heat generation by a power plant of 30 kW_{el} operating for 4000 h per year.

Fig. 5.7 compares the thermal load of the buildings without envelope insulation and the heat produced by a power plant for the entire year. As previously mentioned, a higher thermal power production could be entirely exploited only during the coldest months; the produced heat would be discharged for most of the operational time.
Considering the smallest possible plant size (30 kW_{el}), Fig. 5.8 shows the discounted cash flow for the power plant running for 2000, 4000 and 6000 h and considering scenarios either with or without subsidization. The economic analysis has been performed for the three analysed building configurations (0, 5, 15 cm of the envelope insulation). Considering the incentive regime, power plants with low operational time, e.g. less than 4000 h, move to high payback time due to a long amortisation schedule. Moreover, the feed-in tariff is guaranteed for 20 years, afterwards the revenues have the same order of magnitude of the operational costs with a resulting profit close to zero or even negative. The discounted cash flow, corresponding to the scenario without incentives, shows that the gasification system profitability strictly depends on the incentive paid for the electricity production. Fig. 5.9 compares the revenues of the considered system, and it highlights the importance of the heat valorisation, in particular for the scenario without incentive. With current market prices, the revenue coming from a full utilization of the generated heat would be higher than the revenue for the electricity trade (i.e. simplified purchase & resale arrangements). The revenue coming from heat valorisation has been displayed in EUR/kWh_{el} for comparison purposes, but it can be converted in EUR/kWh_{th} multiplying the power-to-heat ratio (i.e. 0.375).

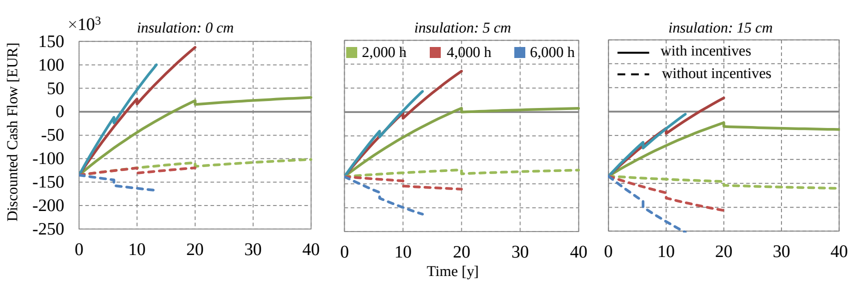

Fig. 5.8 – Discounted cash flows for a power plant of 30 kW_{el}, considering three operational times (2000; 4000; 6000 h) and three building configurations (0, 5, 15 cm of the thermal insulation of the opaque envelope). Incentive regime with solid line and scenario without incentive with dotted line.

Fig. 5.10 shows the payback time and the annual worth for the three analysed building configurations. The choice of the optimal operational time could be based on AW rather than PBT, depending on the optimization target of the investment. Considering the AW, the optimal operational time corresponds to 5000 h (10 006 EUR/y) for the building without envelope insulation, 4000 h (5,748 EUR/y) for the building with 5 cm of insulation and 4000 h (1,914 EUR/y) for the building with 15 cm of insulation. The optimal operating time is close to 4000 h because it corresponds to the heating season duration in which a significant share of heat, produced by the CHP system, is used for both DHW and space heating. Considering the PBT, the optimal operational time corresponds to 8000 h both for the buildings without envelope insulation and for those with 5 cm of insulation (respectively, 6.9 and 9.2 y), and 5000 h for the building with 15 cm of insulation (14.7 y). As far as the configurations with high optimal operating time (i.e. 8000 h) are concerned, it has to be taken into account that the corresponding AW is quite low because considerable heat has to be discharge to the environment since the users require only DHW for almost half of the year. Figs. 5.11 and 5.12 show the incidence of a relative variation (-20 % – +20 %) on investment cost, biomass cost, feed-in tariff, cogeneration bonus and heat valorisation to NPV (Fig. 5.11) and PBT (Fig. 5.12). The graphs correspond to a 30 kW_{el} CHP system operating 4000 h for the three analysed building configurations (0, 5, 15 cm of the envelope insulation). The feed-in tariff has been found to be the parameter that mainly influences both NPV and PBT while the cogeneration bonus, which is related to the useful heat, has been detected as the parameter with the lower impact. These results confirm the need to update the subdivision of the subsidization, increasing the extent of the cogeneration bonus to promote the design of systems that properly valorise the heat share. This finding is also in agreement with the conclusions drawn by Noussan et al. (2013) in a case study of a biomass-fired CHP system coupled with a district heating.

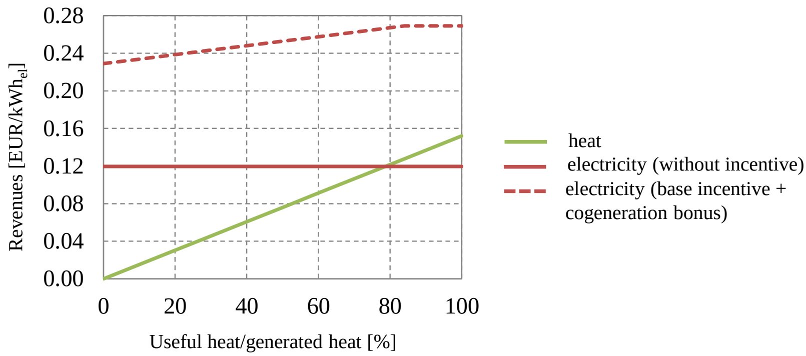

Fig. 5.9 – Revenues from heat and electricity depending on the useful heat (both the revenues refer to the kWh$_{el}$ generated by the power plant). Incentive regime with dotted line and scenario without incentive with solid line.

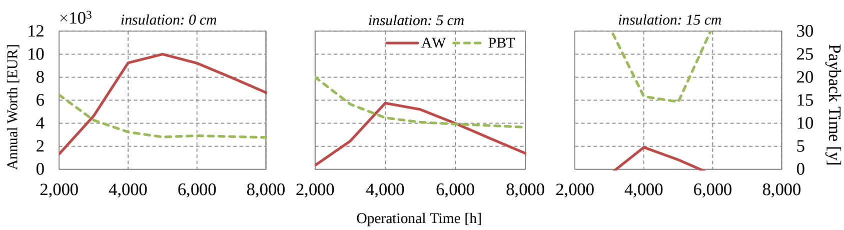

Fig. 5.10 – Annual Worth (AW) and Payback Time (PBT) for a 30 kW$_{el}$ power plant, considering different operational times and building configurations (0, 5, 15 cm of the thermal insulation of the opaque envelope).

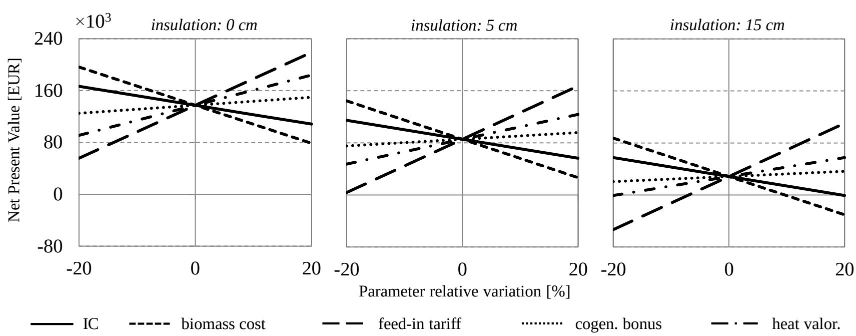

Fig. 5.11 – Incidence of the parameters (IC, biomass cost, feed-in tariff, cogeneration bonus, heat valorisation) on the NPV for a 30 kW$_{el}$ CHP system operating 4000 h for the three analysed building configurations (0, 5, 15 cm of the envelope insulation).

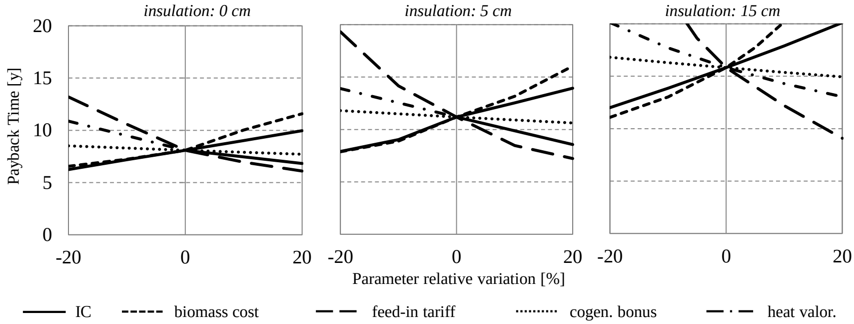

Fig. 5.12 – Incidence of the parameters (IC, biomass cost, feed-in tariff, cogeneration bonus, heat valorisation) on the PBT for a 30 kW_{el} CHP system operating 4000 h for the three analysed building configurations (0, 5, 15 cm of the envelope insulation).

Some detailed results about the energetic assessment are shown in Table 5.3 considering a power plant of 30 kW_{el} and different operational time (i.e. 2000; 4000; 6000; 8000 h). PES is greater than zero for all the three building configurations. For high operational time, the building heat demand covered by CHP is a considerable share but also the discharged heat is considerably high, in particular for the buildings with thermal insulation. These results highlight the complexities satisfying a large share of building heat demand and, having at the same time, a negligible share of heat discharged into the atmosphere.

Table 5.3 – PES, disposed heat and heat by CHP system depending on the operational time (2000; 4000; 6000; 8000 h) for a CHP system of 30 kW_{el}.

		Building Configurations:		
	Oper. time [h]	Insulation: 0 cm	Insulation: 5 cm	Insulation: 15 cm
PES	2000	0.32	0.29	0.22
	4000	0.29	0.23	0.15
	6000	0.22	0.15	0.07
	8000	0.15	0.09	0.03
Disposed Heat by CHP	2000	4 %	13 %	32 %
	4000	14 %	29 %	46 %
	6000	30 %	46 %	59 %
	8000	44 %	56 %	66 %

Building heat	2000	29 %	43 %	46 %
demand	4000	52 %	70 %	73 %
covered by	6000	63 %	80 %	83 %
CHP	8000	67 %	87 %	92 %

5.3 Main findings

This study proposes an integrated approach for the assessment of the energy and economic performance of a biomass gasification CHP system installed in a residential block. This approach allows the estimation of the performance of the system in operation and provides indications for the design of energetically and economically efficient systems.

For all the considered building configurations (12 alternatives), the PES analysis shows the possibility to set-up a biomass gasification CHP that allows a primary energy saving with respect to the separate production of heat and power. The primary energy saving depends on the heat discharged; the less heat is discharged, the larger is PES. A better exploitation of heat could be reached increasing the number of users that are served by the power plant but in that case a district heating system could be a more plausible scenario.

At the current stage, partial or on/off operation of the gasification systems is not a feasible option due to management complexities to reach a steady state operation. Since the gasification power plant should run continuously, the heat discharged is strictly related to both plant size and thermal load profile of the final user. Therefore, the nominal power of the plant has to be considerably lower than the building peak load in order to limit the discharge heat. As a consequence, the heat demand of buildings has to be partially supplied by a back-up boiler, thus losing some benefits given by cogeneration. The gasification power plant, because of its management complexities for the on/off operation, should be installed as base thermal load station.

The economic analysis based on the power plant of 30 kW_{el} shows there is a considerable influence of the useful heat on the discounted cash flow for both the scenario with and without incentive. The useful heat amount is related to the heat load profile, which varies for each building configuration. At the current stage of the technology, the incentive is essential for an economic return of the investment. The use of the heat share generated by a CHP system – even if it is based on renewable energy – is very important to promote high efficiency system in operation. With the current subsidization, the use of the generated heat is not fundamental for the business plan. Such subsidization distorts the energy sector, promoting the electricity generation instead of the primary energy saving.

6. Building refurbishment and DH systems

The recast of Energy Performance of Buildings Directive (EPBD) (European Commission 2010) states that by the end of 2020, all new buildings should be nearly zero-energy buildings, and in the meanwhile, the performance of the buildings that undergo major renovation should be upgraded in order to meet the minimum energy performance requirements in accordance with the cost-optimal level. The Commission Delegated Regulation EU 244/2012 (European Commission 2012) established a methodology for the calculation of the cost-optimal based energy performance requirements for new and existing buildings. The result should be a trade-off between the maximum energy saving and the minimum economic costs.

Moreover, Member States should ensure that, before the construction of new buildings starts, the technical, environmental and economic feasibility of high-efficiency alternative systems is considered. Among these systems, the normative reports: decentralized energy supply systems based on energy from renewable sources, cogeneration, district or block heating or cooling (European Commission 2010). However, the promotion of both building refurbishment and district heating (DH), as suggested by the EPBD recast, seems a contradiction from both the economic and the energy point of view. On the one hand, the reduction of heating demand of the buildings allow the fuel consumption in the DH area to be reduced (Nielsen and Möller 2013). On the other hand, it causes a reduced utilization of the DH capacity with a consequent reduction of both the distribution efficiency (because constant network losses will be a higher fraction if the total heat is reduced) and the revenues. For this reason, the existing DH systems need to be upgraded in order to be an efficient solution in the future, and the construction of new DH network has to properly consider the development of the building stock.
Building refurbishment could reduce the difference of thermal power between the heating season and the period with only DHW demand (Lund et al. 2014). A more constant heat load during the year would enable a higher equivalent utilization time of a new CHP system installed with a proper size. However, also in the case of DH networks, the minimum heat demand could

be very low and would not justify the installation of a CHP plant (Sartor et al. 2014).

The extension of the existing network could be considered as a possible solution to tackle the reduced utilisation of the DH capacity. However, it has to be carefully evaluated, taking into account both the additional heat losses, due to the network extension, and the additional heat need of the new users. This trade-off strictly depends on the energy density of the potential areas and their distance to existing DH networks. Moreover, the economic feasibility of the DH extension is related to its investment costs (Münster et al. 2012; Connolly et al. 2014).

The reduction of heat demand is not considered a barrier for the DH systems in high density areas. In contrast, those systems can lose competitiveness in low heat density areas. According to Persson and Werner (2011), three determining factors emerge as critical: the future competition on the heat market, the current use of district heat, and the future city shapes.

The reduction of the grid temperatures (i.e. supply and return) is another measure, mentioned in literature, to upgrade the DH systems. Both heat exchangers and radiators are usually oversized because they are usually designed for the most critical weather condition. Actually, this condition rarely occurs and, therefore, a reduced network temperature could be sufficient to satisfy the building heat need. A lower temperature means lower network losses and thus higher distribution efficiency of the DH network. The control of the DH mass flow, by means of pumps with inverters, could also be implemented to increase the heat transfer while reducing return temperature and pumping power (Kuosa et al. 2013; Yan et al. 2013). Moreover, the use of a control algorithm (i.e. adaptive control) to produce the lowest possible return temperature of the network enables a further improvement of the DH efficiency (Lauenburg and Wollerstrand 2014).

According to Gustafsson et al. (2010), the grid supply temperature should be used as an indicator of the outside temperature to control the temperature of the heating system of the buildings. Moreover, a customised system control curve (i.e. correlation between the system supply temperature and the local outdoor temperature) should be defined for each DH system, by means of

simulation tools, in order to increase the network ΔT and consequently reduce the pumping power.
A pilot project carried out in Denmark, showed that the low temperature district heating (LTDH), i.e. 55/25 °C (supply/return), is a suitable solution for DH systems in low heat density area with low energy buildings (Li and Svendsen 2012). In accordance with Dalla Rosa and Christensen (2011), LTDH systems in areas with linear heat density of 0.20 MWh m^{-1} $year^{-1}$ are supposed to be feasible from an energy and economic point of view. In addition, a correct use of the buildings by the occupants could lead to a 60 % peak load reduction with significant benefits in terms of efficiency of the DH system (Dalla Rosa and Christensen 2011). In existing DH systems, the DH managers cannot force the users to adopt measures that aim to decrease the temperature level of their heating systems, but they could try to promote it by means of heat price depending on the temperature level.
A study, carried out on a DH plant based on a CHP system, highlighted that a decrease of the DH network temperature of 10 °C can improve the electric efficiency of the ORC generator by one percentage point. Moreover, the temperature reduction could decrease the main losses of the boiler, namely the exhaust latent thermal loss and the exhaust sensible thermal loss (Prando et al. 2015a).
This study aims to define the energy and economic performance of the DH system, considering cost-optimal solutions for the refurbishment of buildings connected to the DH system. The study focuses on micro networks, with less than 20 buildings, since they could be particularly affected by refurbishment of the connected buildings due to the limited number of users. The heating need is calculated by means of TRNSYS 17. The domestic hot water need has been quantified in accordance with UNI/TS 11300-1 (UNI 2008a) and a model of the distribution network has been developed for the purpose. Several measures have been considered for the refurbishment of buildings and a genetic algorithm is used to reduce the number of configurations to investigate among all the possible combinations to get the optimal ones. Firstly, the retrofit measure that minimizes both the energy consumption and the NPV is defined for each considered building. The buildings are then ranked according to increasing cost-optimal NPV and, therefore, each addi-

tional refurbished building in the network creates a new scenario. Each scenario, with a different number of refurbished buildings in the network, has been analysed comparing two strategies as for the supply temperature: the current fixed network temperature − i.e. 90 °C − and the lowest network temperature required by the most critical building. Moreover, an incentive for the promotion of low temperature heat has been considered as a potential measure to improve the DH systems in the near future. Finally, primary energy (EP), NPV, distribution efficiency and the generation-distribution efficiency of the whole DH system have been calculated.

6.1 Materials and methods

6.1.1 Reference buildings

The retrofitting of buildings is investigated by means of several energy simulations in order to find the cost optimal solutions. The multi-objective optimization analysis focuses on different residential buildings representative of the South Tyrol context. The floor area has been sized on the weighted average surface for residential buildings computed from the data provided by the National Statistical Institute (i.e. Istituto Nazionale di Statistica – ISTAT). Each building has been simplified as a base module with a square floor and an internal height of 3.0 m.

Besides, 14 representative buildings have been defined in order to represent a typical set of buildings connected to the micro-grid in South Tyrol. Each building has been assigned to one of the three construction periods according to the statistics provided by National Statistical Institute (i.e. Istituto Nazionale di Statistica – ISTAT). In South Tyrol, 37 % of the residential buildings was built before 1960, 49 % between 1960 and 1991, and 14 % after 1991 (ISTAT 2001). The construction period is important since it is associated with a specific type of building envelope. Hence, it strongly affects the assessment of the interventions that are economically and technically efficient.

The thermal characteristics of the opaque envelope have been chosen according to the abacus of the existing buildings published in the Italian technical report UNI/TR 11552 (UNI 2014). The opaque envelope is a simplified two-layer structure with a massive clay block layer on the internal side

and an insulating layer on the external side. The glazing system is a single-pane glass (buildings before 1991) or double-pane glass (buildings after 1991) with standard timber frame equally distributed on the four vertical walls for a total area of 15 % the floor area. The glazed surface has a solar heat gain coefficient (SHGC) equal to 0.810 both for single-pane and double-pane glass, see Table 6.1. The ventilation rate corresponds to an air change rate per hour of 0.3 h^{-1}, in accordance with UNI/TS 11300-1 (UNI 2008a).
A hydronic system with a radiator emission system has been adopted for all the building classes. The radiators have been modelled by implementing in the software the characteristic curve with an exponent equal to 1.3.
The domestic hot water (DHW) need has been determined in accordance with the Italian technical specification UNI/TS 11300-2 (UNI 2008b). All buildings in the past were equipped with an autonomous system for both floor heating and DHW production, usually a biomass boiler coupled with a storage tank. The tank was reused in the new facility connected to the district heating. For this reason, the DHW needs have been considered uniform over the period 8 AM to 12 PM, that coincides with the charge phase of the storage tank.
The analysis is carried out using the weather conditions of Bolzano, HDD20=2791 K d, which is the most populated city of the province.

Table 6.1 – Characteristic of the envelope and heating system of the reference cases.

Reference building before 1960					
Opaque Envelope				Windows	Single-pane
	Clay	Insulation		U_{gl} (W m^{-2} K^{-1})	5.693
d (m)	0.2	0		SHGC	0.810
λ (W m^{-1} K^{-1})	0.25	0.04		Frame	Std Timber
ϱ (kg m^{-3})	893	40		U_f (W m^{-2} K^{-1})	3.2
c (J kg^{-1} K^{-1})	840	1470		$A_f/A_{wind.}$ (%)	22.2
Reference building between 1960 and 1991					
Opaque Envelope				Windows	Single-pane
	Clay	Insulation		U_{gl} (W m^{-2} K^{-1})	5.693
d (m)	0.2	0.01*		SHGC	0.810
λ (W m^{-1} K^{-1})	0.25	0.04		Frame	Std Timber
ϱ (kg m^{-3})	893	40		U_f (W m^{-2} K^{-1})	3.2
c (J kg^{-1} K^{-1})	840	1470		$A_f/A_{wind.}$ (%)	22.2
Reference building after 1991					
Opaque Envelope				Windows	Double-pane
	Clay	Insulation		U_{gl} (W m^{-2} K^{-1})	3.44
d (m)	0.2	0.05		SHGC	0.757
λ (W m^{-1} K^{-1})	0.25	0.04		Frame	Std Timber
ϱ (kg m^{-3})	893	40		U_f (W m^{-2} K^{-1})	2.63
c (J kg^{-1} K^{-1})	840	1470		$A_f/A_{wind.}$ (%)	22.2

*equivalent to an air cavity with a thermal resistance of 0.25 m^2 K W^{-1}

6.1.2 Refurbished buildings performance and economic analysis

The research aims to analyse the extent to which the refurbishment of building connected to district heating can become an issue for the district heating manager. For this reason, the main standard energy saving measures that affect the reduction of the energy needs of the building have been investigated. The following measures have been considered in this analysis, and the thermo-physical parameters of the new solutions are reported in Table 6.2:

- external insulation of the vertical walls (VW) with a possible thickness increment from 1 cm (0.39 in) to 20 cm (7.87 in) using a 1 cm (0.39 in) step;

- external insulation of the roof (RW) with a possible thickness increment from 1 cm (0.39 in) to 20 cm (7.87 in) using a 1cm (0.39 in) step;
- external insulation of the floor (FW) with a possible thickness increment from 1 cm (0.39 in) to 20 cm (7.87 in) using a 1cm (0.39 in) step and screed replacement (SR);
- replacement of existing glazing systems with higher thermal performance windows such as double or triple-pane with either high or low solar heat gain coefficients. Besides, also the frames are replaced with an improved aluminium frames with thermal break;
- installation of a mechanical ventilation system with heat recovery (MVHRS) to control the air exchange;
- replacement of the high temperature hydronic system with a underfloor heating, that ensure a reduction of the supply water temperature of the house. Also this intervention requires the screed replacement (SR).

  Additionally, the substitution of the windows causes the reduction of the infiltration rates that becomes a half of the original values.

Table 6.2 – Refurbishment measures, IC without VAT and parameters for the economic analysis.

Opaque Envelope: Insulation Layer			
Thermal characteristic of Polystyrene EPS			IC (EUR m^{-2}) (1)
λ (W m^{-1} K^{-1})	0.04		t = thickness (cm)
c (J kg^{-1} K^{-1})	1470		$IC_{VW} = 1.6\ t + 38.53$
ϱ (kg m^{-3})	40		$IC_{HW} = 1.88\ t + 8.19$
Transparent Envelope			
Aluminium Frame with thermal break Uf = 1.2 (W m^{-2} K^{-1})			
Glazing	U_{gl}	SHGC	IC (EUR m^{-2}) (1)
DH – Double, high SHGC (4/9/4, krypton, low-e)	1.140	0.608	$IC_{DH} = 404.33$
DL – Double, low SHGC (6/16/6, krypton, low-e)	1.099	0.352	$IC_{DL} = 439.06$
TH – Triple, high SHGC (6/12/6/12/6 krypton,low-e)	0.613	0.575	$IC_{TH} = 477.65$
TL – Triple, low SHGC (6/14/4/14/6 argon, low-e)	0.602	0.343	$IC_{TL} = 454.49$

<table>
<tr><td colspan="4">Mechanical ventilation heat recovery system (MVHRS)</td></tr>
<tr><td>Ventilation Rate ($m^3 h^{-1}$)</td><td colspan="2"></td><td>IC (EUR) (1)</td></tr>
<tr><td>Power ($W/(m^3/h)$)</td><td colspan="2">0.4</td><td>IC_{MV} = 6000 EUR</td></tr>
<tr><td colspan="4"></td></tr>
<tr><td colspan="4">Parameters for the economic analysis</td></tr>
<tr><td>Heat price (2)</td><td>0.10 EUR kWh^{-1}</td><td>Electricity Cost (4)</td><td>0.25 EUR kWh_{el}^{-1}</td></tr>
<tr><td>Increase heat price (3)</td><td>2.8 %</td><td rowspan="2">Increase electricity price (3)</td><td rowspan="2">1.71 %</td></tr>
<tr><td>VAT</td><td>10 %</td></tr>
<tr><td></td><td></td><td>Real Interest Rate</td><td>3 %</td></tr>
</table>

(1) (Penna et al. 2014); (2) (Gasser and Meran 2014); (3) (European Commission 2009); (4) domestic customer (AEEG 2013)

The reference prices (see Table 6.2) of the different refurbishment measures are obtained from a survey comparing the prices in different zones of the national territory (Penna et al. 2014). The prices are also expressed in USD considering the average exchange rate of the last 10 years. The NPV for each retrofit solution is based on the methodology proposed by the regulation EU 244/2012 (European Commission 2012) and computed according to the EN 15459:2009 (UNI 2007) procedure. A lifespan of 30 years has been used in the calculation for the evaluation of the initial investment cost (IC), the running costs (i.e. maintenance, operational and energy costs), the replacement cost, due to periodic substitution of building elements, and the residual value at the end of the calculation. All the refurbishment measures have been considered to be implemented without any loan. The running costs caused by the heating and power consumption have been computed by means of a dynamic simulation model with a time step of 1 hour. The dynamic simulations have been carried out by means of TRNSYS which is validated in accordance with BESTEST (Neymark et al. 2005) and recently compared with other simulation tools (Pernigotto and Gasparella 2013), therefore, the obtained results are considerably independent by the choice of the simulation tool.
Two scenarios have been investigated for the heat price. The first scenario considers a constant price of 0.10 EUR kWh^{-1}, and this is the current scenario in South Tyrol. In the second one, the heat price has been determined in

accordance with the temperature level of the required heat. For a supply temperature of 75 °C, the price has been set at 0.10 EUR kWh^{-1}, while for 50 °C it has been set at 0.09 EUR kWh^{-1}, with a linear trend in between. The heat price equation is reported hereinafter:

$$Price_{heat} = 0.10 + \frac{0.010}{25} \cdot (T_{\substack{supply \\ secondary}} - 75) \qquad [\text{EUR kWh}^{-1}] \qquad (1)$$

where $T_{supply,\ secondary}$ is the temperature supply at the secondary hydraulic circuit, expressed in °C.

The full parametric analysis of the energy conservation measures would take a considerable computational time. To overcome this problem, a Genetic Algorithm code has been implemented in Matlab environment (Holland 1975; Haupt and Haupt 2004; Penna et al. 2014). The algorithm used to discover the cost-optimal mixing of the energy saving solutions is the elitist Non-dominated Sorting Genetic Algorithm (NSGA-II) developed by Deb et al. (2002). The fitness function, used in the analysis, is a Matlab code that launches automatically the TRNSYS model for the building energy simulation. After the model execution, the function reads the TRNSYS output file and post-processes the results. The code defines the initial population of the parameters by using a Sobol's sequence sampling (Saltelli et al. 2004). This pseudo random number generator avoids the oversampling of same region that can occur with random sampling. Moreover, Sobol's sequence is a low-discrepancy sequence, which aims to give a uniform distribution of values, and has the advantages of reducing the random behaviour of the genetic algorithm and giving a good individuals' collection as initial population. In the Matlab code, a tournament selection without replacement TSWOR with 0.5 fraction has been adopted. Similarly, the crossover and mutation have been implemented using a arithmetic crossover fraction of 0.8 and a uniformly distributed random value for mutation.

The refurbishment measures, that allow the minimization of both the heat demand and NPV, define the cost-optimal configurations. These configurations correspond with the so-called Pareto front that has been defined for each building connected to the network.

6.1.3 Numerical model of the DH system

A numerical model has been developed to simulate the thermal behaviour of a DH network and calculate its performance. The network implemented in the model has been defined as an average of 13 micro networks located in South Tyrol, a mountainous area in northern Italy. The study focused on micro DH − total length shorter than 3 km – because of the limited number of users which are connected to the grids. A high number of buildings could be a problem due to a high computational time required for the building simulation. Moreover, these networks could be particularly affected by refurbishment of the connected buildings due to the limited number of users. However, the results of this study can be extended to larger systems.

The network consists of pre-insulated steel pipe, whose main characteristics are reported in Table 6.3. The piping has been chosen on the basis of the commercial sizes regulated by the standard EN 253. The pipes are considered to be installed 80 cm underground on average.

Table 6.3 – Characteristics of the pre-insulated pipes for district heating network.

DN (mm)	20	25	32	40	50	65	80	100	125	150
$t_{ins.}$ (mm)	29	25	31	28	29	29	32	39	39	36
$\lambda_{ins.}$ (W m^{-1} K^{-1})	0.03									

The network has been designed on the basis of the design heat load of the connected buildings, which has been calculated in accordance with the European normative EN 12831:2003 (CEN 2003). This approach can be used to calculate the size of the network piping, the heat exchanger of each substation and the boiler. In accordance with the normative, the design heat load is calculated considering the transmission and ventilation heat losses without taking into account the solar and internal heat gains. For residential buildings, the minimum ventilation thermal loss is calculated with an air change rate per hour of 0.5 ACH. According to the national specification (UNI 2006), the external design temperature for Bolzano, county town of South Tyrol, is -15 °C.

The mass flow rate, through the heat exchanger of each building substation, has been calculated on the basis of the design heat load and the temperature

difference (supply and the return of the primary network). The piping from the generation system to each building is sized to keep the water velocity lower than 2 m s^{-1} in the main branches (transportation pipes) and 1.75 m s^{-1} in the secondary branches (distribution pipes) (Vallios et al. 2009). Furthermore, the specific total pressure drop is kept below 980 Pa/m in order to avoid high electricity consumption of the circulation pump.
The heat transfer coefficient between the water and the ground is calculated for each segment of the network depending on its diameter, insulation thickness and length. The heat loss of the entire network is hourly computed depending on the network temperatures and ground temperature. The ground temperature at a depth of 80 cm is computed with Trnsys 16.1 considering a mean surface temperature of 12.6 °C (UNI 1994), an amplitude of the surface temperature of 10.1 °C (UNI 1994), a soil thermal conductivity of 2 W m^{-1} K^{-1}, a soil density 2500 kg m^{-3} and a soil specific heat of 0.8 kJ kg^{-1} K^{-1}. The network temperature is defined hourly in accordance with the temperature requirement of the most critical building in terms of temperature. The radiators of each building have been sized to provide the nominal power at the design heat load condition with an average temperature of around 70 °C, i.e. typical value if no control strategy is adopted. During the heating season, in particular for the refurbished buildings, the heating load of each building is lower than the design heat load. For this reason, the radiator temperature, and therefore the network temperature, can be lower. On this basis, the minimum temperature required on the network has been calculated hourly and it represents the minimum theoretical temperature for the network.
The temperature drop along the network has not been considered because of its negligible contribution; the farthest building is about 0.4 km from the plant and the temperature drop has been estimated to be around 3 °C/km. The minimum limit temperature of the network has been fixed at 65 °C in order to ensure the domestic hot water (DHW) production (Brand et al. 2013). Although a lower temperature in the supply line − i.e. 50–55 °C − could be sufficient for DHW production, it strongly depends on the heat exchanger characteristics (Brand et al. 2010; Dalla Rosa and Christensen 2011).

The size of the pellet boiler has been determined in accordance with the design load calculated through the EN 12831:2003 (CEN 2003), as mentioned at the beginning the section. The generation efficiency has been considered to be 0.9 at nominal load and 0.88 at 30 % of the nominal load, considering a linear trend in between (KWB 2014). These values have been used for the calculation of the pellet consumption of the boiler. The circulation pump has been considered to be coupled with a motor for fixed speed operation. Its electricity consumption has been hourly calculated depending on the water mass flow rate and pressure drop in each segment of the network.

6.1.4 Energy and economic analysis of the district heating

The refurbished buildings, after the multi-objective optimization, have been ranked from the lowest to the highest NPV. The buildings on the top of the list are more likely to be refurbished because of the lower NPV permitted by the optimal refurbishment solution. The DH scenario changes every time that an additional building connected to the network is refurbished. For each scenario (15 in total considering the reference case with no refurbished buildings), distribution efficiency, generation-distribution efficiency, EP and NPV of the district heating have been calculated.

The distribution efficiency of the district heating system has been calculated with the following formula:

$$\eta_{\text{distribution}} = 1 - \frac{E_{\substack{\text{network}\\ \text{loss}}}}{E_{\text{boiler}}} \tag{2}$$

where $E_{\text{network, loss}}$ (kWh) is the network heat loss and E_{boiler} (kWh) is the output heat from the boiler.

The generation-distribution efficiency of the district heating system has been calculated with the following formula:

$$\eta_{\substack{\text{generation}\\ \text{distribution}}} = \frac{E_{\text{h}} + E_{\text{DHW}}}{m_{\text{pellet}} \cdot LHV_{\text{pellet}} + E_{\text{e}} \cdot f_{PE}} \tag{3}$$

where E_{h} (kWh) is the space heating need, E_{DHW} (kWh) is the DHW need, m_{pellet} (kg) is the pellet consumption of the boiler, LHV_{pellet} (kWh kg^{-1}) is the lower heating value of pellet, E_{e} (kWh) is the electricity self-consumption of the auxiliaries and f_{PE} is the conversion coefficient from electrical to primary energy. In Italy, f_{PE} is currently fixed at 2.174 (AEEGSI 2008) but it is periodically updated according to the average electrical efficiency of the national grid. The lower heating value of pellet has been considered 4.7 kWh kg^{-1} (UNI 2011).

The EP (kWh $year^{-1}$) of the DH system has been calculated with the following formula:

$$EP = m_{\text{pellet}} \cdot LHV_{\text{pellet}} + E_{\text{e}} \cdot 2.174 \quad (4)$$

The NPV of the DH system has been calculated as the sum of the discounted cash flow over a period of 30 years (Dalla Rosa and Christensen 2011; Reidhav and Werner 2008). The present work investigates the refurbishment of the existing DH systems and, therefore, does not consider the investment costs of both plant and network. The formula for NPV is the following:

$$NPV = \sum_{t=0}^{t=30} \frac{(E_{\text{h}} + E_{\text{DHW}}) \cdot p_{heat} - m_{\text{pellet}} \cdot p_{\text{pellet}} - E_{\text{e}} \cdot p_{\text{electricity}} - m_{ash} \cdot p_{\substack{\text{ash}\\ \text{disposal}}} - C_{\text{maint.}}}{(1+i)^t} \quad (5)$$

where p_{heat} is the price of the heat delivered to the users, p_{pellet} is the price of the input pellet and $p_{electricity}$ is the price of electricity used by the auxiliary equipment, m_{ash} is the ash production, $p_{ash,disposal}$ is the price for ash disposal, $C_{maint.}$ is the maintenance cost, t is the time of the cash flow and i is the discount rate (i.e. i = 3 %). The inflation rates of electricity and heat have been considered to be 1.71 % and 2.8 %, respectively (see Table 6.2). The inflation of pellet price, as well as the remaining prices, has been considered the same as that of heat (i.e. 2.8 %). Ash production has been calculated as 1.5 % the pellet consumption (UNI 2011). Table 6.4 reports the operational costs (pellet, auxiliary electricity, ash disposal, maintenance), and the revenues (heat trade) required to perform an economic analysis, VAT and other taxes excluded.

Table 6.4 – Prices for heat, pellet, electricity, ash disposal and maintenance.

	Price	Reference
Heat sale (EUR /kWh)	0.10	Networks survey
Pellet (EUR /t)	263.5	(IRE 2014)
Aux. Electricity* (EUR /kWh)	0.1358	(AEEG 2013)
Ash disposal (EUR /t)	150	Networks survey
Maintenance (EUR /kW)	3.2	(Viessmann 2013)
Boiler substitution (EUR)	70	(Viessmann 2013)

*Industrial customer

Moreover, both EP and NPV have been calculated considering two additional scenarios with different floor areas in order to assess the influence of the size of the buildings on both energy and economic analysis. The calculation of the cost-optimal measures of new buildings takes a considerable computational time, therefore the building stock has been divided into two categories; the buildings that are smaller than the median and the ones that are larger. A scenario with smaller buildings has been defined considering twice the buildings below the median and a scenario with larger buildings has been defined considering twice the buildings above the median.

Finally, the installation of a CHP system has been considered as potential measure to improve the DH profitability. A gasification system has been considered as possible solution to produce electricity – to be delivered to the national grid – and heat that can be delivered to the buildings through the DH network – the excess heat is considered to be discharged to the atmosphere. The smallest CHP system available in the market has been considered to be operated continuously for entire year. In this case the biomass boiler is used as back-up boiler and to supply heat when the DH demand is higher than the CHP heat production. The economic analysis for the DH system with a CHP generator has been conducted considering the costs in Table 6.4 and in Table 6.5, namely the investment costs (IC), the operational costs, the feed-in tariff and the revenues (VAT and other taxes excluded) related to the CHP system. The details of the energy and economic performance of the gasification system are reported in section 5.2.4.

Table 6.5 – Costs for the economic analysis (Prando et al. 2014a).

Item	Price
IC, gasifier (EUR kW_{el}^{-1})	4000
IC, engine (EUR kW_{el}^{-1})	500
Maintenance cost (EUR kWh_{el}^{-1})	0.050
Biomass cost (EUR t^{-1})	165
Feed-in-tariff (EUR kWh_{el}^{-1})	0.220
Cogeneration bonus (EUR kWh_{el}^{-1})	0.040
Char disposal (EUR t^{-1})	150

6.2 Results and discussion

6.2.1 DH network survey

The survey of the 13 micro DH networks located in South Tyrol is summarised in Fig. 6.1 (Autonomous Province of Bolzano 2014). Most of them have similar features, in terms of energy demand, and the distance from the plant follows a linear trend according to the consumption. The buildings that are particularly far from the plant generally have a high heat demand that justifies the effort to cover such a distance. Fig. 6.1 reports also the average network (marked in dashed line) that has been elaborated as arithmetic mean in terms of number of buildings and length of each pipe segment. Table 6.6 reports the distance of each building from the power plant in terms of piping length.

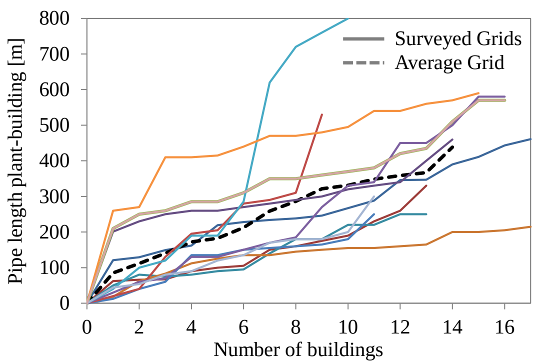

Fig. 6.1 – Pipe length from the power plant to the buildings for the surveyed networks and average network.

Table 6.6 – Pipe length from the power plant to each building for the elaborated average network.

Building #	1	2	3	4	5	6	7	8	9	10	11	12	13	14
Pipe length (m)	85	112	140	172	183	212	259	286	321	331	348	358	367	438
Floor area (m^2)	126	182	422	375	245	75	139	111	129	341	392	89	356	179

6.2.2 Building retrofitting

The multi-objective optimization has been carried out in accordance with the cost-optimal approach for each building connected to the network. Fig. 6.2 and Fig. 6.3 show the Pareto front for all the buildings connected to the DH network. The blue dots in the graph are the ones that optimize both the NPV and heat demand (i.e. cost-optimal refurbishment measures of minimum heat demand). The red dots correspond to the reference case. Fig. 6.2 refers to the scenario with constant heat price while Fig. 6.3 refers to the scenario with incentive for the LT heat (i.e. lower heat price for heat required at lower temperature). Among the different cost-optimal configurations (Pareto front) of each building, the one with the lowest NPV is selected as the refurbishment measure that would be adopted by the building owner.

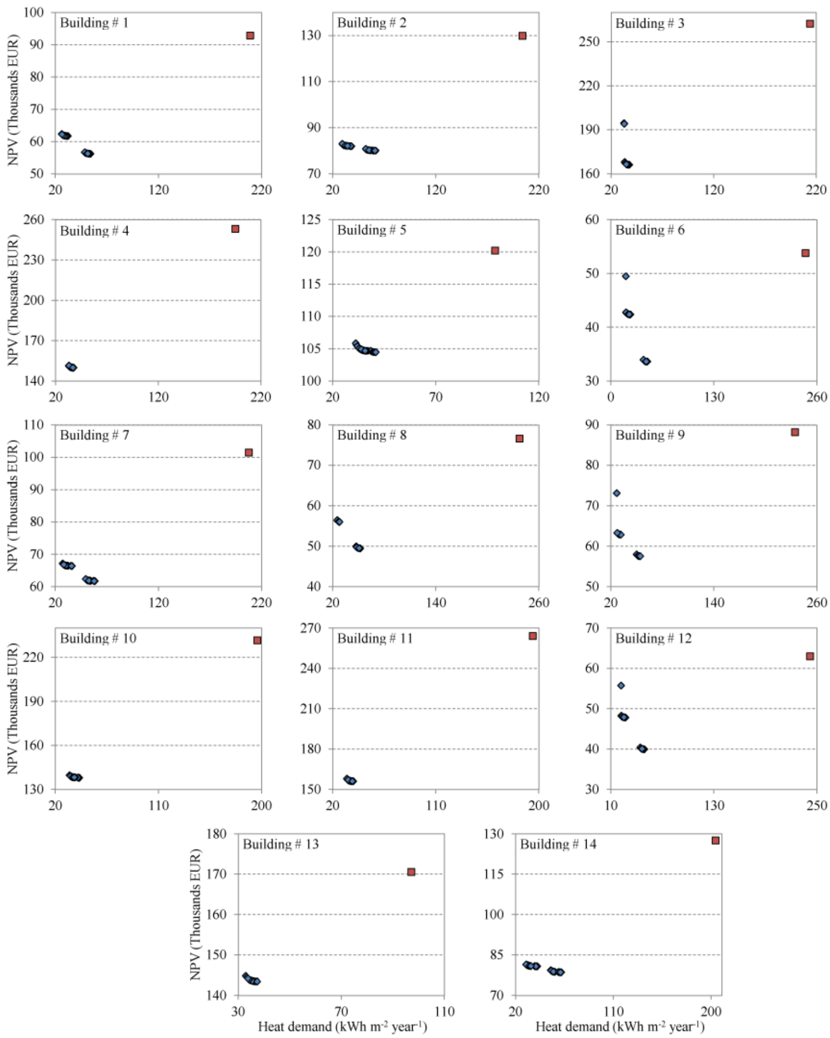

Fig. 6.2 – NPV and EP for the reference case (red dots) and the cost-optimal configurations (blue dots) of the buildings for the scenario with constant heat price.

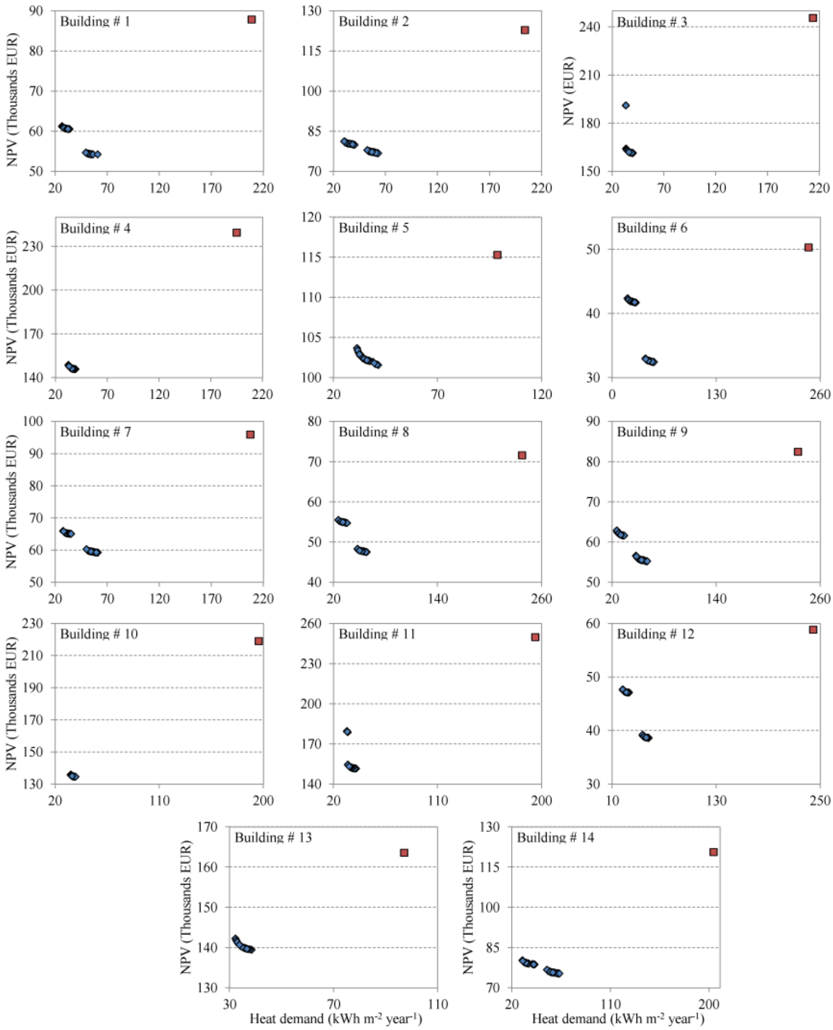

Fig. 6.3 – NPV and EP for the reference case (red dots) and the cost-optimal configurations (blue dots) of the buildings for the scenario with incentive for the LT heat.

Table 6.7 – Building configurations of both reference case and cost-optimal refurbishment for the scenario with a constant heat price.

	Reference case						Cost-optimal					
B	Insulation			Window	Ventilation	ES	Insulation			Window	Ventilation	ES
	W	R	F				W	R	F			
#	cm	cm	cm	-	-	-	cm	cm	cm	-	-	-
1	1	1	1	SGL	NAT	H_T	20	19	15	T_H	NAT	L_T
2	1	1	1	SGL	NAT	H_T	18	17	10	T_H	NAT	L_T
3	0	0	0	SGL	NAT	H_T	19	18	12	T_H	NAT	L_T
4	1	1	1	SGL	NAT	H_T	18	17	10	T_H	NAT	L_T
5	5	5	5	D_H	NAT	H_T	18	16	9	D_H	NAT	L_T
6	0	0	0	SGL	NAT	H_T	19	18	10	T_H	NAT	H_T
7	1	1	1	SGL	NAT	H_T	18	17	11	D_H	NAT	H_T
8	0	0	0	SGL	NAT	H_T	19	18	10	T_H	NAT	H_T
9	0	0	0	SGL	NAT	H_T	18	16	10	T_H	NAT	H_T
10	1	1	1	SGL	NAT	H_T	18	17	10	T_H	NAT	L_T
11	1	1	1	SGL	NAT	H_T	17	17	10	T_H	NAT	L_T
12	0	0	0	SGL	NAT	H_T	19	18	11	T_H	NAT	L_T
13	5	5	5	D_H	NAT	H_T	18	19	13	T_H	NAT	L_T
14	1	1	1	SGL	NAT	H_T	17	16	10	D_H	NAT	H_T

B=building, W=wall, R=roof, F=floor, ES=emission system.

Tables 6.7 and 6.8 report the building configurations of both the reference case and the cost-optimal refurbishment for the scenario with a constant heat price (Table 6.7) and for the scenario with the heat price depending on the temperature level (Table 6.8).

Once the cost-optimal configurations have been defined, the buildings have been ranked from the lowest to the highest NPV, since a smaller NPV values correspond with refurbished buildings more likely to be realized among the whole building stock, assuming a rational approach of the decision makers. Table 6.9 reports both the NPV and the specific space heating demand of each reference case and refurbished building for the scenario with constant heat price. Table 6.10 reports the same information but for the scenario with an incentive for the LT heat (i.e. lower heat price for heat at lower temperature). Moreover, in both the tables the best performance of each refurbished

building (energy optimal) are reported. These results depend on the range of each refurbishment measure, as defined in the previous section.
The results of the optimization depend on the performance of the refurbishment measures, their costs to be implemented and operated, as well as the starting performance and the physical characteristics of the buildings.

Table 6.8 – Building configurations of both reference case and cost-optimal refurbishment for the scenario with the heat price depending on the temperature level.

	Reference case						Cost-optimal					
B	Insulation			Win-	Venti-	ES	Insulation			Win-	Venti-	ES
	W	R	F	dow	lation		W	R	F	dow	lation	
#	cm	cm	cm	-	-	-	cm	cm	cm	-	-	-
1	1	1	1	SGL	NAT	H_T	15	14	12	D_H	NAT	H_T
2	1	1	1	SGL	NAT	H_T	17	17	10	T_H	NAT	H_T
3	0	0	0	SGL	NAT	H_T	17	18	11	T_H	NAT	L_T
4	1	1	1	SGL	NAT	H_T	18	19	15	T_H	NAT	L_T
5	5	5	5	D_H	NAT	H_T	19	19	13	T_H	NAT	L_T
6	0	0	0	SGL	NAT	H_T	19	19	14	T_H	NAT	H_T
7	1	1	1	SGL	NAT	H_T	18	16	9	D_H	NAT	H_T
8	0	0	0	SGL	NAT	H_T	18	16	10	T_H	NAT	L_T
9	0	0	0	SGL	NAT	H_T	17	15	9	D_H	NAT	H_T
10	1	1	1	SGL	NAT	H_T	18	19	11	T_H	NAT	L_T
11	1	1	1	SGL	NAT	H_T	19	20	16	T_H	MV	L_T
12	0	0	0	SGL	NAT	H_T	18	17	10	T_H	NAT	H_T
13	5	5	5	D_H	NAT	H_T	18	19	13	T_H	NAT	L_T
14	1	1	1	SGL	NAT	H_T	18	20	15	T_H	NAT	L_T

B=building, W=wall, R=roof, F=floor, ES=emission system, MV=MVHRS.

Table 6.9 – Ranking (i.e. from the lowest to the highest cost-optimal NPV) of the refurbished buildings for the scenario with a constant heat price.

	Reference case		Energy-optimal		Cost-optimal*	
Build.	NPV,	E_h,	NPV,	E_h,	NPV*,	E_h,
#	$\times 10^3$ EUR	kWh m^{-2} y^{-1}	$\times 10^3$ EUR	kWh m^{-2} y^{-1}	$\times 10^3$ EUR	kWh m^{-2} y^{-1}
6	53.8	245.4	49.5	19	33.6	46.0
12	63.0	241.8	55.7	21.9	40.0	49.1
8	76.6	237.4	56.5	25.2	49.5	52.0
1	92.9	208.8	62.35	26.1	56.2	54.1

Build. #	NPV, ×10³ EUR	E_h, kWh m⁻² y⁻¹	NPV, ×10³ EUR	E_h, kWh m⁻² y⁻¹	NPV*, ×10³ EUR	E_h, kWh m⁻² y⁻¹
9	88.2	234.3	73.1	26.9	57.5	54.4
7	101.4	207.5	67.1	27.1	61.7	58.2
14	127.6	204.1	81.4	29.7	78.6	62.0
2	129.9	203.9	83	29.2	80.1	61.6
5	120.2	98.7	105.9	31.2	104.5	40.9
10	231.6	196.0	139.6	32.3	137.9	40.8
13	170.5	97.1	144.8	32.9	143.4	37.3
4	253.3	194.9	151.5	32.7	150.0	37.4
11	264.2	194.4	157.9	32.4	156.1	37.9
3	262.4	213.8	194.6	32.5	166.2	37.6

*Table sorted by ascending NPV (cost-optimal).

Table 6.10 – Ranking (i.e. from the lowest to the highest cost-optimal NPV) of the refurbished buildings for the scenario with the heat price depending on the temperature level.

	Reference case		**Energy-optimal**		**Cost-optimal***	
Build. #	**NPV, ×10³ EUR**	**E_h, kWh m⁻²y⁻¹**	**NPV, ×10³ EUR**	**E_h, kWh m⁻²y⁻¹**	**NPV*, ×10³ EUR**	**E_h, kWh m⁻²y⁻¹**
6	50.3	245.4	42.4	19.3	32.4	52.3
12	58.9	241.8	47.7	22.2	38.7	52.1
8	71.6	237.4	55.5	25.6	47.5	58.1
1	87.8	208.8	61.3	26.5	54.2	60.8
9	82.5	234.3	62.9	25.2	55.2	60.4
7	95.9	207.5	66.0	27.6	59.2	61.1
14	120.6	204.1	80.3	29.5	75.4	63.4
2	122.8	203.9	81.3	30.0	76.8	62.9
5	115.3	98.7	103.7	31.2	101.6	41.4
10	219.0	196.0	135.9	33.3	134.7	37.5
13	163.6	97.1	142.3	32.3	139.5	38.5
4	239.5	194.9	148.8	32.4	145.9	39.3
11	249.8	194.4	179.7	31.5	151.7	39.4
3	245.6	213.8	191.1	32.9	161.5	39.8

*Table sorted by ascending NPV (cost-optimal).

6.2.3 DH system

Fig. 6.4 shows the heat share delivered to the network for the scenario with high supply temperature "T=90 °C" (column with texture in Fig. 6.4) and the scenario with low supply temperature "T min". For the latter, the graph reports a column for each additional refurbished building. Heat for DHW is constant for both refurbished and not refurbished buildings and it is 45 MWh year^{-1}. In the case where the network temperature is constant at 90 °C (194 °F) during the year, the network heat loss is 168 MWh year^{-1} (first column with texture in Fig. 6.4). In the case of minimum grid temperature, the heat loss is also quite constant for almost all the degrees of refurbishment (i.e. 114 MWh year^{-1}) while it is slightly lower when the last building is refurbished (i.e. 106 MWh year^{-1}) – see solid column in Fig. 6.4. The reduction of the network losses is strictly related to the buildings to be refurbished because only one building can prevent the reduction of the network temperature. The only implementation of the minimum network temperature required by the buildings (not yet refurbished), enables a considerable reduction of the network loss (i.e. 32 %) – compare the first two columns of Fig. 6.4. Only the refurbishment of all the buildings enable a further small reduction of the network loss (i.e. 5 %).

Fig. 6.5a and Fig. 6.5b report the distribution efficiency for both the scenarios with "T=90 °C" (Fig. 6.5a) and the one with "T min" (Fig. 6.5b). Fig. 6.5c and Fig. 6.5d report the generation-distribution efficiency for both the scenarios with "T=90 °C" (Fig. 6.5c) and the one with "T min" (Fig. 6.5d). The blue columns represent the reference case (i.e. no refurbished building), the red columns refers to half of the buildings being refurbished, and the green columns refers to all the buildings being refurbished. The efficiency is particularly low (< 0.35 for all the scenarios) in the months when only heat for DHW is required. The efficiency reduction is also significant when all the buildings of the stock are refurbished, nevertheless, the scenario with the minimum network temperature partially compensate for the DH capacity reduction deriving from the refurbishment.

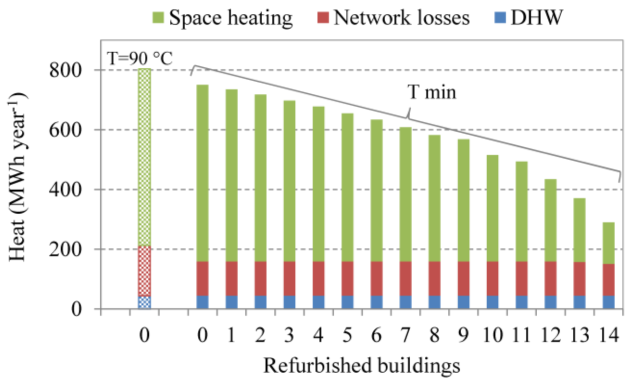

Fig. 6.4 – Heat shares delivered to the network for the scenario with constant network temperature (column with texture) and minimum network temperature (solid columns).

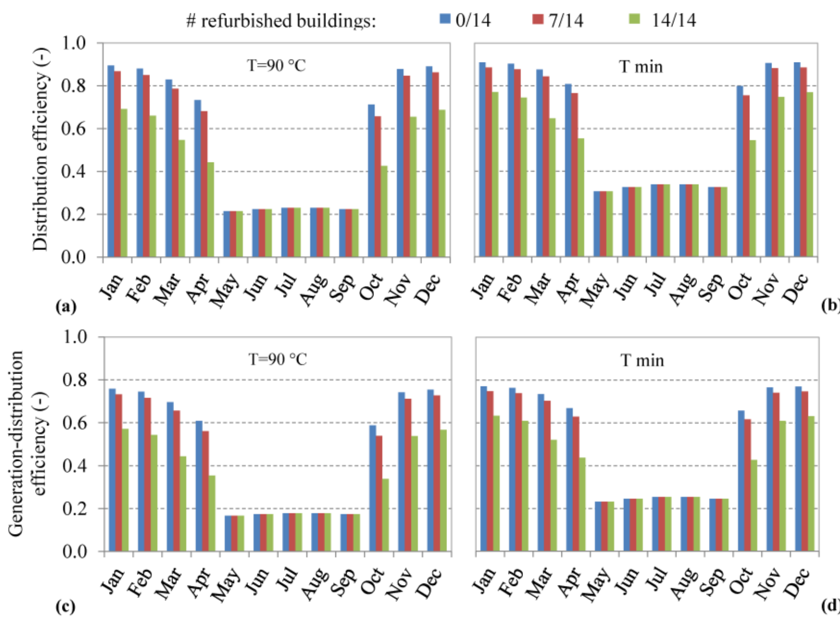

Fig. 6.5 – Distribution (a,b) and generation-distribution (c,d) efficiency of the DH system for each month.

NPV and EP of the DH system have been calculated and displayed in Fig. 6.6. From the DH manager's point of view, a positive NPV is expected from the operation of the DH system. The blue dots (i.e. T=90 °C) correspond to the case in which a constant network temperature of 90 °C is kept along the network. The red dots (i.e. T min) correspond to the cases in which the minimum network temperature, the one required by the most critical building, is adopted. The green dots correspond to the scenario with both the minimum network temperature and the incentive on the heat price (i.e. price reduction for low temperature heat). The dots with black border correspond to the reference cases (i.e. no refurbished building). Each point refers to an additional refurbished building and therefore to a new DH state. For all the DH scenarios, a complete refurbishment of the buildings would lead to a negative NPV, that means the DH system would be no longer profitable. The operation of the DH system with the minimum network temperature (red dots) allows a constant benefit in terms of NPV and EP, and partially compensates for the economic profitability loss deriving from the refurbishment: the case with "T min" and 6 refurbished buildings has a similar NPV as the starting configuration with constant temperature network T=90 °C. The scenario with both minimum network temperature and incentive for low temperature heat (green dots) shows that trend is slightly less negative because the incentive promotes the use of heat at LT, however the economic loss deriving from a heat price discount is not paid back.

Fig. 6.7 shows EP and NPV considering different sizes of the connected buildings. According to the survey, the reference buildings have a floor area as reported in Table 6.6, that corresponds to an average area of the buildings stock of 225 m^2. A scenario with smaller buildings involves buildings with a floor area between 75 m^2 and 178 m^2 − average area of the buildings stock is 121 m^2 − while a scenario with larger buildings correspond to floor area between 182 m^2 and 421 m^2 − average area of the buildings stock is 330 m^2. The EP, and therefore NPV, is much higher for larger buildings. Nevertheless, for a high number of refurbished buildings, the NPV for smaller and larger buildings is not considerably different because the income, coming from heat trade, is a minor share of the cash flow, that is dominated by costs to manage the network. This result is similar for both the scenarios with "T=90 °C" and "T min".

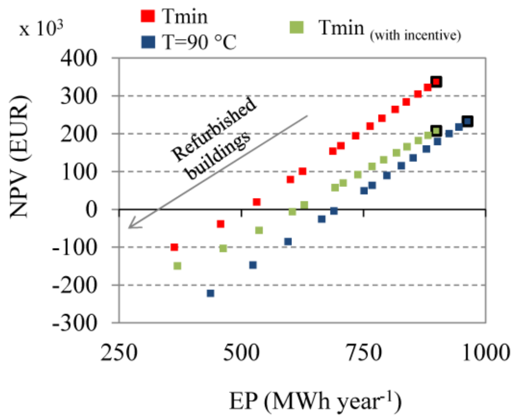

Fig. 6.6 – NPV and EP of the DH system for the three scenarios: T=90 °C, T_{min}, $T_{min, with\ incentive}$.

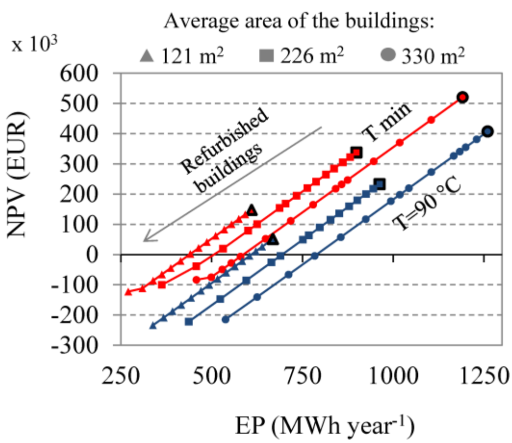

Fig. 6.7 – NPV and EP of the DH system for larger and smaller buildings.

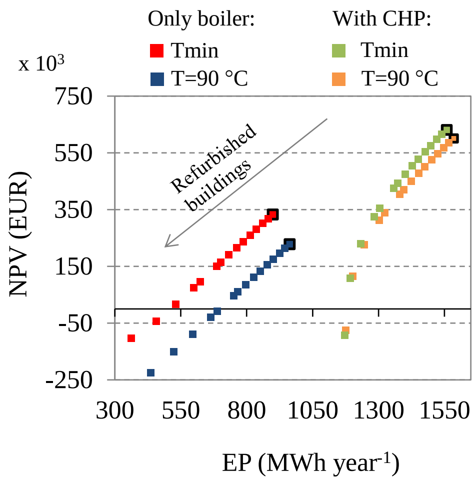

Fig. 6.8 – NPV and EP of the DH system for T=90 °C, T_{min} with (red and blue dots) and without CHP system (green and yellow dots).

Finally, the installation of a CHP system (30 kW_{el} and 80 kW_{th}) has been investigated. The minimum size currently available in the market has been selected in order to limit the heat discharge (see section 5.3.2). The plant has been considered to be constantly operated for the whole year, which is the most profitable strategy with the Italian incentive on the electricity production (Prando et al. 2014a). Fig. 6.8 shows EP and NPV considering the scenario with and without CHP system. The dots with black border correspond to the reference cases (i.e. no refurbished building). The scenarios with CHP system enable a higher NPV due to the revenues from the electricity sale, however, also EP is higher due to the CHP input energy to produce electricity. The benefit coming from the implementation of the minimum temperature is weaker – the two curves are closer – because the dominant revenue is due to the electricity sale (in particular when the buildings are refurbished). The slope of the curves (orange and green) is higher—increasing the refurbished building—because the EP of the CHP system is constant even if the heat required by the DH is lower.

The NPV of the abovementioned scenarios is reported depending on the linear heat density (MWh m^{-1} $year^{-1}$) in Fig. 6.9. The linear heat density is defined as the ratio between the heating annually sold to the customers and the trench length of the DH network. Studies in literature states that areas with a linear heat density of 0.2–0.3 MWh (m year)$^{-1}$ can be supplied by DH in a cost-efficient way (Dalla Rosa and Christensen 2011; Zinko et al. 2008), which is confirmed by the present study. Moreover, the graph in Fig. 6.9 highlights that the implementation of a CHP system could shift this threshold to 0.15 MWh (m year)$^{-1}$.

NPV and PES of the DH system are reported in Fig. 6.10. Each point refers to an additional refurbished building and the dots with black border correspond to the reference cases (i.e. no refurbished building). PES is lower when the minimum network temperature is implemented because the heat demand is reduced and therefore a larger amount of heat has to be discharged – since the CHP system is not operated at partial load. Although the Italian incentive regime enables the profitability for all the considered scenarios, none of them have positive primary energy saving (PES) index, as reported in Fig. 6.10.

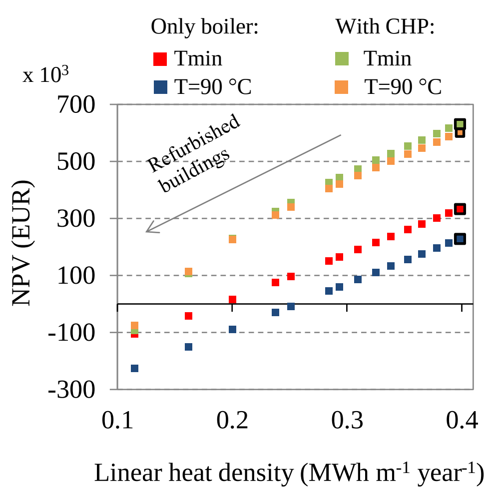

Fig. 6.9 – NPV and EP of the DH system for T=90 °C, T_{min} with (red and blue dots) and without CHP system (green and yellow dots).

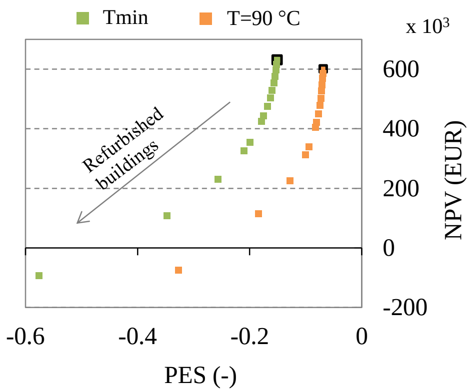

Fig. 6.10 – NPV and PES of the DH system for T=90 °C, T_{min}.

6.3 Main findings

This study aims to define the energy and economic performance of the DH system considering cost-optimal solutions for the refurbishment of buildings connected to the DH system. The heating need of the buildings has been calculated by means of TRNSYS 17, and a model of the distribution network has been developed for the purpose of the present study. Several measures have been considered for the refurbishment of the buildings and a genetic algorithm has been used to reduce the number of investigated configurations to find the cost-optimal ones. Among these cost-optimal refurbishments, the one with the minimum NPV has been adopted as the most probable from the user point of view. The results of the optimization depend on the performance of the refurbishment measures as well as their costs to be implemented and operated.

The buildings have been then ranked with increasing NPV, of which the first are more likely to be implemented. Every time that a renovation took place on a building, a new scenario was created. Each scenario, with a different number of refurbished buildings in the network, has been analysed comparing two strategies as for the supply temperature of the network: a constant temperature of 90 °C and the lowest temperature required by the most critical building. The only implementation of the minimum network temperature required by the buildings (no refurbished building), enables a reduction of 32 % of the network loss. This is possible because both heat exchangers and radiators are usually oversized, since they are designed for the most critical weather condition. Only the refurbishment of all the buildings enables a further 5 % reduction of the network loss. The reduction of network loss is strictly related to the buildings to be refurbished because only one building can prevent the reduction of the network temperature.

The refurbishment of all the buildings leads to a negative NPV that means the DH system is no more profitable. The operation of the DH system with the minimum network temperature allows a constant benefit in terms of NPV and EP, and partially compensate for the loss economic profitability deriving from the refurbishment. An incentive for the promotion of low temperature heat has been also considered as a potential measure to improve the DH performance. This scenario shows a trend that is slightly less negative because the incentive promotes the use of heat at LT, however the economic loss deriving from a heat price discount has been not repaid. EP—and therefore NPV—are much higher for larger buildings. Nevertheless, for a high number of refurbished buildings, the NPV for smaller and larger buildings is not considerably different because the cash flow is dominated by costs of the network management (heat sale is a negligible share). Finally, the implementation of a CHP system allows higher NPV mainly due to the revenue from electricity trade. Areas with a linear heat density of 0.15 MWh per meter on a yearly basis can be supplied by DH-CHP in a cost-efficient way.

7. Conclusions

This research work focuses on two main aspects of energy conversion systems based on lignocellulosic biomass. On the one hand it deals with the conversion of biomass into energy and the performance of the analysed systems. On the other hand it focuses on the distribution, matching the generated heat to the end users, with the respective energy efficiency. These two parts are complementary and both their efficiencies contribute to the overall performance of the whole system. In this work, the experimental study of the plants has been supplemented with the modelling of the main components in order to study in detail both the current performance of the systems and the potential improvements.

A consolidated and widely diffused biomass-based CHP technology consists of a boiler fed with solid lignocellulosic biomass coupled with an ORC generator. In South Tyrol, 13 existing plants implement this technology. The first section of the present thesis focuses on the monitoring of the energy performance of a biomass boiler coupled with an ORC generator in a DH context. The assessment has been supplemented with the results of a calibrated model of the ORC generator in order to carry out some predictions for different management strategies of the system.

The net electric efficiency of the whole plant (i.e. boiler and ORC), is 9.9 % at 94 % of the nominal power load and 9.1 % at 79 % of the nominal power load. This is a flexible system because its performance is not particularly penalised at partial load. However, the subsidisation for renewable sources promotes the nominal load operation – discharging part of the cogenerated heat – in order to maximize electricity production. Since the maximum ORC plant load depends on the amount of thermal power that can be discharged, high network temperature is set to increase the rejected heat and thus the electricity production, even if the electric efficiency is penalised.

A thermodynamic model of the ORC generator has been developed with the objective to investigate different management strategies of the system. The numerical results are in close agreement with the monitored data, therefore the developed model shows some significant prediction capabilities. An evaluation on the sensitivity of the electric performance of the ORC plant at varying working conditions shows that the condensing temperature is the most influential parameter, while the evaporating pressure has a lower impact. For a pre-fixed electric load, higher values of the ORC electric efficiency could be reached by decreasing the mean temperature of the primary network. For example, a reduction of 10 °C of the mean primary network temperature would lead to an increase in the electric efficiency of the ORC generator of about one percentage point.

The analysis of the boiler losses highlighted that the exhaust latent thermal loss and the exhaust sensible thermal loss account for 9 % and 16 % of the boiler input power, respectively. A further exploitation of both sensible and latent exhaust heat shares could considerably improve the efficiency of the boiler. However, this measure should be integrated with a reduction of the DH network temperature that would enable a higher heat recovery at lower temperature.

More than 50 % of the ORC heat output is used to dry the woodchips; therefore, a further detailed analysis on the energy effectively used for the drying process would be essential to optimise the plant operation. In addition, the operation of the driers is not automated but it is handled manually in batch mode with consequent management inefficiencies. An automatic and continuous drying process would permit a considerable reduction of the drying heat share and a consequent improvement of the global efficiency of the system. Nonetheless, the subsidisation on the electricity production strongly increases the electricity worth and does not promote the valorisation of the generated heat. In this perspective, there is less interest to improve the efficiency of the drying section that is also operated as an air cooler which allows for an increase in the discharged heat and, therefore, in electricity production.

A different technology – particularly promising for the small scale generation – although often not completely commercially mature, consists of downdraft gasifiers coupled with ICE. The net electric efficiency of a representative system for the current situation in South Tyrol (i.e. gasifier and ICE) is around 18.3 %. Nevertheless, small gasification systems are designed to operate at nominal load. It means they should be installed as base thermal load stations. The coupling of a biomass dryer section is considered a suitable option to improve the recovery of useful heat because of the low moisture content required by the gasifier. However, the subsidisation promotes a nominal load operation – discharging part of heat – in order to maximize the electricity production. Finally, char has a disposal cost that could be tackled with the application of sustainable solutions which aim to valorise these by-products. In particular, it has also a residual energy content that make it attractive for further use in the energy chain.

These two monitoring activities have been carried out for two different technologies that have the same purpose: the combined generation of heat and power. However, it is worth highlighting that the two selected plants have different sizes, as detailed in chapter 2 and 3. The plant based on combustion is about 20 times larger than the plant based on gasification, therefore, this has to be considered for the comparison of these two systems.

One of the main technology barriers for the development of the gasification systems is the presence of tar in the producer gas. It mainly causes the clogging of filters and valves and the corrosion of the metallic components. For this specific issue, a general screening of the tar present in the raw producer gas has been carried out for a small open top gasifier developed at the Indian Institute of Science.

The tar sampling procedure has been carried out using both IPA and hexane in order to define the capability of two different solvents to dissolve tar. The results highlighted there is not considerable difference using IPA rather than hexane. Nevertheless, IPA is easier to handle due to its higher boiling point.

The GC-MS analyses on the collected samples highlighted that tar is mainly composed of light aromatic compounds, where benzene and toluene account for about 70 % of the total detected tar. The gravimetric tar is roughly one order of magnitude smaller than tar amount detected in the collected samples by means of GC-MS analysis. Moreover, GC-MS analysis on the gravimetric tar highlighted that most of the detected compounds have a MW higher than 150 g mol^{-1} and correspond to light and heavy PAH compounds, however, the main fraction of gravimetric tar is expected to be GC un-detectable. The two approaches for the determination of tar in the producer gas – GC-MS on collected sample and gravimetric tar – have different capabilities and have to be used depending on the downstream application of the gasification system.

The tar content values have been detected to be higher when coconut shell is used in the gasification process. Nevertheless, the compounds that enhance the difference are mainly benzene and toluene. Considering the rest of the compounds, the gasification of Casuarina woodchip rather than coconut shell has a similar tar content in the producer gas.

In the second part of this work, the matching between the heat generated by the CHP plant and the heat demand of the final users has been studied. Furthermore, the impact of the building refurbishment on the energy and economic performance of the plant has been discussed.

An integrated approach for the assessment of the energy and economic performance of a biomass gasification CHP system installed in a residential block has been developed. This approach allows the estimation of the performance of the system in operation and provides indications for the design of systems energetically and economically efficient.

For all the considered building configurations (12 alternatives), the PES analysis shows the possibility to set-up a biomass gasification CHP that allows a primary energy saving with respect to the separate production of heat and power. The primary energy saving depends on the heat discharged: the less heat is discharged, the larger is PES. A better exploitation of heat could be reached increasing the number of users that are served by the power plant but in that case a district heating system could be a more plausible scenario.

At the current stage, partial or on/off operation of the gasification systems is not a feasible option at these scales due to management complexities to reach a steady state operation. Since the gasification power plant should run continuously, the heat discharged is strictly related to both plant size and thermal load profile of the final user. Therefore, the nominal power of the plant should be considerably lower than the building peak load in order to limit the discharge heat. As a consequence, the heat demand of buildings has to be partially supplied by a back-up boiler, thus losing some benefits given by cogeneration. The gasification power plant, because of its management

complexities for the on/off operation, should be installed as base thermal load station.
The economic analysis based on the power plant of 30 kW_{el} shows a considerable influence of the useful heat on the discounted cash flow for both the scenario with and without incentive. The useful heat amount is related to the heat load profile, which varies for each building configuration. At the current stage of the technology, the financial incentive is essential for an economic return of the investment. The use of the heat share generated by a CHP system – even if it is based on renewable energy – is very important to promote high efficiency system in operation. With the current subsidization, the use of the generated heat is not a fundamental contribution to the business plan. Such a subsidization distorts the energy sector promoting the electricity generation instead of the primary energy saving.
Finally, the energy and economic impact of the buildings refurbishment on the DH plant has been investigated. The multi-objective optimization – i.e. minimisation of both EP and NPV of a building – has been carried out in accordance with the cost-optimal approach for each building connected to the network. Several measures have been considered for the refurbishment of the buildings and a genetic algorithm has been used to reduce the number of investigated configurations to find the cost-optimal ones. Among the different cost-optimal configurations of each building, the one with the lowest NPV is selected as the refurbishment measure that would be adopted by the building owner.
Each scenario, with a different number of refurbished buildings in the network, has been analysed from the DH point of view, comparing two strategies as for the supply temperature of the network: a constant temperature of 90 °C and the lowest temperature required by the most critical building. The only implementation of the minimum network temperature required by the buildings (no refurbished building), enables a reduction of 32 % of the network losses. This is possible because both heat exchangers and radiators are usually oversized, since they are usually designed for the most critical weather condition. Only the refurbishment of all the buildings enable a further 5 % reduction of the network loss. The reduction of network loss is strictly related to the buildings to be refurbished because only one building

can prevent the reduction of the network temperature. The refurbishment of all the buildings leads to a negative NPV that means the DH system is no more profitable. The operation of the DH system with the minimum network temperature allows for a constant benefit in terms of NPV and EP, and partially compensates for the loss of economic profitability deriving from the refurbishment. An incentive for the promotion of low temperature heat has been also considered as a potential measure to improve the DH performance, however, the economic loss deriving from a heat price discount has not been repaid. EP—and therefore NPV – is much higher for larger buildings, however, NPV for smaller and larger buildings is not considerably different for a high number of refurbished buildings because the cash flow is dominated by network management costs. Finally, the implementation of a CHP system allows higher NPV mainly due to the revenue from electricity sale, therefore, areas with a linear heat density of 0.15 MWh $(m\ year)^{-1}$ can be supplied by DH-CHP in a cost-efficient way.

In conclusion, this study also has a local impact on the territory because it reports the current performance of the existing biomass energy systems and highlights the potential improvements to be implemented in South Tyrol. Some guidelines for both designer and the political arena can be identified from this research work. First of all, a system should match as much as possible the heat production with the users' needs and this should be done from the designing phase. A stringent requirement in this regard should be defined by the energy policy at provincial level, since it is not available at national level. Both combustion and gasification systems should be promoted, the former for its capability of operation at partial load and the latter for its superior electric efficiency. Another important aspect regards the implementation of LT district heating in order to improve distribution efficiency. Considering the high number of DH networks, the local administration should impose the reduction of the operational temperature for both existing and new installations. This measure is particularly urgent considering the current trend of refurbishment of the buildings connected to the network.

Nomenclature

Abbreviations

ACH	air change per hour
CHP	combined heat and power
DH	district heating
DHW	domestic hot water
D_H	Glazing system with double-pane glass and high SHGC
D_L	Glazing system with double-pane glass and low SHGC
EP	primary energy
el	electricity
f	conversion coefficient
h	heating
HRVG	heat recovery vapour generator
H_T	high temperature emission system (radiator)
i	real discount rate
IC	investment cost
ICE	internal combustion engine
LT	low temperature
L_T	low temperature emission system (underfloor heating)
MDM	octamethyltrisiloxane
MVHRS	mechanical ventilation system with heat recovery
NAT	natural ventilation
NPV	net present value
O&M	operation and maintenance
ORC	organic Rankine cycle
SHGC	solar heat gain coefficient
SGL	Glazing system with single-pane glass and high SHGC
T_H	Glazing system with triple-pane glass and high SHGC
T_L	Glazing system with triple-pane glass and low SHGC
VAT	Value Added Tax

Symbols

A	area (m^2)
C	carbon mass fraction of biomass on as received basis (%)
CO	carbon monoxide molar fraction of the dry flue gas (%)
CO_2	carbon dioxide molar fraction of the dry flue gas (%)
c_p	specific heat at constant pressure ($J\ K^{-1}\ kg^{-1}$)
c_{pmd}	specific heat on volume basis of dry flue gas in standard conditions ($J\ K^{-1}\ m^{-3}$)
c_{pmw}	specific heat on volume basis of water vapour in standard conditions ($J\ K^{-1}\ m^{-3}$)
f	energy fraction (-)
E	energy (J)
H	hydrogen content of the fuel on as received basis (% wt.)
h	enthalpy ($J\ kg^{-1}$)
HDD20	heating degree days calculated with a reference temperature of 20°C
k	coverage factor (-)
LHV	lower heating value ($J\ kg^{-1}$)
m	mass (kg)
$\dot{m}$	mass flow rate ($kg\ s^{-1}$)
n	time of the cash flow, years
P	power (W)
p	pressure (Pa)
Q	volume flow rate ($m^3\ s^{-1}$)
R	mass of residues passing through the grate (% wt.)
S	boiler surface (m^2)
t	temperature (°C)
U	thermal transmittance ($W\ m^{-2}\ K^{-1}$)
w	moisture content of the test fuel (% wt.)

Greek symbols

α	convection heat transfer coefficient (W m^{-2} K^{-1})
ΔT	temperature difference (°C)
ε	heat exchange efficiency (-)
λ	thermal conductivity (W m^{-1} K^{-1})
ϱ	density (kg m^{-3})
η	efficiency (-)
τ	temperature difference between the condensing MDM and the cooling water at the pinch point of the condenser (K)

Subscripts

A	thermal heat loss in the flue gas
a	MDM saturated liquid at evaporating pressure
aux	auxiliaries
B	chemical heat loss in the flue gases
b	biomass
boil	boiler
c	condensation
cond	MDM superheated vapour at regenerator outlet
cf	cooling fluid
D	heat loss through the boiler surface
d	design
el	electric
evap	evaporation
f	frame
fg	flue gas
gen	generator
gl	glass
in	input
is	isentropic
m	mechanical
nom	nominal
off	off-design
out	output

to	thermal oil
p	pump
PE	electricity-to-primary energy
pp	pinch point
r	MDM saturated liquid at regenerator outlet
reg	regenerator
res	residues
surf	surface
t	turbine
th	thermal
U	loss through unburned fuel in the ash
v	vapour of MDM
wind	window
1	MDM saturated liquid at condensing pressure
3	MDM superheated vapour at evaporating pressure
4	MDM at turbine outlet

References

AEEGSI (Italian Regulatory Authority for Electricity, Gas and Water). 2008. Approval EEN 3/08 Update of the conversion coefficient from kWh to tons of oil equivalent related to the mechanism of the energy efficiency certificates (In Italian: Delibera EEN 3/08 Aggiornamento del fattore di conversione dei kWh in tonnellate equivalenti di petrolio connesso al meccanismo dei titoli di efficienza energetica).

AEEGSI (Italian Regulatory Authority for Electricity, Gas and Water). 2013. Annual report on the state of services and regulatory activities (In Italian: Relazione annuale sullo stato dei servizi e sull'attività svolta). Milan (Italy).

Agency for environment of the Autonomous Province of Bolzano, www.provincia.bz.it/agenzia-ambiente/energia/biomassa.asp [Accessed: 1st October 2014].

Ahmed, T.Y., Ahmad, M.M., Yusup, S., Inayat, A., Khan, Z. 2012. Mathematical and computational approaches for design of biomass gasification for hydrogen production: A review, Renewable and Sustainable Energy Reviews 16(4), pp. 2304–2315.

Ahrenfeldt J., Thomsen T. P., Henriksen U., and Clausen L. R. 2011. Biomass gasification cogeneration – A review of state of the art technology and near future perspectives. Applied Thermal Engineering 50(2), pp. 1407–1417.

Akhtari, S., Sowlati, T., and Day, K. 2014. Economic feasibility of utilizing forest biomass in district energy systems – A review. Renewable and Sustainable Energy Reviews 33, pp. 117–127.

Aigner, I., Wolfesberger, U., Hofbauer, H. 2009. Tar Content and Composition in Producer Gas of Fluidized Bed Gasification and Low Temperature Pyrolysis of Straw and Wood – Influence of Temperature. Available at: www.bioenergy2020.eu/files/publications/pdf/Tar_Content_and_Composition_in_Producer_Gas_of_Fluidized_Bed_Gasification_and_Low_Temperature_Pyrolysis_of_Straw_and_Wood_%E2%80%93_Influence_of_Temperature.pdf [Accessed: 20th January 2015].

Alanne, K., Saari, K., Kuosa, M., Jokisalo, J., and Martin, A. R. 2012. Thermo-economic analysis of a micro-cogeneration system based on a rotary steam engine (RSE). Applied Thermal Engineering 44, pp. 11–20.

Alberti, L., Bianchi, N., Member, S., Boglietti, A., Cavagnino A. 2014. Core Axial Lengthening as Effective Solution to Improve the Induction Motor Efficiency Classes, Industry Applications IEEE Transaction, pp. 3391–3398.

Algieri, A. and Morrone, P. 2013. Energetic analysis of biomass-fired ORC systems for micro-scale combined heat and power (CHP) generation. A possible application to the Italian residential sector, Applied Thermal Engineering 71(2), pp. 751–759.

Angrisani, G., Roselli, C., Sasso, M., Rosato, A., Sibilio, S. 2011. MCHP in the residential sector (in Italian), AICARR Journal 11, pp. 54–61.

Angrisani, G., Canelli, M., Rosato, A., Roselli, C., Sasso, M., Sibilio, S. 2013. Load sharing with a local thermal network fed by a microcogenerator: Thermo-economic optimization by means of dynamic simulations, Applied Thermal Engineering 71(2), pp. 628–635.

Anis, S. and Zainal Z.A. 2011. Tar reduction in biomass producer gas via mechanical, catalytic and thermal methods: A review, Renewable and Sustainable Energy Reviews 15, pp. 2355–2377.

Asadullah, M. 2014. Barriers of commercial power generation using biomass gasification gas: A review. Renew. Sustain. Energy Rev. 29, pp. 201–215.

Aung, N. Z. 2008. Modification of Diesel engine to producer gas engine. Jurnal ilmiah teknologi energi 1, pp. 29–41.

Autonomous Province of Bolzano. 2014. Energy service of the Autonomous Province of Bolzano (In Italian: Ufficio Risparmio Energetico Provincia di Bolzano).

Baggio, P., Baratieri, M., Gasparella, A., Longo, G.A. 2008. Energy and environmental analysis of an innovative system based on municipal solid waste (MSW) pyrolysis and combined cycle. Applied Thermal Engineering 28, pp.136–144.

Bang-Møller C., Rokni M., and Elmegaard B. 2011. Exergy analysis and optimization of a biomass gasification, solid oxide fuel cell and micro gas turbine hybrid system. Energy 36(8), pp. 4740–4752.

Baratieri, M., Baggio, P., Fiori, L., Grigiante, M. 2008. Biomass as an energy source: thermodynamic constraints on the performance of the conversion process, Bioresource Technology 99(15), pp. 7063–7073.

Baratieri, M., Baggio, P., Bosio, B., Grigiante, M., Longo, G.A. 2009. The use of biomass syngas in IC engines and CCGT plants: A comparative analysis, Applied Thermal Engineering 29(16), pp. 3309–3318.

Barbieri, E.S., Spina, P.R., Venturini, M. 2012. Analysis of innovative micro-CHP systems to meet household energy demands, Applied Energy 97, pp. 723–733.

Bergman, P.C.A., Paasen, V.B., Boerrigter, H. 2002. The novel ''OLGA'' technology for complete tar removal from biomass producer gas, Pyrolysis and Gasification of Biomass and Waste, Expert Meeting, September 30, 2002, Strasbourg, France.

Biedermann, F., Carlsen, H., Obernberger, I., and Schöch, M. 2004a. Small-scale CHP Plant based on a 75 kWel Hermetic Eight Cylinder Stirling Engine for Biomass Fuels – Development, Technology and Operating Experiences. In 2nd World Conference and Exhibition on Biomass for Energy, Industry and Climate Protection, 1–4. Rome, Italy.

Biedermann, F., Carlsen, H., Schöch, M., and Obernberger, I. 2004b. Operating experiences with a small-scale CHP pilot plant based on a 35 kWe hermetic four cylinder stirling engine for biomass fuels, Graz, Austria, Available at: www.bios-bioenergy.at/en/electricity-from-biomass/stirling-engine.html [Accessed: 10th October 2014].

Bini, R., and Manciana, E. 1996. Organic Rankine Cycle turbogenerators for combined heat and power production from biomass. In 3rd Munich Discussion Meeting "Energy conversion from Biomass Fuels Current Trends and Future Systems" Munich (Germany), pp. 96A00412: 1–8.

Bocci, E., Sisinni, M., Moneti, M., Vecchione, L., Di Carlo, A., and Villarini, M. 2014. State of Art of Small Scale Biomass Gasification Power Systems: A Review of the Different Typologies. Energy Procedia 45, pp. 247–256.

Börjesson, M., and Ahlgren, E. O. 2012. Biomass CHP Energy Systems: A Critical Assessment. Compr. Renewable Energy 5, pp. 87–97.

Boschiero Do Espirito Santo, D. 2014. An Energy and Exergy Analysis of a High-Efficiency Engine Trigeneration System for a Hospital: A Case Study Methodology Based on Annual Energy Demand Profiles. Energy and Buildings 76, pp. 185–198.

Branchini, L., De Pascale, A., Peretto, A. 2013. Systematic comparison of ORC configurations by means of comprehensive performance indexes. Applied Thermal Engineering 61, pp. 129–140.

Brand, M., Dalla Rosa, A., Svendsen, P.S. 2010. Performance of Low-Temperature District Heating Systems for Low-Energy Houses. In: The Future for Sustainable Built Environments with High-Performance Energy Systems Conference. Munich, Germany.

Brand, M., ,Svendsen, S. 2013. Renewable-based low-temperature district heating for existing buildings in various stages of refurbishment. Energy 62, pp. 311–319.

Brandoni, C. and Renzi, M. 2015. Optimal sizing of hybrid solar micro-CHP systems for the household sector, Applied Thermal Engineering 75, pp. 896–907.

Burkhardt GmbH, 2013. Available at: www.burkhardt-gmbh.de/en/energy/wood_gasification [Accessed: 5th August 2013].

Calise, F., Capuozzo, C., Carotenuto, A., Vanoli, L. 2014. Thermoeconomic analysis and off-design performance of an organic Rankine cycle powered by medium-temperature heat sources, Solar Energy 103, pp. 595–609.

Castellano, P. J., Volk, T. A., and Herrington, L. P. 2009. Estimates of technically available woody biomass feedstock from natural forests and willow biomass crops for two locations in New York State. Biomass and Bioenergy 33(3), pp. 393–406.

CEN (European Committee for Standardization). 2003. EN 12831: Heating system in buildings – Method for calculation of the design heat load.

CEN (European Committee for Standardization). 2008. EN 15316-3-1 Heating systems in buildings – Method for calculation of system energy requirements and system efficiencies – Part 3–1: Domestic hot water systems, characterisation of needs (tapping requirements), CEN, Brussels (Belgium).

CGPL (Combustion Gasification & Propulsion Laboratory). 2014. Technology of Biomass Gasification, Bangalore (India), Indian Institute of Science (IISC), Available at: http://cgpl.iisc.ernet.in/site/Technologies/Biomass Gasification/tabid/68/Default.aspx [Accessed: 10th June 2014].

Chiang, K.-Y., Chien, K.-L., and Lu, C.-H. 2012. Characterization and comparison of biomass produced from various sources: Suggestions for selection of pretreatment technologies in biomass-to-energy. Applied Energy 100, pp. 164–171.

Connolly, D., Lund, H., Mathiesen, B. V., Werner, S., Möller, B., Persson, U., Boermans, T., Trier, D., Østergaard, P.A., Nielsen, S. 2014. Heat Roadmap Europe: Combining district heating with heat savings to decarbonise the EU energy system. Energy Policy 65, pp. 475–489.

Coronado, C.R., Yoshioka, J.T., Silveira, J.L. 2011. Electricity, hot water and cold water production from biomass. Energetic and economical analysis of the compact system of cogeneration run with woodgas from a small downdraft gasifier, Renewable Energy 36(6), pp. 1861–1868.

Corria, M.E., Cobas, V.M., and Lora, E.S. 2006. Perspectives of Stirling engines use for distributed generation in Brazil. Energy Policy 34, pp. 3402–3408.

CTI. 2013. GL 904 "Biogas from anaerobic fermentation and producer gas" (In Italian: GL 904 "Biogas da fermentazione anaerobica e syngas biogenico") CTI (Italian Thermo-technical Committee). Available at: www.cti2000.it/index.php?controller=documenti&action=showDocuments&argid=33 [Accessed: 10th October 2014].

Daianova, L., Dotzauer, E., Thorin, E., Yan, J. 2012. Evaluation of a regional bioenergy system with local production of biofuel for transportation, integrated with a CHP plant. Applied Energy 92, pp. 739–749.

Dalla Rosa, A. and Christensen, J. E. 2011. Low-energy district heating in energy-efficient building areas. Energy 36(12), pp. 6890–6899.

Dasappa, S., Paul, P.J., Mukunda, H.S., Rajan, N.K.S., Sridhar, G., Sridhar, H.V. 2004. Biomass gasification technology – a route to meet energy needs. Current Science 87(7), pp. 908–916.

Dasappa, S., Subbukrishna, D. N., Suresh, K. C., Paul, P. J., and Prabhu, G. S. 2011a. Operational experience on a grid connected 100 kWe biomass gasification power plant in Karnataka, India. Energy for Sustainable Development 15(3), pp. 231–239.

Deb, K., Pratap, A., Agarwal, S. 2002. A Fast and Elitist multi-objectives genetic algorithm: NSGA-II, IEE Transactions on Evolutionary Computation, vol.6 n.2, pp.182–197.

Demirbas, A. 2001. Biomass resource facilities and biomass conversion processing for fuels and chemicals. Energy Conversion and Management 42, pp. 1357–1378.

Devi, L., Ptasinski, K.J., Janssen, F.J.J.G. 2003. A review of the primary measures for tar elimination in biomass gasification processes. Biomass and Bioenergy 24, pp. 125–140.

Devi, L., Ptasinski K.J., Janssen F.J.J.G., Van Paasen S.V.B., Bergman P.C.A., Kiel J.H.A. 2005. Catalytic decomposition of biomass tars: use of dolomite and untreated olivine. Renewable Energy 30(4), pp. 565–587.

Difs, K., Wetterlund, E., Trygg, L., and Söderström, M. 2010. Biomass gasification opportunities in a district heating system. Biomass and Bioenergy 34(5), pp. 637–651.

Dong, L., Liu, H., and Riffat, S. 2009. Development of small-scale and micro-scale biomass-fuelled CHP systems – A literature review. Applied Thermal Engineering 29(11–12), pp. 2119–2126.

Duvia, A., and Guercio, A. 2009. Technical and economic aspects of Biomass fuelled CHP plants based on ORC turbogenerators feeding existing district heating networks. In Proceedings of the 17th European Biomass Conference. Hamburg, Germany. Available at: www.turboden.eu/it/public/downloads/09A06400_paper_orc_turboden_clotilde.pdf [Accessed: 1st October 2014].

ECB (European Central Bank). 2014. Euro exchange rates. Available at: www.ecb.europa.eu/stats/exchange/eurofxref/html/eurofxref-graph-usd.en.html [Accessed: 30th November 2014].

Elliott, DC. 1988. Relation of reaction time and temperature to chemical composition of pyrolysis oils. In: Soltes EJ, Milne TA, editors. Proceedings of the ACS symposium series 376, pyrolysis oils from biomass.

ENEA (Italian National Agency for New Technologies, Energy and Sustainable Economic Development) 2014. Available at: www.enea.it/it/enea_informa/le-parole-dellenergia/fonti-rinnovabili-scenari-e-politiche/italia-meccanismi-di-incentivazione [Accessed: 1st October 2014].

European Commission. 2009. EU energy trends to 2030.

European Commisssion. 2012. Commission delegated regulation (EU) No 244/2012 of 16 January 2012, Official J. of the European Union 81, pp. 18–36.

Exergy. 2014. Available at: www.exergy-orc.com/applications/biomass [Accessed: 1st October 2014].

Faaij, A., Van Ree, R., Waldheim, L., Olsson, E., Oudhuis, A., van Wijk, A., Daey-Ouwens, C., Turkenburg, W. 1997. Gasification of biomass wastes and residues for electricity production. Biomass and Bioenergy 12(6), pp. 387–407.

Fagbenle, R.L., Oguaka, A.B., Olakoyejo, O.T. 2007. A thermodynamic analysis of a biogas-fired integrated gasification steam injected gas turbine (BIG/STIG) plant, Applied Thermal Engineering 27(13), pp. 2220–2225.

Ferrari, M.L., Pascenti, M., Sorce, A., Traverso, A., and Massardo, A.F. 2014. Real-time tool for management of smart polygeneration grids including thermal energy storage. Applied Energy 130, pp. 670–678.

Fumo, F., Mago, P.J., Chamra, L.M. 2009. Energy and economic evaluation of cooling, heating, and power systems based on primary energy, Applied Thermal Engineering 29(13), pp. 2665–2671.

Gabbrielli, R. 2012. A novel design approach for small scale low enthalpy binary geothermal power plants, Energy Conversion and Management 64, pp. 263–272.

Gerun, L., Paraschiv, M., Vîjeu, R., Bellettre, J., Tazerout, M., Gøbel, B. 2008. Numerical investigation of the partial oxidation in a two-stage downdraft gasifier. Fuel 87(7), pp. 1383–1393.

GSE (The Italian Regulatory Authority for Electricity and Gas). 2013. www.gse.it/en/ridssp/SimplifiedPurchaseandResaleArrangements(RID)/ Pages/default.aspx, Simplified purchase & resale arrangements [Accessed: 1st October 2013].

Gustafsson, J., Delsing, J., and van Deventer, J. 2010. Improved district heating substation efficiency with a new control strategy. Applied Energy 87(6), pp. 1996–2004.

Han, J., and Kim, H. 2008. The reduction and control technology of tar during biomass gasification/pyrolysis: An overview. Renewable and Sustainable Energy Reviews 12(2), pp. 397–416.

Hasler, P., and Nussbaumer, T. 1999. Gas cleaning for IC engine applications from fixed bed biomass gasification. Biomass and Bioenergy 16, pp. 385–395.

Hasler, P., Nussbaumer, T. 2000. Sampling and analysis of particles and tars from biomass gasifiers. Biomass and Bioenergy 18, pp. 61–66.

Haupt, R.L., Haupt, S.E. 2004. Pratical Genetic Algorithm, II. ed. John Wiley & Sons, Hoboken/New Jersey.

Hawkes, A., Leach, M. 2007. Cost-effective operating strategy for residential micro-combined heat and power, Energy 32(5), pp. 711–723.

Henriksen, U., Ahrenfeldt, J., Jensen, T., Gøbel, B., Bentzen, J., Hindsgaul, C., Sørensen, L. 2006. The design, construction and operation of a 75kW two-stage gasifier. Energy 31(10–11), pp.1542–1553.

Hernández, J.J., Ballesteros, R., Aranda, G. 2013. Characterisation of tars from biomass gasification: Effect of the operating conditions. Energy 50, pp. 333–342.

Heywood J.B. 1988. Internal Combustion Engine Fundamentals, McGraw-Hill, New York (U.S.).

Hofbauer, H. 2009. Gas production for Polygeneration Plants, Proceedings of ICPS – International Conference on Polygeneration Strategies 2009, Vienna.

Hofmann, P., Panopoulos, K.D., Aravind, P.V., Siedlecki, M., Schweiger, A., Karl, J. 2009. Operation of solid oxide fuel cell on biomass product gas with tar levels >10 g Nm−3, Int. J. Hydrogen Energy 34, pp. 9203–9212.

Holland, J.H. 1975. Adaptation in natural and artificial systems. University of Michigan Press, Ann Arbor.

Huang, Y., Mcilveen-wright, D.R., Rezvani, S., Huang, M.J., Wang, Y.D., Roskilly, A.P., Hewitt, N.J. 2013. Comparative techno-economic analysis of biomass fuelled combined heat and power for commercial buildings, Applied Energy 112, pp. 518–525.

ICF International. 2008. Technology Characterization: Steam Turbines. Environmental Protection Agency (EPA), Available at: www.epa.gov/chp/technologies.html [Accessed: 10th October 2014].

IRE (Institute for the Economic Research). 2014. Price list of the Chamber of Commerce of Bolzano (www.camcom.bz.it/it-IT/IRE/Dati_economici/

listini_prezzi.html?idBlock=1534). Available at: www.camcom.bz.it/ 19338.pdf [Accessed: 4th May 2014].

ISTAT (The National Institute of Statistics). 2001. 14° Building and population census (In Italian: 14° Censimento generale delle popolazioni e delle abitazioni). Avaiilable at: http://dawinci.istat.it/MD/ [Accessed: 4th May 2014].

Jess, A. 1996. Mechanisms and kinetics of thermal reactions of aromatic hydrocarbons from pyrolysis of solid fuels. Fuel 75(12), pp. 1441–8.

Joelsson, A., Gustavsson, L. 2009. District heating and energy efficiency in detached houses of differing size and construction, Applied Energy 86(2), pp. 126–134.

Jordan, C.A. and Akay, G. 2012. Occurrence, composition and dew point of tars produced during gasification of fuel cane bagasse in a downdraft gasifier. Biomass and Bioenergy 42, pp. 51–58.

Kalina, J. 2011. Integrated biomass gasification combined cycle distributed generation plant with reciprocating gas engine and ORC, Applied Thermal Engineering 31, pp. 2829–2840.

Kaltschmitt, M., Streicher, W. & Wiese, A. 2007. Renewable Energy: Technology, Economics and Environment, Springer Berlin Heidelberg, Berlin.

Keeley, K.R. 1988. A theoretical investigation of the part-load characteristics of LP steam turbine stages, in: CEGB memorandum RD/L/ES0817/M88, Central Electrical Generating Board.

Kinoshita, C.M., Wang, Y., Zhou, J. 1994. Tar formation under different biomass gasification conditions, Journal of Analitical and Applied Pyrolysis 29(2), pp. 169–181.

Knoef, H. A. M. 2012. Handbook on biomass gasification. (BTG biomass technology group BV, Ed.) Combustion (II edition.). Enschede (The Netherlands).

Kölling, A., Siemers, W., Hellwig, U., Sachno, N., Schröder, S., and Senkel, N. 2014. High Temperature Biomass Fired Stirling Engine (HTBS). In International Conference on Renewable Energies and Power Quality. Cordoba (Spain).

Kongtragool, B., and Wongwises, S. 2003. A review of solar-powered Stirling engines and low temperature differential Stirling engines. Renewable and Sustainable Energy Reviews 7(2), pp. 131–154.

Koppatz, S., Pfeifer, C., Hofbauer, H. 2011. Comparison of the performance behaviour of silica sand and olivine in a dual fluidised bed reactor system for steam gasification of biomass at pilot plant scale. Chemical Engineering Journal 175, pp. 468–483.

Kuosa, M., Kontu, K., Mäkilä, T., Lampinen, M., and Lahdelma, R. 2013. Static study of traditional and ring networks and the use of mass flow control in district heating applications. Applied Thermal Engineering 54(2), pp. 450–459.

KWB (Kraft und Wärme aus Biomasse). 2014. Available at: www.kwb-heating.co.uk/fileadmin/media/%C3%96sterreich/Downloads/Technik_Planung/TP_Powerfire_2014_EN_Low.pdf [Accessed: 2nd December 2014].

Lauenburg, P., and Wollerstrand, J. 2014. Adaptive control of radiator systems for a lowest possible district heating return temperature. Energy and Buildings 72, pp. 132–140.

Lauri, P., Havlík, P., Kindermann, G., Forsell, N., Böttcher, H., and Obersteiner, M. 2014. Woody biomass energy potential in 2050. Energy Policy 66, pp. 19–31.

Lee, U., Balu, E., Chung, J.N. 2013. An experimental evaluation of an integrated biomass gasification and power generation system for distributed power applications, Applied Energy 101, pp. 699–708.

Li, C., Suzuki, K. 2009. Tar property, analysis, reforming mechanism and model for biomass gasification—An overview. Renewable and Sustainable Energy Review 13(3), pp. 594–604.

Li, H., and Svendsen, S. 2012. Energy and exergy analysis of low temperature district heating network. Energy 45(1), pp. 237–246.

Lund, H., Šiupšinskas, G., Martinaitis, V. 2005. Implementation strategy for small CHP-plants in a competitive market: the case of Lithuania, Applied Energy 82(3), pp. 214–227.

Lund, H., Andersen, A. N., Østergaard, P. A., Mathiesen, B. V., and Connolly, D. -2012. From electricity smart grids to smart energy systems

– A market operation based approach and understanding. Energy 42(1), pp. 96–102.

Lund, H., Werner, S., Wiltshire, R., Svendsen, S., Thorsen, J. E., Hvelplund, F., and Mathiesen, B. V. 2014. 4th Generation District Heating (4GDH) Integrating smart thermal grids into future sustainable energy systems. Energy 68, pp. 1–11.

Ma, Z., Zhang, Y., Zhang, Q., Qu, Y., Zhou, J., Qin, H. 2012. Design and experimental investigation of a 190 kWe biomass fixed bed gasification and polygeneration pilot plant using a double air stage downdraft approach. Energy 46, pp. 140–147.

Mahapatra, S., Dasappa, S. 2014. Influence of surface area to volume ratio of fuel particles on gasification process in a fixed bed. Energy for Sustainable Development. 19, pp. 122–129.

Magnusson, D. 2012. Swedish district heating—A system in stagnation: Current and future trends in the district heating sector. Energy Policy 48, pp. 449–459.

Maraver, D., Sin, A., Royo, J., Sebastián, F., 2013. Assessment of CCHP systems based on biomass combustion for small-scale applications through a review of the technology and analysis of energy efficiency parameters, Applied Energy 102, pp. 1303–1313.

Marinitsch, G., Biedermann, F., Carlsen, H., Bovin, J. K., Schöch, M., and Obernberger, I. 2005. Development of a hot gas heat exchanger and a cleaning system for a 35kW el hermetic four cylinder Stirling engine for solid biomass fuels (pp. 1–12). Graz, Austria.

McKendry, P. 2002a. Energy production from biomass (Part 2): Conversion technologies. Bioresource Technology 83(1), pp. 47–54.

McKendry, P. 2002b. Energy production from biomass (Part 3): Gasification technologies. Bioresource Technology 83(1), pp. 55–63.

Michel, R., Rapagnà, S., Di Marcello, M., Burg, P., Matt, M., Courson, C., Gruber, R. 2011. Catalytic steam gasification of Miscanthus X giganteus in fluidised bed reactor on olivine based catalysts. Fuel Processing Technology 92(6), pp. 1169–1177.

Milne, T.A., and Evans, R.J. 1998. Biomass Gasifier "Tars": Their Nature, Formation, and Conversion. Golden (Colorado).

Ministry of the economic development. 2011. Decreto 4 Agosto 2011: Integrazioni al decreto legislativo 8 febbraio 2007, n. 20, di attuazione della direttiva 2004/8/CE sulla promozione della cogenerazione basata su una domanda di calore utile sul mercato interno dell'energia, e modificativa della direttiva 92/42/CE. (in Italian, English title: Decree 4th August 2011: Integrations to legislative decree 8th February 2007, n. 20, for the implementation of the directive 2004/8/CE on the promotion of cogeneration based on useful heat demand on the energy internal market, modifing the directive 92/42/CE), Gazzetta Ufficiale 218, pp. 52–70.

Ministry of the economic development. 2012. Decreto 6 Luglio 2012: Attuazione dell'art. 24 del decreto legislativo 3 marzo 2011, n. 28, recante incentivazione della produzione di energia elettrica da impianti a fonti rinnovabili diversi dai fotovoltaici (in Italian, English title: Decree 6th July 2012: Implementation of art. 24 of the legislative decree 3rd March 2011, n. 28 regarding subsidization of electricity production from power plant based on non-photovoltaic renewable sources), Gazzetta Ufficiale 159, pp. 38–102.

Morf, P. 2001. Secondary reactions of tar during thermochemical biomass conversion. PhD thesis. Zurich: Swiss Federal Institute of Technology Zurich.

Morris, D., Szargut, J. 1986. Standard chemical exergy of some elements and compounds on the planet earth. Energy 11(8), pp. 733–755.

Münster, M., Morthorst, P. E., Larsen, H. V., Bregnbæk, L., Werling, J., Lindboe, H. H., and Ravn, H. 2012 The role of district heating in the future Danish energy system. Energy 48(1), pp. 47–55.

Mwasilu, F., Justo, J. J., Kim, E.-K., Do, T. D., and Jung, J.-W. 2014. Electric vehicles and smart grid interaction: A review on vehicle to grid and renewable energy sources integration. Renewable and Sustainable Energy Reviews 34, pp. 501–516.

Namioka, T., Son, Y., Sato, M., Yoshikawa, K. 2009. Practical method of gravimetric tar analysis that takes into account a thermal cracking reaction scheme. Energy and Fuels 23(12), pp. 6156–62.

Nemanova, V., Nordgreen, T., Engvall, K., Sjöström, K. 2011. Biomass gasification in an atmospheric fluidised bed : Tar reduction with experimental iron-based granules from Höganäs AB , Sweden. Catal Today 176(1), pp. 253–257.Nelson, V. 2011. Introduction to Renewable Energy, A. Ghassemi, ed., CRC Press, Taylor & Francis Group.

Neymark, J., P. Girault, G. Guyon, R. Judkoff, R. LeBerre, J. Ojalvo, and P. Reimer. 2005. The "ETNABESTEST" empirical validation data set. Proceedings of Building Simulation 2005, Montréal, Canada, August 15–18, pp. 839–46.

Nielsen, S. and Möller, B. 2013. GIS based analysis of future district heating potential in Denmark. Energy 57, pp. 458–468.

NIST. 2012. Reference Fluid Thermodynamic and Transport Properties Database, REFPROP 9.

Noussan, M., Abdin, G.C., Poggio, A., Roberto, R. 2013. Biomass-fired CHP and heat storage system simulations in existing district heating systems, Applied Thermal Engineering 71(2), pp. 729–735.

Nuytten, T., Claessens, B., Paredis, K., Van Bael, J., and Six, D. 2013. Flexibility of a combined heat and power system with thermal energy storage for district heating. Applied Energy 104, pp. 583–591.

Obernberger, I., Thonhofer, P., and Reisenhofer, E. 2002. Description and evaluation of the new 1000 kWel Organic Rankine Cycle process integrated in the biomass CHP plant in Lienz, Austria. Euroheat & Power 10, pp. 18−25. Available at: www.turboden.eu/de/public/downloads/report_on_lienz_plant.pdf [Accessed: 1st October 2014].

Olmos, L., Ruester, S., Liong, S., and Glachant, J. 2011. Energy efficiency actions related to the rollout of smart meters for small consumers, application to the Austrian system. Energy 36(7), pp. 4396–4409.

Openshaw, K. 2010. Biomass energy: Employment generation and its contribution to poverty alleviation. Biomass and Bioenergy 34(3), pp. 365–378.

Paethanom, A., Nakahara, S., Kobayashi, M., Prawisudha, P., and Yoshikawa, K. 2012. Performance of tar removal by absorption and adsorption for biomass gasification. Fuel Processing Technology 104, pp. 144–154.

Pagliarini, G., Corradi, C., Rainieri, S. 2012. Hospital CHCP system optimization assisted by TRNSYS building energy simulation tool, Applied Thermal Engineering 44, pp. 150–158.

Pedroso, D. T., Machín, E. B., Silveira, J. L., and Nemoto, Y. 2013. Experimental study of bottom feed updraft gasifier. Renewable Energy 57, pp. 311–316.

Peris, B., Navarro-Esbrí, J., Molés, F., Collado, R., Mota-Babiloni, A. 2014. Performance evaluation of an Organic Rankine Cycle (ORC) for power applications from low grade heat sources, Applied Thermal Engineering, DOI:10.1016/j.applthermaleng.2014.10.034.

Perrot, P. 1998. A to Z of Thermodynamics. Oxford University Press.

Penna, P., Prada, A., Cappelletti, F., Gasparella, A. 2014. Multi-Objectives optimization of Energy Saving Measures in existing buildings. Energy and Buildings 95, pp. 57–69.

Pernigotto, G., Gasparella, A. 2013. Extensive comparative analysis of building energy simulation codes: Heating and cooling energy needs and peak loads calculation in TRNSYS and EnergyPlus for southern Europe climates. HVAC&R Research 19, pp. 481–492.

Persson, U., and Werner, S. 2011. Heat distribution and the future competitiveness of district heating. Applied Energy 88(3), pp. 568–576.

Phuphuakrat, T., Nipattummakul, N., Namioka, T., Kerdsuwan, S., Yoshikawa, K. 2010. Characterization of tar content in the syngas produced in a downdraft type fixed bed gasification system from dried sewage sludge. Fuel 89(9), pp. 2278–2284.

Piacentino, A., Barbaro, C., Cardona, F. 2014. Promotion of polygeneration for buildings applications through sector- and user-oriented "high efficiency CHP" eligibility criteria, Applied Thermal Engineering 71(2), pp. 882–894.

Pohl, E., Diarra, D. 2013. Assessment of primary energy savings by means of CHP systems in domestic energy supply, Applied Thermal Engineering 71(2), pp. 830–837.

Prando, D., Patuzzi, F., Pernigotto, G., Gasparella, A., Baratieri, M. 2014a. Biomass gasification systems for residential application: An integrated simulation approach, Applied Thermal Engineering 71(1), pp. 152–160.

Prando, D., Rizzo, A. M., Vakalis, S., Gasparella, A., Chiaramonti, D., and Baratieri, M. 2014b. Monitoring of two CHP systems based on biomass in northern Italy: boiler-ORC and gasifier-ICE. In the proceedings of the 5th

International Conference on Engineering for Waste and Biomass Valorisation, Rio de Janeiro (Brazil).

Prando, D., Renzi, M., Gasparella, A., Baratieri, M. 2015a. Monitoring of the energy performance of a district heating CHP plant based on biomass boiler and ORC generator, Applied Thermal Engineering 79, pp. 98–107.

Prando, D., Prada, A., Ochs, F., Gasparella, A., Baratieri, M. 2015b. Analysis of the energy and economic impact of cost-optimal buildings refurbishment on district heating systems, HVAC&R Research – Special Issues, Science and Technology for the Built Environment 21(6), pp. 876–891.

Puig-Arnavat, M., Bruno, J. C., and Coronas, A. 2013. Modeling of trigeneration configurations based on biomass gasification and comparison of performance. Applied Energy DOI: http://dx.doi.org/10.1016/j.apenergy.
2013.09.013.

Quoilin, S., Van Den Broek, M., Declaye, S., Dewallef, P., and Lemort, V. 2013. Techno-economic survey of Organic Rankine Cycle (ORC) systems. Renewable and Sustainable Energy Reviews 22, pp. 168–186.

Reidhav, C., Werner, S. 2008. Profitability of sparse district heating. Applied Energy 85, pp. 867–877.

Rentizelas, A., Karellas, S., Kakaras, E., and Tatsiopoulos, I. 2009. Comparative techno-economic analysis of ORC and gasification for bioenergy applications. Energy Conversion and Management 50(3), pp. 674–681.

Renzi, M., and Brandoni, C. 2014. Study and application of a regenerative Stirling cogeneration device based on biomass combustion. Applied Thermal Engineering 67(1–2), pp. 341–351.

Rezaie, B. and Rosen, M.A. 2012. District heating and cooling: Review of technology and potential enhancements. Applied Energy 93, pp. 2–10.

Rivarolo, M., Greco, A., and Massardo, A. F. 2013. Thermo-economic optimization of the impact of renewable generators on poly-generation smart-grids including hot thermal storage. Energy Conversion and Management 65, pp. 75–83.

Rosato, A., Sibilio, S., Ciampi, G. 2013a. Energy, environmental and economic dynamic performance assessment of different micro-cogeneration systems in a residential application, Applied Thermal Engineering 59(1–2), pp. 599–617.

Rosato, A., Sibilio, S. 2013b. Energy performance of a micro-cogeneration device during transient and steady-state operation: Experiments and simulations, Applied Thermal Engineering 52(2), pp. 478–491.

Ruiz, J.A., Juárez, M.C., Morales, M.P., Muñoz, P., Mendívil, M.A. 2013. Biomass gasification for electricity generation: Review of current technology barriers. Renewable and Sustainable Energy Reviews 18, pp. 174–183.

Saidur, R., Abdelaziz, E. a., Demirbas, a., Hossain, M. S., and Mekhilef, S. 2011. A review on biomass as a fuel for boilers. Renewable and Sustainable Energy Reviews 15(5), pp. 2262–2289.

Saltelli, A., Tarantola, S., Campolongo, F., Ratto, M. 2004. Sample generation, in Sensitivity analysis in practice. A guide to assessing scientific models, Chichester (UK): John Wiley & Sons, pp. 193–204.

Sandeep, K. and Dasappa, S. 2014. First and second law thermodynamic analysis of air and oxy-steam biomass gasification. International Journal of Hydrogen Energy 39(34), pp. 19474–19484.

Sartor, K., Quoilin, S., and Dewallef, P. 2014. Simulation and optimization of a CHP biomass plant and district heating network. Applied Energy 130, pp. 474–483.

Senapati, P.K., Behera, S. 2012. Experimental investigation on an entrained flow type biomass gasification system using coconut coir dust as powdery biomass feedstock. Bioresource Technology 117, pp. 99–106.

Sheeba, K.N., Babu, J.S.C., Jaisankar, S. 2009. Air gasification characteristics of coir pith in a circulating fluidized bed gasifier. Energy for Sustainable Development 13(3), pp. 166–173.

Smith, G.P., Golden, D.M., Frenklach, M., Moriarty, N.W., Eiteneer, B., Goldenberg, M., Bowman, C.T., Hanson, R.K., Song, S., Gardiner, W.C., Jr., Lissianski, V.V., Qin, Z. 2013. GRI-Mech 3.0. www.me.berkeley.edu/gri_mech/ [Accessed: 1st October 2013].

Spanner. 2014. Available at: www.holz-kraft.de/en/products/technical-data [Accessed: 2nd June 2014].

Spliethoff, H. 2001. Status of biomass gasification for power production. IFRF Combustion Journal, Available at: www.industrial.combustion.ifrf.net/paper_download.html?paperId=29 [Accessed: 11th November 2014]

Sridhar, G., Paul, P.J., Mukunda, H.S. 2001. Biomass derived producer gas as a reciprocating engine fuel – an experimental analysis, Biomass and Bioenergy 21, pp. 61–72.

Ståhl, K., and Neergaard, M. 1998. IGCC power plant for biomass utilization, Värnamo, Sweden. Biomass and Bioenergy 15(3), pp. 205–211.

SWD. 2013. Commission staff working document accompanying the Communication "A new EU Forest Strategy: for forests and the forest-based sector" Available at: http://ec.europa.eu/agriculture/forest/strategy/staff-working-doc_en.pdf [Accessed: 2nd June 2014].

The European Parliament and the Council of the European Union. 2004. Directive 2004/8/EC of the European Parliament and of the council of 11 February 2004 on the promotion of cogeneration based on a useful heat demand in the internal energy market and amending Directive 92/42/EEC, Official Journal of the European Union 52, pp. 50–60.

The European Parliament and the Council of the European Union. 2009. Directive 2009/28/EC of the European Parliament and of the council of 23 April 2009 on the promotion of the use of energy from renewable sources and amending and subsequently repealing Directives 2001/77/EC and 2003/30/EC, Official Journal of the European Union 140, pp. 16–62.

The European Parliament and the Council of the European Union. 2010. Directive 2010/31/EU of the European Parliament and of the council of 19 May 2010 on the energy performance of buildings (recast), Official Journal of the European Union 153, pp. 13–35.

The European Parliament and the Council of the European Union. 2012. Directive 2012/27/EU of the European Parliament and of the council of 25 October 2012 on the promotion of the use of energy from renewable sources and amending and subsequently repealing Directives 2001/77/EC and 2003/30/EC, Official Journal of the European Union 315, pp. 1–56.

Tomasi, C., Baratieri, M., Bosio, B., Arato, E., Baggio, P. 2006. Process analysis of a molten carbonate fuel cell power plant fed with a biomass syngas, Journal of Power Sources 157(2), pp. 765–774.

Turboden. 2014. Available at: www.turboden.eu/it/products/products-chp.php [Accessed: 1st October 2014].

UNI (Italian Organization for Standardization). 1994. UNI 10349 Heating and cooling of buildings – Climatic data.

UNI (Italian Organization for Standardization). 2006. UNI EN 12831 Heating systems in buildings – Method for calculation of the design heat load.

UNI (Italian Organization for Standardization). 2007. EN 15459 – Energy performance of buildings: economic evaluation procedure for energy systems in buildings.

UNI (Ente Nazionale Italiano di Normazione). 2008a. UNI/TS 11300-1 Energy performance of buildings – Part 1: Evaluation of energy need for space heating and cooling (In Italian: Determinazione del fabbisogno di energia termica dell'edificio per la climatizzazione estiva ed invernale), UNI, Milan (Italy), 2008.

UNI (Ente Nazionale Italiano di Normazione). 2008b. UNI/TS 11300-2 Energy performance of buildings – Part 2: Evaluation of primary energy need and of system efficiencies for space heating and domestic hot water production (In Italian: Determinazione del fabbisogno di energia primaria e dei rendimenti per la climatizzazione invernale e per la produzione di acqua calda sanitaria), UNI, Milan (Italy).

UNI (Ente Nazionale Italiano di Normazione). 2010. UNI 9182 Impianti di alimentazione e distribuzione d'acqua fredda e calda – Progettazione, installazione e collaudo (in English: Hot and cold water supply and distribution installations Design, testing and management criteria), UNI, Milan (Italy), 2010.

UNI (Italian Organization for Standardization). 2011. UNI EN 14961-2 Biocombustibili solidi – Specifiche e classificazione del combustibile – Parte 2: Pellet di legno per uso non industriale.

UNI (Italian Organization for Standardization). 2014. UNI TR 11552 Abacus of the opaque components of the builidngs – Thermo-physical parameters (In Italian: Abaco delle strutture costituenti l'involucro opaco degli edifici – Parametri termofisici).

U.S. Department of Energy. 2013. EnergyPlus – Testing and Validation [Online]. Available at: apps1.eere.energy.gov/buildings/energyplus/

energyplus_testing.cfm. EnergyPlus – Testing and Validation [Accessed: 5th October 2013].

Vakalis, S., Prando, D., Patuzzi, F., Mimmo, T., Gasparella, A., Tirler, W., Dal Savio, S., Chiaramonti, D., Prussi, M., Bararieri, M. 2013. Experiences in biomass gasification in South Tyrol: the "GAST" project, in: EU BC&E 2013 – European Biomass Conference and Exhibition, ETA Florence (ed.), Copenhagen (Denmark), pp. 891–901.

Vakalis, S., Prando, D., Patuzzi, F., Mimmo, T., Gasparella, A., Tirler, W., Dal Savio, S., Chiaramonti, D., Prussi, M., Bararieri, M. 2014. Measuring the performance of biomass small scale gasification plants by implementing mass and energy balances, in: 4th Central European Biomass Conference, Graz (Austria), Available at: www.cebc.at/en/service/presentations/ electricity-from-solid-biomass-friday [Accessed: 1st October 2014].

Vallios, I., Tsoutsos, T., Papadakis, G. 2009. Design of biomass district heating systems. Biomass and Bioenergy 33, pp. 659–678.

Van Loo, S., and Koppejan, J. (Eds.). 2008. The Handbook of Biomass Combustion and Co-firing. London (UK): Earthscan.

Van Paasen S.V.B., Kiel, J.H.A., Veringa, H.J. 2004. Tar formation in a fluidised-bed gasifier. ECN Biomass, 2004. Available at: www.ecn.nl/ docs/library/report/2004/c04013.pdf?q=tar [Accessed: 20th January 2015].

Van Ree, R., Oudhuis, A.B.J., Faaij, A., Curvers, A.P.W.M. 1995. Modelling of a biomass-integrated-gasifier/combined-cycle (BIG/CC) system with the flowsheet simulation programme ASPEN+, Energy research Centre of the Netherlands (ECN), Petten (The Netherlands), 1995.

Viessmann. 2013. Boiler fed by lignocellulosic biomass (In Italian: L'impianto termico a biomassa legnosa). Bressanone: Viessmann Engineering Srl.

Wetterlund, E., M. Söderström, 2010. Biomass gasification in district heating systems – The effect of economic energy policies, Applied Energy 87(9), pp. 2914–2922.

Wood, S.R., and Rowley, P.N. 2011. A techno-economic analysis of small-scale, biomass-fuelled combined heat and power for community housing. Biomass and Bioenergy 35(9), pp. 3849–3858.

Xue, X., Wang, S., Sun, Y. and Xiao F. 2014. An interactive building power demand management strategy for facilitating smart grid optimization. Applied Energy 116, pp. 297–310.

Yan, A., Zhao, J., An, Q., Zhao, Y., Li, Y.H. Huang. 2013. Hydraulic performance of a new district heating systems with distributed variable speed pumps. Applied Energy 112, pp. 876–885.

Yu, H., Zhang, Z., Li, Z., Chen, D. 2014. Characteristics of tar formation during cellulose, hemicellulose and lignin gasification. Fuel 118, pp. 250–256.Veringa, H.J. 2005. Advanced techniques for generation of energy from biomass and waste, 1–24, Energy research Centre of the Netherlands (ECN), Available at: www.ecn.nl/fileadmin/ecn/units/bio/Overig/pdf/Biomassa_voordelen.pdf [Accessed: 1st October 2014].

Zinko, H., Bøhm, B., Kristjansson, H., Ottosson, U., Rama, M., Sipila, K. 2008. District heating distribution in areas with low heat demand density. International Energy Agency 2008.

The author

Dario Prando is a research fellow at the Free University of Bozen-Bolzano. His research focuses on both experimental and modelling studies of energy systems based on renewable sources, specializing mainly on biomass-to-energy systems for distributed generation applications, with a particular attention to the gasification-based plants. Thanks to the experience gained from a multidisciplinary research team, his study is complemented by analysis of district heating networks and the connected buildings, especially considering the building refurbishment and the integration of renewable energy.